Titre: Title:	Biomass Gasification Integrated into a Reference Canadian Kraft Mill
Auteur: Author:	Pardis Rofouieeraghi
Date:	2012
Type:	Mémoire ou thèse / Dissertation or Thesis
Référence: Citation:	Rofouieeraghi, P. (2012). Biomass Gasification Integrated into a Reference Canadian Kraft Mill [Mémoire de maîtrise, École Polytechnique de Montréal]. PolyPublie. https://publications.polymtl.ca/789/

URL de PolyPublie: PolyPublie URL:	https://publications.polymtl.ca/789/
Directeurs de recherche: Advisors:	Jean Paris, & Michel Perrier
Programme: Program:	Génie chimique

UNIVERSITÉ DE MONTRÉAL

BIOMASS GASIFICATION INTEGRATED INTO A REFERENCE CANADIAN KRAFT MILL

PARDIS ROFOUIEERAGHI

DÉPARTEMENT DE GÉNIE CHIMIQUE

ÉCOLE POLYTECHNIQUE DE MONTRÉAL

MÉMOIRE PRÉSENTÉ EN VUE DE L'OBTENTION
DU DIPLÔME DE MAÎTRISE ÈS SCIENCES APPLIQUÉES

(GÉNIE CHIMIQUE)

FÉVRIER 2012

UNIVERSITÉ DE MONTRÉAL

ÉCOLE POLYTECHNIQUE DE MONTRÉAL

Ce mémoire intitulé:

BIOMASS GASIFICATION INTEGRATED INTO A REFERENCE CANADIAN KRAFT MILL

présenté par: ROFOUIEERAGHI Pardis

en vue de l'obtention du diplôme de: MAÎTRISE ÈS SCIENCES APPLIQUÉES

a été dûment accepté par le jury d'examen constitué de:

M. TAVARES Jason R., Ph.D., président

M. PARIS Jean, Ph.D., membre et directeur de recherche

M. PERRIER Michel, Ph.D., membre et codirecteur de recherche

M. PRETO Fernando, Ph.D., membre

Dedication

To my beloved grandfather,

Karim Kahrizi

Acknowledgements

First, I would like to state my deep appreciation to my advisor Professor Jean Paris for his diligence, experience, and trust and to Professor Michel Perrier for his supports. Many thanks to my friends and classmates for their supports, Maria Mironova, Milad Aghabararnejad, Tatiana Rafione, and Omid Ebrahimpour who I am filled with gratitude for his continuous company. Finally, I would like to thank my mother and my father, Parvin and Reza, and to my brother, Pouya with deep appreciation and sincere admiration for their love and supports.

Résumé

L'intégration de la bioraffinerie forestière dans l'industrie des pâtes et papiers crée une augmentation de la demande d'énergie. Comme l'industrie des pâtes et papiers est un des plus gros consommateurs de biomasse ligneuse au Canada, les déchets (écorces, liqueur noire, etc.) de cette industrie peuvent être utilisés pour répondre à la demande énergétique des usines de pâtes et papiers. Les ressources en biomasse peuvent également être utilisées pour produire des biocarburants, de l'électricité et des produits chimiques de spécialité. Le processus de gazéification est la méthode la plus efficace pour utiliser le potentiel énergétique de la biomasse. Dans cette étude, un bilan de masse et d'énergie ainsi qu'une analyse économique et environnementale d'un procédé de gazéification intégré à une usine Kraft de référence ont été réalisé. Pour ce faire, un modèle d'un procédé de gazéification comprenant une unité de séchage de la biomasse, une unité de gazéification ainsi que des unités de nettoyage des gaz a été simulé sur MATLAB puis sur Aspen Plus. Ce modèle a par la suite été lié à une simulation d'une usine Kraft de référence développée sur la plateforme CADSIM Plus. Un modèle thermodynamique d'équilibres modifiés pour le gazéificateur de biomasse a été développé afin d'améliorer la précision de la modélisation en équilibre. Le modèle a été évalué en utilisant aussi bien des données commerciales que des données provenant de la littérature. Deux études de cas pour la gazéification de la biomasse intégrée à usine Kraft de référence ont été évaluées. La comparaison des données du modèle d'équilibre avec les données expérimentales disponibles à partir de circuler gazogènes de biomasse à lit fluidisé a indiqué que le modèle d'équilibre nettement sous-estimer le rendement en méthane. Dans le modèle modifié, un modèle de dégazage est utilisé pour modérer l'écart du méthane basé sur la reconnaissance du fait que le méthane qui est initialement généré dans le processus de dégazage de la biomasse, ne pas réformer par des réactions de gazéification. Un modèle de dévolatilisation générale semi-empirique est appliqué pour prédire la composition des gaz volatils. Deux coefficients empiriques sont calculés à partir des données empiriques disponibles pour des expériences de dégazage de la biomasse. Les atomes correspondants de carbone et d'hydrogène à partir du méthane rendement prédite par le modèle de dévolatilisation sont éliminés du courant d'entrée gazéificateur. Le modèle modifié donne une meilleure estimation de la composition du gaz de synthèse à partir d'un air soufflé gazéifier de biomasse à lit fluidisé circulant en comparaison avec les données d'équilibre et deux données d'équilibre modifiés sont tirés de la littérature. Dans le premier cas, le produit issu de la gazéification de la biomasse est utilisé pour substituer le carburant fossile utilisé dans le four à chaux. Dans le second cas, la gazéification de la biomasse a été intégrée à un cycle combiné (cogénération). La faisabilité technique de ces deux scénarios a été démontrée. Une analyse économique pour les deux scénarios tenant compte du coût total en capital, des coûts d'exploitation et des recettes et considérant également la réduction des taxes sur les émissions de CO_2 a été réalisée.

Abstract

The integration of forest biorefinery into the pulp and paper industry introduces increased energy demands to the mills. As the pulp and paper industry is the largest woody biomass consumer in Canada, biomass resources such as bark, wood wastes, and black liquor that are used by pulp mills can be processed to supply energy demands of the mills and biorefinery units. Also, pulp and paper biomass resources can generate renewable biofuels, electricity, and chemicals. Gasification process is the most efficient method for utilizing the energy potential of biomass. The principle of this study is to perform mass and energy, economic, and environmental analyses for an integrated gasification process into a reference Canadian Kraft mill. To achieve this, a model of a complete gasification process including biomass drying, gasifier and gas cleaning units was simulated in MATLAB and Aspen Plus and then linked to a reference Kraft process that has been developed on the CADSIM Plus platform. A modified thermodynamic equilibrium model is developed to improve the prediction of syngas composition and heating values. Thermodynamic calculations are implemented based on non-stichiometric formulation to develop an equilibrium gasifier model. Comparison of equilibrium model data with available experimental data from circulating biomass fluidized bed gasifiers indicated that the equilibrium model significantly under-estimate the methane yield. In the modified model, a devolatilization model is employed to moderate the methane deviation based on acknowledgement the fact that methane which is initially generated in the biomass devolatilization process, does not reform through gasification reactions. A general semi-empirical devolatilization model is applied to predict the composition of volatile gases including methane composition. Two empirical coefficients are calculated from empirical data for available biomass devolatilization experiments. The corresponding atoms of carbon and hydrogen from predicted methane yield by devolatilization model are removed from the gasifier input stream. The modified model gives better estimation of the syngas composition from an air-blown circulating biomass fluidized bed gasifier in comparison with equilibrium data and two modified equilibrium data are taken from the literature. Two case studies for integrated biomass gasification with the reference Kraft are evaluated: using wood gasified to fire lime kiln, and integrated biomass gasification combined cycle. In the first scenario, the feasibility of replacing natural gas with syngas from wood residues gasification to fire the Kraft mill lime kiln is assessed. For the second scenario, the feasibility of replacement of the existing bark boiler with the integrated biomass gasification combined cycle is analyzed. Technical practicability of both scenarios based on the mass and energy balances derived from gasification process model is investigated. To evaluate the economic viability for both scenarios, total capital costs, operating costs, and revenues which achieved through lime kiln fossil fuel reduction, and also CO_2 emissions taxes are considered. The net present worth, NPV for 20 years payback period and 10% interest rate are estimated for the two case studies. It has been shown that gasified biomass is an attractive alternative lime kiln fuel for mills with access of woody biomass and concerns in reduction of fossil greenhouse gas emissions. Moreover, if the necessity of new bark boiler installation considered, the replacement of the existing bark boiler with integrated gasification combined cycle is technically viable. The results also show that the replacement of bark boiler has the potential to contribute to reduce global CO_2 emissions. Economic analysis proves the replacement of bark boiler with gasification power unit is economically feasible.

Table of Contents

List of Figures

List of Tables

NOTATION

A_C: corresponding corrected carbon utilized in the calculations.
A_{C0}: True values of the carbon in the system
A_H: corresponding corrected hydrogen utilized in the calculations.
A_{H0}: true values of the hydrogen in the system
b_k : number of atoms of the k_{th} element in a molecule of species i
$b*$: element abundance vector modified with kinetic carbon conversion, dimensionless
C_1: cost of the equipment at capacity q_1
C_2: cost of the equipment at capacity q_2
E: activation energy (kJ/mol)
F_k : cash flow at the end of the k period
G: system Gibbs free energy (kJ/mol)
IR: interest rate for each year
i : species index
K_1: equilibrium constant for water-gas shift reaction
K_2: equilibrium constant for $C + 2H_2 \rightarrow CH_4$
k_0: pre-exponential constant (s^{-1})
L: plant life
M, N: generic chemical species (atom or molecule)
M_i : molecular weight of product i at time t
m, n : coefficient of atomic carbon and hydrogen for tar
m_w: number of moles of water vapor (dry basis)
N' : total number of species considered
$n_{CH_4,dev}$: The number of moles of methane produced in the devolatilization step, per kilogram of biomass
ni = number of moles of species
n_t : total number of gaseous moles in the reactor
$n_{z\alpha}$: inert moles in phase a (mol)
P : pressure (N/m^2)
P_x : partial pressure of species
q_i: capacity of equipment
R : ideal gas constant 8.314 (J/mol/K)
R-squared: statistic fitting factor
SSE: explained sum of squares
T : thermodynamic temperature (K)
u_α : phase split of differential change in total moles of the system
V_i : yield of product i at time t
V_{i*}: ultimate yield of i at high temperature and long times
X_C: carbon conversion into gaseous products
X_{CH_4}: methane conversion by steam reforming
x,y,z : normalized coefficient of atomic hydrogen, oxygen, and nitrogen for biomass molecule
x_1-x_5 :number of moles of H_2, CO, CO_2, H_2O, and CH_4
x_g : number of moles of oxygen for gasification
Y_{gas}: gas yield of pyrolysis product

adt: standard dry ton
AGR: acid Gas Removal
ASU: air separation unit

CFB: circulating fluidized bed
daf : dry, ash fre
DME: dimethyl-ether
DC: direct cost
ER: equivalence ratio
HHV : higher heating value
HRSG: heat recovery steam generator
IC: indirect costs
IRR: internal rate of return
LP: low pressure
MJ: mega joule
MM: million
MP: medium pressure
MW: megawatt
MWth: megawatt thermal
Nm^3: normal cubic meter
NREL: National Renewable Energy Laboratory
NPV: net product value
TCI: total capital investment
TDIC: total direct and indirect cost
TIC: total installed cost
TJ: tetra joule
TPEC: total purchased equipment cost
TPI: total plant investment

Greek Letter

ΔG_T: Gibbs free energy (kJ/kmol)
ΔH: enthalpy changes (kJ/kmol)
ΔH_f: heat of formation (kJ/mol)
$£(n, \lambda)$= Lagrange function
α: phase index
β : elemental availability, or fractional achievement of equilibrium, dimensionless
β_C: availability of carbon, dimensionless
$\beta_{C,1}$: fraction of carbon converted into gaseous species, dimensionless
$\beta_{C,2}$: fraction of carbon converted into methane, dimensionless
$\beta_{C\ to\ CH_4}$: fraction of carbon and hydrogen converted into methane
β_H :availability of hydrogen, dimensionless
γ : mass fraction of gas species in the volatile gases
δ_{ij}: Kronecker delta
θ : exponential factor
λ_k: Lagrange multiplier for the k_{th} element
μ_i: molar free energy of species i (kJ/mol)
μ^*_i : standard chemical potential of species i (kJ/mol)
π: total number of phases in system
ω : acentric factor
τ: payback time
φ_i: fugacity coefficient of species i
ψk: function related to Lagrange multiplier

CHAPTER 1: Introduction

1.1. Problem introduction

Converting pulp and paper mills to biorefinery-based mills has the potential to help with difficulties such as a decrease in demand for pulp and paper products and increases in energy costs. Reduction of greenhouse gas emissions is also an important driver for converting mills into biorefineries. Kraft pulping process which produces approximately 60% of global pulp and paper products consumes significant amounts of energy generated from fossil fuels. By-products and wood residues resulting from a Kraft mill and black liquor are major biomass resources that can be applied to generate energy and value-added products. On the other hand, the implementation of biorefinery units into a Kraft mill can have two compounded effects on the steam system: it can create additional steam demand for the extraction and conversion units, and reduce steam production capacity. The installation of an integrated gasification system to process wood residues is an attractive solution to avoid increased dependency on fossil fuels and eventually to eliminate their use.

Gasification for enhancing biomass energy utilization is relatively mature compared with other possible technologies. Biomass gasification is a thermochemical conversion method to convert biomass feed into the synthesis gas product via partial oxidation of feedstock in the presence of air, oxygen and/or steam. The produced syngas can be applied directly to produce renewable fuels, energy and other products or it can be subsequently processed in synthesis reactors to generate liquid fuels such as ethanol, DME and mixed alcohols.

In order to precisely investigate the integration of biomass gasification process into a Kraft mill, a comprehensive model of a gasification plant is required. The core of the simulation is the model of the gasification chamber. Most available models are based on equilibrium assumptions. However, equilibrium modeling is valid only when the gasification temperature is high enough and the residence time is larger than the time required to complete the reactions. Due to absence of these conditions, equilibrium models estimate inaccurate syngas composition. In the present study, the equilibrium model is modified to take into account the fact that the biomass gasification occurs in two steps: devolatilization followed by partial oxidation and char gasification.

Finding an alternative fuel for lime kilns which are utilized in Kraft mills to convert lime mud ($CaCO_3$) to lime (CaO) through calcination reactions is an opportunity to reduce fossil fuel consumption in pulp and paper industries. The heat demand of the reaction is generally provided by burning natural gas or fuel oil in the lime kiln. Typically, 8.44 GJ per ton of lime product is required to heat lime kiln process (Francey et al., 2009). Using gasified wood residues to fire in lime kilns is an alternative which will reduce the dependency on fossil fuel consumption.

In addition, the integration of biomass gasification with a pulp and paper mills for electricity and steam production has the capability of reducing greenhouse gas emissions with positive economic benefits. Although, considerable interest has been exhibited in biofuel production, several studies have shown that the combined heat and electricity generation and heating applications are more cost effective (Wetterlund et al., 2011), (Rodrigues et al., 2007), (Wahlund et al., 2004), (Azar et al., 2003), (Dornburg and Faaij, 2001)).

In this study, integration of biomass gasification with a Canadian reference Kraft mill is investigated. As the recovery boiler does not supply the whole steam demand of the mill, a bark boiler is utilized to generate the required Kraft steam. The replacement of the existing bark boiler with a biomass gasifier is studied. In economic evaluation, it is assumed that a new investment would be made to replace an existing bark boiler system which had attained the end of its life. Moreover, the environmental benefits of the replacement are considered. Additionally, the use of gasified biomass as an alternative fuel to fire the lime kiln is investigated. Economic and environmental analyses as well as a technical study are performed to verify the feasibility of the implementation of an integrated gasification process into the reference Kraft mill.

1.2. Kraft pulping process

The Kraft process is the most efficient pulping process to transform woody biomass into paper and pulp. A schematic diagram of the Kraft mill is shown in Figure 2.1. First, to liberate the cellulose fibers, the white liquor, mixture of NaOH and Na_2S, is used to heat the wood in the digester to degrade wood into cellulose, lignin and hemicelluloses. Then, after washing and bleaching cellulose fibers are drained, pressed, and thermally dried in a pulp machine.

The dissolved materials include hemicelluloses, cellulose, lignin and together with various others organics are called black liquor and are sent to a series of multi-effect evaporators and concentrators, where it is concentrated from 13-17% solids to 65-85% solids to form a strong black liquor. Subsequently, the concentrated black liquor is burned in a Tomlinson recovery boiler to generate steam and to recover the chemical smelt. Typically, the high pressure steam produced in the recovery boiler is sent to a steam turbine to generate and LP steam. The chemical smelt which is highly concentrated in sodium carbonate and calcium carbonate is recovered through the conversion of sodium and sulfur compounds to sodium carbonate (Na_2CO_3) and sodium sulfide (Na_2S) under local reducing conditions. The smelt leaving the recovery boiler is dissolved in water to form green liquor, which is followed by the causticization of sodium carbonate with lime to convert Na_2CO_3 to NaOH. The causticized green liquor known as white liquor, which contains NaOH and Na_2S is recycled to the digester. The precipitated calcium carbonate ($CaCO_3$) is separated from the white liquor, washed and dewatered to form lime mud. To recover the lime for reusing in the causticizing unit, the lime mud recovers through the calcination reaction in a lime kilns process as follows:

$$CaCO_3(s) \rightarrow CaO(s) + CO_2(g) \qquad (1)$$

The required heat for the endothermic calcination reaction is provided by directly firing fuels in the lime kiln (Smook, 1990).

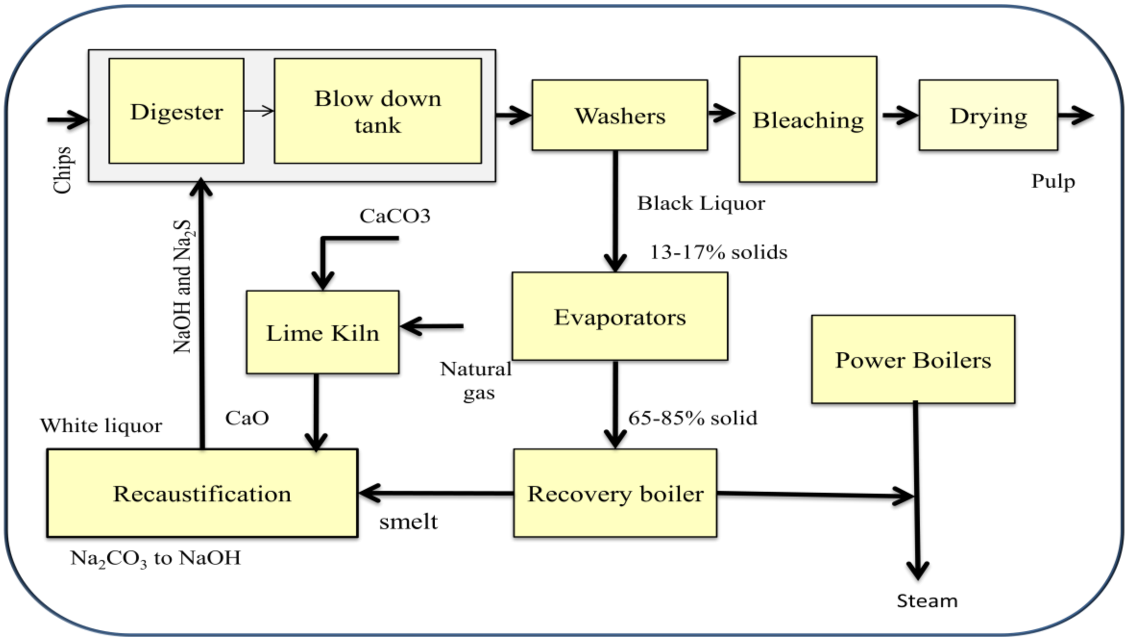

Figure 1.1. Schematic diagram of a Kraft pulping process

1.3. Integrated gasification into pulp and paper industry

The economic and environmental benefits of integrated gasification processes for a variety of industrial plants for electricity production and biofuel generation have been previously studied. Generally, the study of integration of gasification into pulp and paper industries includes two different types of processes: gasification of black liquor generated by the reference mill and woody biomass gasification. Although, integrated black liquor gasification in pulp mills has received considerable attention over recent years ((Lindblom, 2007),(Andersson and Harvey, 2006), (Berglin and Berntsson, 1998), (Larson et al., 2003)), only a few studies have investigated the integration of biomass gasification. Some studies have considered both biomass and black liquor gasification integration into pulp and paper mills. For example, (Naqvi et al., 2010) replaced the old bark boiler with a new power boiler with a higher capacity of power and steam production in order to compensate for the energy amount of black liquor that converted to biofuels (Figure 2.2). As well, (Consonni et al., 2009) considered both black liquor and biomass gasification for integration into an American pulp and paper mill. Seven configurations to produce mixed alcohols, dimethyl ether, and Fischer-Tropsch liquids were proposed in their study. The economic analysis confirmed that gasification-based Kraft mill biorefinery introduced significant benefits.

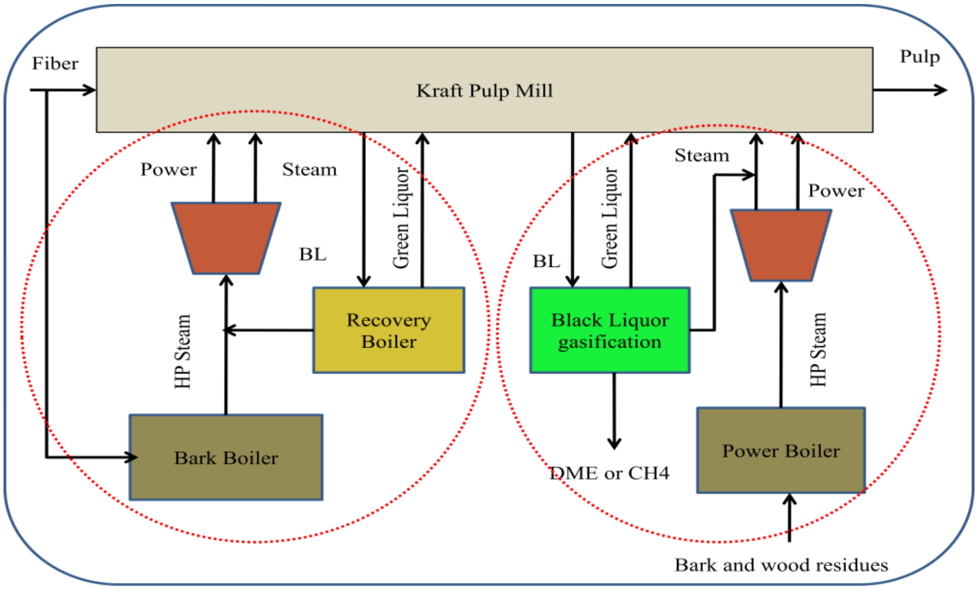

Figure 1.2. Replacement of recovery boiler with black liquor gasification

Recently, (Wetterlund et al., 2011) evaluated the integration of biomass gasification with pulp and paper production. Two biomass gasification scenarios were considered in their work: Biomass Integrated Gasification Dimethyl Ether production (BIGDME) and Biomass Gasification Integrated Combined Cycle (BIGCC). The results showed that energy market parameters strongly influence the profitability of biomass gasification integration with pulp and paper industry. The BIGDME case performs better than BIGCC when district heating is also utilized, whereas greenhouse gas emissions are reduced more in the BIGCC case. While, considerable interest has been shown in standalone biomass gasification in literature and industry; a few studies have been performed on the integration of biomass and wood residues gasification with a Kraft mill (Wetterlund et al., 2011),(Consonni et al., 2009). The integration of wood residues gasification with a Kraft mill in order to substitute the lime kiln fossil fuel can be an attractive alternative. After the enormous increases in oil prices in early 1980's, several lime kiln gasification processes were installed. The Ahlstrom Pyroflow CFB gasifier was installed in 1983 at the Wisa Forest Pulp and Paper Mill in Pietarsaari, Finland to apply gasified wood residues for firing the lime kiln. The target of 85% replacement of oil was obtained in few months with two years payback period. Since then, between 1985 and 1986, three more gasifiers, two in Sweden (25 MWth at Norrsundet Bruks, AB, Norrsundet and 27 MWth at ASSI, Karlsborg Bruk, Karlsborg) and one in Portugal (15 MWth at Portucel, Rodao Mill), were built and installed for firing lime kilns. These gasifiers produce lime kiln fuel from bark and waste wood (Abdul Salam et al., 2010).

1.4. General objective

The aim of the present study is to evaluate the technical, economic and environmental effects of integrated woody biomass gasification with a reference Kraft mill. In the present study, two different scenarios are considered:

- Using the syngas generated from biomass gasification as an alternative fuel for the lime kiln.
- Applying a biomass integrated gasification combined cycle, BIGCC, to generate steam and electricity in a combined heat and power plant.

In order to obtain the mass and energy balances for the above mentioned scenarios, a complete simulation for the different gasification units is required. Since the gasifier model is the heart of the simulation, using an accurate gasifier model to predict the syngas composition can be a great benefit. One of the simulation objectives is to generate a precise model of biomass gasification. The modified thermodynamic equilibrium model for biomass gasifier will be developed based on the minimization of Gibbs free energy. The model of biomass dryer, Syngas cooling and cleaning, and heat and power units would be implemented in Aspen Plus. The modified gasifier model would be developed in MATLAB and would be linked to the simulation of other process units in Aspen Plus and to a reference Kraft mill which has been simulated in CADSIM Plus through Excel.

1.5. Structure and organization

In chapter 2, the important parameters and concepts that should be considered in the gasification process are reviewed. As the development of gasifier model is the key target of the present thesis, the research review on gasification modeling receive more attention in this chapter.

In chapter 3, the specific objectives and overall methodology are presented.

In chapter 4, the results and techniques used in developing the simulation model for different steps of the gasification plant are illustrated. Also, the model validation of each unit is demonstrated.

In chapter 5, the feasibility analysis of replacing fossil fuel in lime kilns with the produced synthesis gas from the biomass gasification is discussed. Furthermore, the viability of the replacement of existing bark boiler in the reference Kraft mill with an integrated biomass gasification combined heat and power unit is also investigated.

Finally, in chapter 6, the conclusions and recommendations are presented.

CHAPTER 2: OVERVIEW OF BIOMASS GASIFICATION

2.1. Biomass gasification Process

The main gasification parameters include biomass type and properties, gasifier type, gasification temperature, gasification agents, and flowrates of biomass and oxidizing agents.

2.1.1. Biomass feed

Although, biomass gasifiers are flexible for a variety of biomass feedstocks, the type of biomass has significant effects in the overall syngas composition and operational issues. The biomass types are categorized based on the following parameters (Quaak et al., 1999):

- **Moisture content**

Biomass having high moisture content requires additional heat for evaporation of the moisture. Biomass with high moisture content reduces the gasification temperature causing incomplete cracking of the hydrocarbons generated in the pyrolysis step. Additionally, the moisture content in the presence of CO increases the amount of H_2 through the water gas shift reaction. As a result, the CH_4 content increases in the presence of the high H_2 content. In general, the heating value of the syngas is reduced with higher moisture contents. The reduction can be explained by decreases in the CO content compared with the increase in the amounts of H_2 and CH_4 (Zainal et al., 2001).

- **Ash content**

The amount of inorganic components and ash content are important parameters especially when gasification occurs in high temperatures**.**

- **Volatile matter content**

The amount of biomass which is released when the biomass is heated up to 400 °C is called volatile matter. High difference in the amount of volatiles in biomass (70-75%) compared to coal (20-25%) causes a significant variations between them.

- **Proximate analysis**

The proximate analysis categorizes the biomass in terms of moisture content, volatile content, fixed carbon, ash content, and heating value.

- **Ultimate analysis**

The major components are carbon, hydrogen, and oxygen. Generally, biomass includes small amounts of nitrogen and sulfur**.** The ultimate analysis gives the composition of the biomass in weight percentage of carbon, hydrogen and oxygen as well as sulfur and nitrogen.

- **Heating value** (HHV)

Biomass heating value is given on wet, dry, or dry and ash free basis. For all biomass feed types, higher heating value on a dry and ash free basis is in the order of 20 MJ/kg.

2.1.2. Biomass dryer

The moisture content of “fresh” woody biomass is typically 50% to 55%. In order to decrease the required heat to raise the gasifier temperature, the moisture content needs to be reduced in a dryer. For gasification, the best possible moisture range of biomass after drying is 10-15 wt%. A biomass dryer is an essential unit in a gasification process and influences the feasibility of the gasification plant. The heat source, biomass feed characteristics, and electricity cost determines the selection of the biomass dryer. The most common biomass drying technologies are:

- Flue gas dryer

A flue gas-based dryer has the advantage of using flue gas which improves the net mill energy efficiency. However, a large flow of flue gas is needed because of the low temperature of flue gas. The large volume of flue gas mandates a big biomass dryer with considerable electricity consumption. Also, there is a biomass contamination risk from impurities of flue gas. Typical energy estimation for a flue gas dryers is about 3200 kJ/kg H_2O (Wimmerstedt and Linde, 1998). Typically, around 2600 kJ/kg water is required to evaporate the moisture. Extra heat is needed to compensate energy losses and to heat biomass feed. To avoid huge dryers with high electricity consumption, biomass dryers in gasification plants utilize hot gas generator to burn a portion of the produced syngas for use in the biomass dryer. Generally, about 25% of the produced syngas is applied for drying.

- Air dryer

Recently, low temperature air dryers have received significant interest for biomass drying system because of the low grade heat and low gas emissions (Heyene, 2010). The heat demand for a low temperature air dryer is about 2700 KJ/Kg H_2O (Holmberg and Ahtila, 2005).

- Steam dryer

As steam dryers have the potential to recover a large amount of the input heat through the moisture condensation, considerable attention has been shown for heat integration in steam dryers (De Kam et al., 2009). Due to energy recovery in steam dryers, the net heat demand for a steam dryer is about 600 KJ/Kg H_2O (Heyene, 2010).

2.2. Air biomass gasification

Thermochemical conversion techniques of biomass are categorized by the amount of air, residence time, temperature, and the heat transfer rate in the process. Supplying stochiometric air results in combustion while treatment without air/oxygen leads to in pyrolysis products. Gasification is the conversion of biomass into a gas, syngas, by partial oxidation at high temperature around 700-1000˚C in the presence of a gasifying medium such as air, oxygen or steam (Demirbas, 2009). Syngas from biomass is a mixture of carbon monoxide (CO), carbon dioxide (CO_2), hydrogen (H_2), water (H_2O) and a small amount of methane (CH_4).

Biomass gasification has the potential for higher efficiency in comparison with existing technologies. The gasification process can be divided after drying into three steps (Figure2.3): 1. Pyrolysis or devolatilization 2. Partial oxidation 3. Char gasification

2.2.1. Pyrolysis

Pyrolysis is thermal degradation of biomass and does not require oxygen/air. In the initial pyrolysis step, the biomass converts to char (solid phase), tar (liquid phase), and volatiles (gaseous phase):

$$Biomass \rightarrow char + tar + volatiles \qquad (2)$$

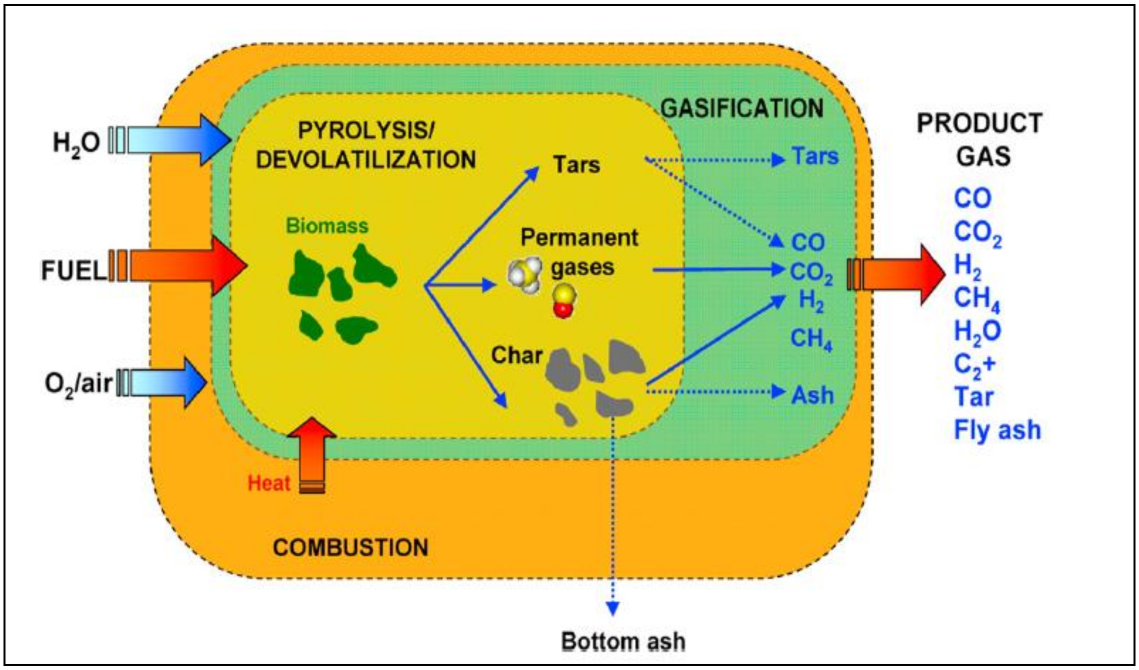

Figure 2.1. Gasification procedures (Gomez-Barea and Leckner, 2010)

The generated volatile matter in the pyrolysis step is a mixture of CO, CO_2, H_2, H_2O, and CH_4 (Kaushal et al., 2010):

$$VM = y_{CO}CO + y_{CO_2}CO_2 + y_{H_2}H_2 + y_{H_2O}H_2O + y_{CH_4}CH_4 + y_{P.Tar}Tar \tag{3}$$

The produced tar converts by thermal cracking, reforming, and partial oxidation in the secondary pyrolysis reactions as follows (Gomez-Barea and Leckner, 2010):

$$C_nH_m + \left({}^{n}/_{2}\right)O_2 \rightarrow nCO + \left({}^{m}/_{2}\right) \qquad \text{Partial oxidation} \tag{4}$$

$$C_nH_m + nCO_2 \rightarrow 2nCO_2 + \left({}^{m}/_{2}\right)H_2 \qquad \text{Dry reforming} \tag{5}$$

$$C_nH_m + nH_2O \rightarrow nCO_2 + \left({}^{m}/_{2} + n\right)H_2 \qquad \text{Steam reforming} \tag{6}$$

$$C_nH_m + \left(2n - {}^{m}/_{2}\right)H_2 \rightarrow nCH_4 \qquad \text{Hydrogenation} \tag{7}$$

$$C_nH_m \rightarrow \left(n - {}^{m}/_{4}\right)C + \left({}^{m}/_{4}\right)CH_4 \qquad \text{Thermal cracking} \tag{8}$$

C_nH_m is considered as the tar formulation.

2.2.2. Partial oxidation

In the Oxidation step, the volatile gases and the produced char react with O_2 to supply the required heat for endothermic gasification reactions (Gomez-Barea and Leckner, 2010):

$$C + O_2 \rightarrow CO_2 \qquad \Delta H = -394\ kj/mol \tag{9}$$

$$C + {}^{1}/_{2}\,O_2 \rightarrow CO \qquad \Delta H = -111\ kj/mol \tag{10}$$

$$CO + {}^{1}/_{2}\,O_2 \rightarrow CO_2 \qquad \Delta H = -283\ kj/mol \tag{11}$$

$$H_2 + {}^{1}/_{2}\,O_2 \rightarrow H_2O \qquad \Delta H = -242\ kj/mol \tag{12}$$

$$CH_4 + 2O_2 \rightarrow CO_2 + 2H_2O \qquad \Delta H = -800\ kj/mol \tag{13}$$

$$CO + H_2O \rightarrow CO_2 + H_2 \qquad \Delta H = -41\ kj/mol \tag{14}$$

2.2.3. Char gasification

Char reacts with $\mathrm{CO_2}$, $\mathrm{H_2O}$, and $\mathrm{H_2}$ in the gasification step. The char gasification reactions are slow compared to the pyrolysis reactions. The char gasification step includes the following reactions (Gomez-Barea and Leckner, 2010):

$$C + CO_2 \rightarrow 2CO \qquad \Delta H = +173\ kj/mol \tag{15}$$

$$C + H_2O \rightarrow CO + H_2 \qquad \Delta H = +131 kj/mol \tag{16}$$

$$C + 2H_2 \rightarrow CH_4 \qquad \Delta H = -75 kj/mol \tag{17}$$

2.3. Operating conditions

Several parameters affect the performance of a gasifier. Biomass type, gasifier type, gasifying agent, equivalence ratio, and temperature are the most important parameters influencing the gas product quality:

2.3.1. Gasifier type

Several types of reactors have been used as biomass gasifiers. The gasifiers can be classified based on the way in which the biomass feed and the gasifying agents are contacted and the hydrodynamics. Fixed bed and Fluidized bed are the most well known types of gasifiers. Among the fixed bed reactors, downdraft and updraft are the most common gasifiers. Furthermore, Bubbling and Circulating Fluidized Bed are the most common fluidized bed gasifiers (Figure 2.4).

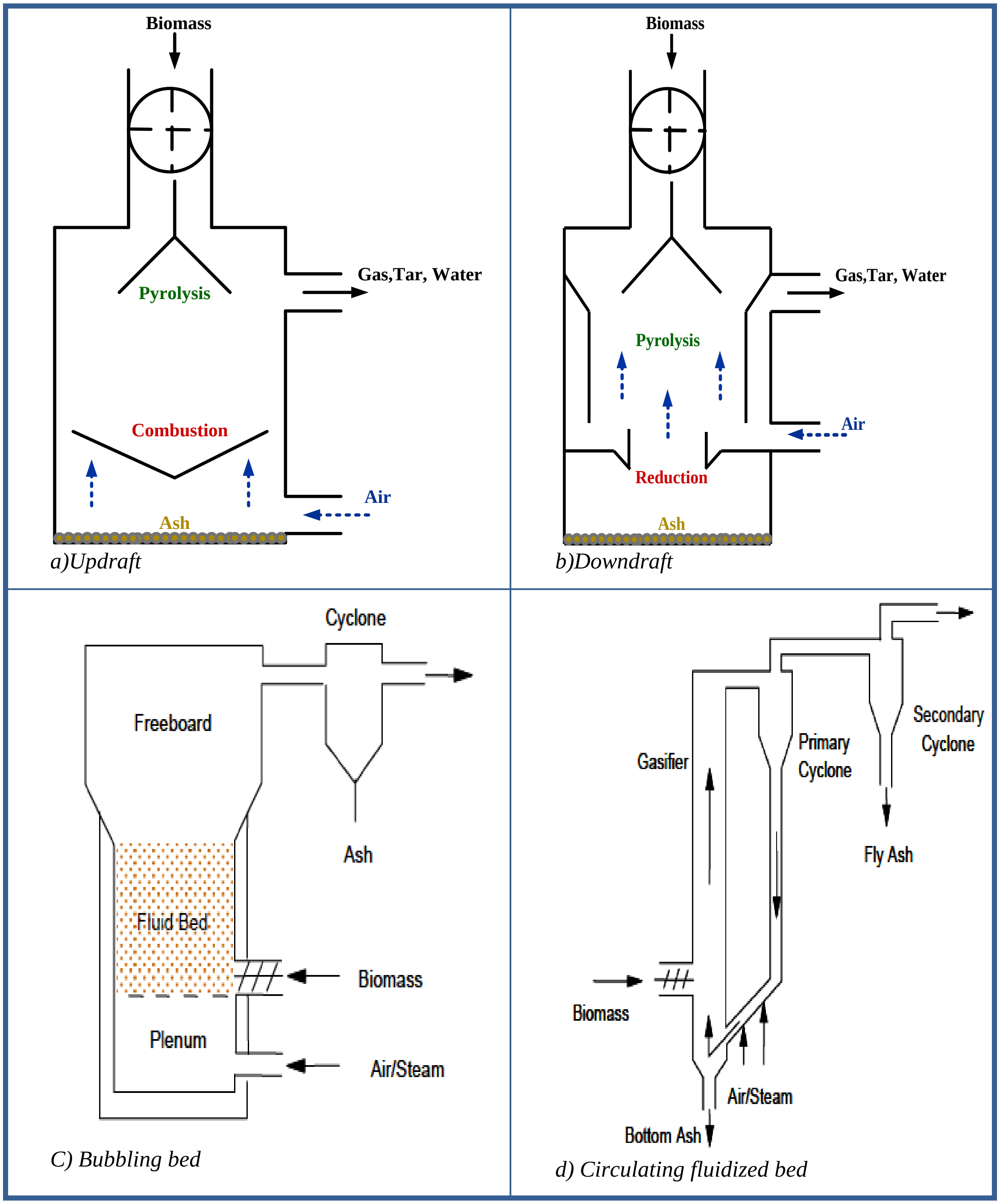

Figure 2.2. Gasifier types, (Stassen et al., 2002)

In the updraft gasifier, the biomass and the gasifying agent move in opposite directions. As the syngas formed is not forced to pass through the hot high temperature zone, the tar content is high in the syngas from this type of gasifier. On the other hand, in the downdraft gasifier, the biomass and gasifying agent both move in the same direction. The amount of tar is lower than that in an updraft gasifier. In fluidized bed gasifiers, feedstock is fluidized in a bed of material like sand/silica with a gasifying medium which can be air or steam. A fluidized bed gasifier can provide higher throughput, heating value and efficiency by improving mass and heat transfer. Circulating fluidized bed has an advantage over the bubbling bed gasifier in term of mass conversion efficiency. It reduces particulate content in the syngas output by trapping solid material in the gas phase in a hot cyclone and recirculating back to the gasification bed (Warnecke, 2000).

The selection of gasifier type depends on many factors such as fuel type, size, moisture content and ash content. Table 2.1 lists the advantages and disadvantages of various gasifier types (EPA-CHP, 2007).

Table 2.1. Advantages and disadvantages of gasifier types

Gasifier	**Advantage**	**Disadvantage**
Updraft fixed bed	✓ Handle high moisture ✓ No carbon in ash	× Feed size limits × High tar yields × Scale limitations × Low heating value
Downdraft fixed bed	✓ Small-scale applications ✓ Low particulates ✓ Low tar	× Feed size limits × Scale limitations × Low heating value gas × Moisture-sensitive
Bubbling fluid bed	✓ Large-scale applications ✓ Direct/indirect heating ✓ Produce high heating value gas	× Medium tar yield × Higher particle loading
Circulating fluid bed	✓ Large-scale applications ✓ Produce high heating value gas	× Medium tar yield × Higher particle loading
Entrained flow fluid	✓ Potential for low tar ✓ Potential for low methane ✓ Produce high heating value gas	× Large amount of carrier gas × Higher particle loading × Particle size limits

2.3.2. Gasifying agent

Common gasifying agents are air, oxygen, steam, and carbon dioxide. The required gas composition is an important factor in the choice between steam and air gasification. If methane is the desired product, steam gasification is the preferred method. When hydrogen and carbon monoxide are the desired products, e.g. for Fischer-Tropsch synthesis, air gasification is more suitable. In air gasification, the syngas will contain at least 38% nitrogen. Consequently, the product gas will have a low heating value of around 4–7 MJ/Nm^3. This dilution can be avoided by using pure oxygen for gasification or by steam gasification. Pure oxygen gasification produces higher quality gas (10–18 MJ/Nm^3). However, due to the high separation cost of oxygen from air, it is not economic (Schuster et al., 2001). As well, the heating value of the syngas can be enhanced by adding steam or CO_2 as the gasifying agent. Steam and CO_2 gasification require an external heat supply for the endothermic gasification reactions. Main advantages and technical challenges based on the gasifying agent, gasifier type and the operation are summarized in Table 2.2.

Table 2.2. Conditions of different gasifying agents (Wang et al., 2008)

Gasifying Agent	**Advantage**	**Conditions**
Air	✓ Moderate char and tar content	✗ Low heating value (3–6 MJ N/m^3) ✗ Large amount of N_2 in syngas
Steam	✓ High heating value (10–15 MJN/m^3) ✓ H_2-rich syngas	✗ External heat supply ✗ High tar content ✗ Catalytic tar reforming
Carbon dioxide	✓ High heating value ✓ High H_2 and CO and low CO_2	✗ External heat supply ✗ Catalytic tar reforming

2.3.3. Equivalence ratio

Equivalence ratio (ER) is defined as the ratio of the air/oxygen to the stoichiometric air/oxygen. ER has a significant effect on syngas composition. By increasing ER, the combustible products are reduced and higher amount of CO_2 is formed. Hence, the heating value of the produced syngas is considerably reduced. As a result, ER plays an important role in determining the overall syngas quality. It should be optimized in order to increase the gasification efficiency.

2.3.4. Temperature

The temperature of a gasifier depends on a variety of parameters such as the moisture content, ER, and heat losses from the system (Corella and Sanz, 2005). Typical temperatures suggested for biomass gasification in a fluidized bed are around 800-1000°C. Higher temperatures increase the carbon conversion. Also, an increase in temperature reduces the tar and char contents inside the gasifier (Zainal et al., 2002). Therefore, higher gas yields can be achieved due to reduction in the char and tar quantities.

2.4. Evaluation criteria

The performance of gasification process is generally evaluated by using following criteria (Rao et al., 2004):

- **The cold gas efficiency (CGE)**

The cold-gas efficiency, CGE, excluding the heating value of the condensable (tars), is defined as the percentage of the fuel heating value converted into the heating value of the product gas:

$$CGE = \frac{\left\{Gas\ yield\left(Nm^3kg^{-1}\ fuel\right) \times HHVof\ gas\ MJ\ Nm^{-3}\right\}}{\left\{HHV\ of\ fuel\ MJ\ kg^{-1}\right\}} \times 100 \qquad (18)$$

HHV (Higher Heating Value) of the dry gas at the standard state of 101.3kPa and 273 K is a function of gas composition, (Lide and Kehiaian, 1994):

$$\begin{aligned} HHV = (12.75[H_2] + 12.63[CO] + 39.82[CH_4] + 63.43[C_2H_4] \\ + \cdots)/100 \end{aligned} \qquad (19)$$

Where the species contents are given in mol%, and their heating value of combustion, in MJ/Nm$^{3.}$

- **Carbon conversion efficiency (η_c):**

Carbon conversion is defined as follows:

$$\eta_c = 1 - \frac{Total\ rate\ of\ carbon\ in\ the\ gas\ product\ stream}{Total\ rate\ of\ carbon\ in\ the\ feed\ stream} \qquad (20)$$

2.5. Biomass gasifier modeling

A variety of models have been proposed from complex CFD models to simple models based on overall heat and mass balances (Gomez-Barea and Leckner, 2010). Based on the aim of present study, thermodynamic equilibrium modeling approach is selected to predict the syngas composition and gasifier efficiency. The equilibrium modeling is briefly described in the next section.

2.5.1. Thermodynamic equilibrium modeling

Thermodynamic equilibrium modeling provides a reasonable estimation when the reaction temperature and residence time are high enough. Equilibrium conditions are difficult to achieve in practical operating conditions and results obtained from thermodynamic equilibrium modeling can serve as the maximum limit on syngas composition. Numerous equilibrium models have been utilized for biomass and coal gasification in the literature (Kinoshita et al., 1991), (Mansaray et al., 2000), (Li et al., 2001), (Mathieu and Dubuisson, 2002), (Altafini et al., 2003), (Li et al., 2004) (Tang and Kitagawa, 2005), (Jand et al., 2006), (Jarungthammachote and Dutta, 2007), (Nikoo and Mahinpey, 2008), (Huang and Ramaswamy, 2009), (Hannula and Kurkela, 2010).

Equilibrium models can be classified into two approaches: Stochiometric and Non Stochiometric (Smith and Missen, 1982):

2.5.1.1. Stochiometric models

Stochiometric formulation of biomass gasification has been mostly applied in the literature (Zainal et al., 2001),(Schuster et al., 2001),(Melgar et al., 2007), (Huang and Ramaswamy, 2009),(Gautam et al., 2010). In the next section, brief details of stochiometric formulation are clarified.

Assuming that the biomass formula is $CH_xO_yN_z$ and gasification products contain the gas species of H_2, CO, CH_4, CO_2, H_2O, and N_2, the gasification reaction can be written as (Gautam et al., 2010):

$$CH_xO_yN_z + m_WH_2O + x_g(O_2 + 3.76N_2) \rightarrow x_1CO + x_2H_2 + x_3CO_2 + x_4H_2O + x_5CH_4 + (\frac{z}{2} + 3.76x_g)N_2 \quad (21)$$

The stochiometric formulation needs a specified reaction mechanism. If water gas shifts (Equation (14)) and methane formation (Equation (17)) reactions are considered as the two major equilibrium reactions that occur in the gasification process, then the equilibrium constant for these equations as the function of their molar composition can be written as follows:

$$K_1 = \frac{n_{CO_2}n_{H_2}}{n_{CO}n_{H_2O}} = \frac{x_3x_2}{x_1x_4} \quad (22)$$

$$K_2 = \frac{n_{CH_4}n_t}{n_{H_2}^2} = \frac{x_5n_t}{x_2^2} \quad (23)$$

Minimization of Gibbs free energy is used to determine the value of K_1 and K_2:

$$ln\,K = \frac{-\Delta G_T}{RT} \quad (24)$$

There are six unknown variables (x_1-x_5, x_g) two of which are calculated from Equations (22) and (23), three of them are calculated from mass balances of atoms of carbon, hydrogen, oxygen, and the final unknown is specified from an enthalpy balance equation.

2.5.1.2. Non-stochiometic models

The non-stochiometric formulation has been extensively applied for biomass gasification modeling ((Li et al., 2004),(Jand et al., 2006)). In the non-stochiometric modeling, the gasification reaction mechanism is not required. The elemental composition of biomass indicated from ultimate analysis is the only essential input of non-stochiometric formulation. The non-stochiometric formulation is based on minimizing the Gibbs free energy at the fixed temperature and pressure, subjecting to the element abundance constraints.

$$\min G(n) = \sum_{i=1}^{N} n_i\mu_i \quad (25)$$

$$\sum_{i=1}^{N} a_{ki} n_i = b_k \qquad K = 1,2,\dots,M \tag{26}$$

2.5.1.3. Pseudo equilibrium models

Equilibrium modeling results in a reasonable prediction when temperature is high enough and residence time is larger than the time needed to complete the reactions (Gomez-Barea and Leckner, 2010). As these conditions do not occur in exisiting gasifiers, overestimation and underestimation of produced gas composition occurs in equilibrium modeling. Generally, equilibrium model overestimates the yields of CO and H_2, and underestimates the yield of CO_2 and CH_4. Pseudo equilibrium models by means of empirical relations increase the prediction accuracy of syngas composition. Only, a few number of pseudo equilibrium models have been developed in the literature. Hereafter, the related publications are reviewed.

A straightforward approach for correcting an equilibrium model is implementing the equilibrium relations at a temperature lower than the actual gasifier temperature, i.e. a quasi equilibrium temperature. (Kersten et al., 2003) showed that for the char gasification reaction with $H_{2,}$ CO_2, and H_2O for temperatures in the range of 740-910 ˚C, the measured unconverted carbon was similar for the equilibrium when evaluated at temperatures in the range of 450-580 ˚C.

(Jayah et al., 2003) considered two of the steps for modelling of gasification process, pyrolysis and gasification. The maximum temperature of system and the composition of produced gas were calculated via a pyrolysis model. The deviation between empirical and model data was corrected by calibration of gasification zone data. In the calibration, the amount of estimated methane was replaced with experimental measurement data of methane.

(Li et al., 2004) proposed a phenomenological model to estimate the performance of a circulating fluidized bed gasifier based on the experimental data from gasification of numerous types of woody biomass. The structure of the model is illustrated in Figure 2.5. The model assumed that the produced methane in gasification comes from the pyrolysis step. The amounts of methane and unconverted carbon are estimated and removed from the equilibrium model input stream.

The availability parameter, β, is defined and multiplied in elemental composition to modify the abundance vector:

$$b^* = (\beta_C n_C, \beta_H n_H, \beta_O n_O, \beta_N n_N, \beta_S n_S) \tag{27}$$

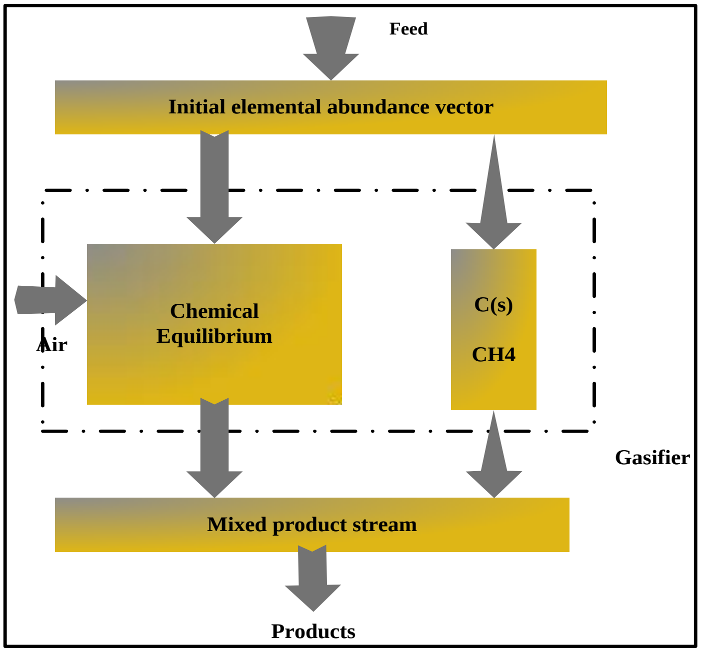

Figure 2.3. Structure of (Li et al., 2004)phenomenological model

The amount of carbon converted in pyrolysis step to methane that is not achieved in equilibrium ($\beta_{C,2}$) is removed from the fraction of carbon converted into gaseous species ($\beta_{C,1}$) in order to calculate the available overall fraction of carbon entering chemical equilibrium (β_C). One mole of methane contains four moles of hydrogen. The available hydrogen is estimated from availability of carbon:

$$\beta_{C,1} = 0.25 + 0.75exp({}^{-ER}/_{0.23}) \tag{28}$$

$$\beta_{C,2} = 0.11(1 - ER) \tag{29}$$

$$\beta_C = \beta_{C,1} - \beta_{C,2} \tag{30}$$

$$\beta_H = 1 - \frac{4\beta_{C,2} n_C}{n_H} \tag{31}$$

They supposed that complete conversion for other elements in the model which introduces some prediction errors in syngas composition. The estimations of CH_4 and H_2O contents improved in comparison with the estimations calculated from a pure equilibrium model. Similar to results reported in previous work (Ruggiero and Manfrida, 1999), the predicted H_2 component is higher than actual data. They considered this deviation to be a result of the fractional availability of water to water gas shift reaction. They mentioned that considering the unconverted carbon as a solid pure carbon is as another source of equilibrium modeling deviation, while the actual unconverted carbon stays more as coke (CH_x) which decreases the availability of both carbon and hydrogen.

(Jand et al., 2006) proposed a method to improve the equilibrium modeling of high temperature biomass gasification. They considered two main stages for modeling: fast pyrolysis and methane and char gasification. To modify the underestimation of char and methane in the rigorous equilibrium model output, the carbon and hydrogen elemental balance constraint corrected as follows:

$$A_C = A_{C_0} X_C - n_{CH_4,dev}(1 - X_{CH_4}) \tag{32}$$

$$A_H = A_{H_0} - 4n_{CH_4,dev}(1 - X_{CH_4}) \tag{33}$$

Where

A_{C0}: True values of the carbon in the system

A_{H0}: True values of the hydrogen in the system

A_C: Corresponding corrected carbon utilized in the calculations.

A_H: Corresponding corrected hydrogen utilized in the calculations.

X_C: Carbon conversion into gaseous products

$n_{CH_4,dev}$: The number of moles of methane produced in the devolatilization step, per kilogram of biomass.

X_{CH_4}: Methane conversion by steam reforming

X_C is typically in the range of 0.8-0.9 depending on the temperature, ER steam, and the gasifier type. The value of $n_{CH4,dev}$ is estimated 5.5 mol/kg as a result of the (Jand et al., 2006) experiment for steam gasification of sawdust. They claimed that X_{CH4} is non-zero when a catalyst is utilized in the gasification process. In this condition, a proper approximation can be (X_{CH4}=1/3). For active reforming catalysts, higher values (up to X_{CH4} = 2/3) should be considered. For air gasification, an insignificant conversion of methane (X_{CH4} = 1/4) can be approximated.

The (Jand et al., 2006) model in comparison with (Li et al., 2004) model is more consistent with experimental data. Table 2.3 illustrates the comparison of the proposed and a base equilibrium model with one of experimental data. The results were obtained for X_C = 0.85 and the methane conversion assumed to be negligible. As shown in the Table 2.3, good agreement is observed between the results from the modified model and the experimental data.

Table 2.3. Comparison between models output and experimental data at T=851˚C

	plant results	**(Jand et al., 2006)** ***model***	***straightforward equilibrium***
gas yield, Nm^3 dry/kg daf biomass	2.04	2.10	2.64
H_2, vol %	11.9	11.9	24.5
CO, vol %	14.2	15.4	28.7
CO_2, vol %	16.4	15.7	6.6
CH_4, vol %	4.0	6.5	0.01
C_2, vol %	1.45	0.0	0.0
C_6+, vol %	0.03	0.0	0.0
N_2, vol %	51.4	50.5	40.3
NH_3, vol %	n.d.	0.001	0.002
H_2O, vol % wet	12.4	12.0	5.9
char + tar, g C/kg daf biomass	69.2	74.7	0

(Melgar et al., 2007) recommended an equilibrium model based on the chemical equilibrium and minimization of free Gibbs energy. They calculated the reactor temperature using energy balance equations and then estimated the output gas composition as a function of the temperature. The chemical equilibrium constants and the thermodynamic properties that are functions of temperature were adapted in iterations of temperature calculations. They investigated the influence of two operating parameters, the relative gasifying fuel/air ratio and the biomass moisture content on the maximum temperature that can be reached.

(Jarungthammachote and Dutta, 2008) used the minimization free Gibbs energy approach to estimate the concentrations of output gas for a spouted fluidized bed biomass gasifier. They modified the equilibrium model by considering the carbon conversion in the constraints and also in the energy balance equations. The procedure for the calculation of the reaction temperature is illustrated in Figure 2.6. First, concentrations of the output gas based on the minimization of Gibbs free energy are calculated in the initial temperature. Next, the ΔH that is a negative value based on the energy balance calculation is obtained. The reaction temperature is repeatedly reduced until the ΔH becomes zero. Otherwise, the temperature is increased. Next, the composition of the produced gas is calculated and accordingly the energy balance is checked. The procedure is continued until ΔH approaches zero.

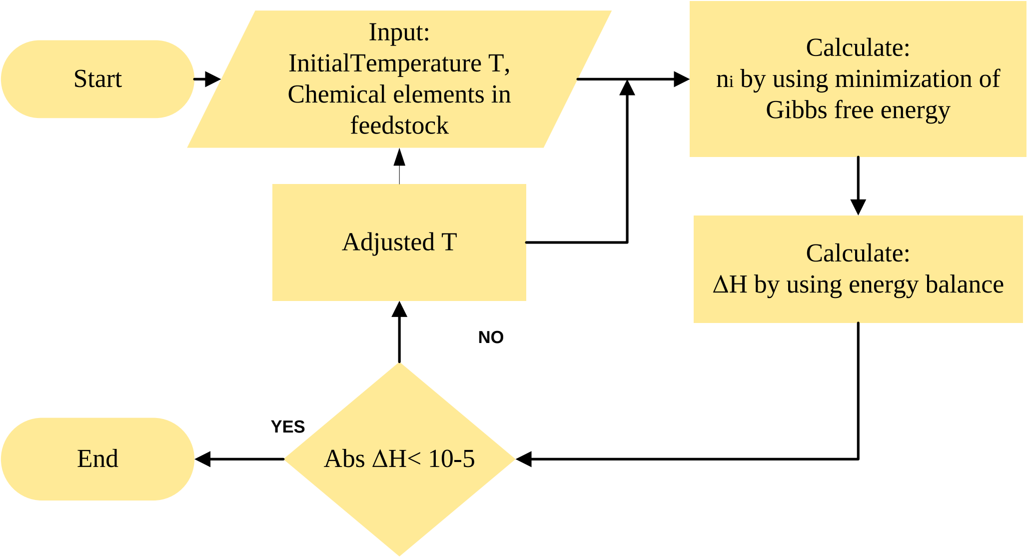

Figure 2.4. Procedure of temperature estimation, (Jarungthammachote and Dutta, 2008)

They assumed that the observed differences between the experimental and calculated data are mainly generated due to ignoring the carbon conversion. Thus, the model was modified by considering carbon conversion. The average value of 60% was considered as the carbon conversion. The modified model results showed that the concentrations of CO and CO_2 are much closer to the empirical data that those from non-modified equilibrium model. However, the overestimation of CO composition causes the higher heating value (HHV) compared to the actual HHV.

(Huang and Ramaswamy, 2009) developed an equilibrium thermodynamic model based on the stochiometric approach with and without considering char. The models were modified by fitting the methane and carbon monoxide compositions to the constant values which were determined from experimental data. They multiplied the two coefficients to the equilibrium constants of steam methane reforming reaction (Equation (17)) and water gas shift reaction (Equation (14)) reactions in order to consider fractional achievement of equilibrium for methane and carbon monoxide. The two coefficients were estimated by setting up the fractions of methane and carbon monoxide in the dry output gas in the average values computed from experimental data.

The most important bottleneck of the reviewed pseudo equilibrium models is that the majority of the proposed models are attempts to improve the performance of the equilibrium modeling for particular gasification conditions. As a result, a significant lack of a comprehensive pseudo equilibrium model in literature was observed.

2.6. Devolatilization model

Considering that a devolatilization model is employed in the proposed model, in this section a brief review of devolatilization (pyrolysis) model is presented.

The goal of a devolatilization model is to estimate the yields of pyrolysis products, gas, tar, and char. A devolatilization model can be classified as basic, distributed activation energy, and structural models (Souza-Santos, 2004). Basic models are a single reaction or a combination of several reactions. The kinetic parameters (activation energy and kinetic constant) and reaction order are specified through experiments. Although, a large number of studies have been investigated to specify the kinetic parameters; a considerable deviation is observed between the parameters. The combination of series and parallels reactions (Figure 2.7) improves the modeling accuracy (Di Blasi, 2008) , (Rath et al., 2002). The most important problem in this approach is that kinetics of the reactions is not well known.

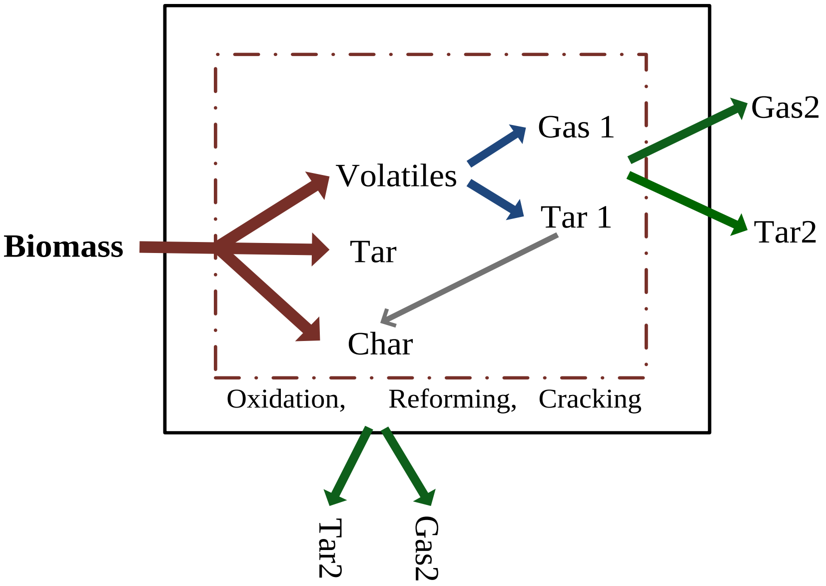

Figure 2.5. Pyrolysis process

The distributed activation energy pyrolysis method expresses the activation energy by a continuous distribution function, developed by fitting empirical data of volatiles over time. This method is more applicable for complex structure such as coal (de Diego et al., 2002).

The published pyrolysis models generally estimate only the overall yields of volatile, tar, and char. To predict the yield of gas products, empirical correlations have been utilized (Hajaligol et al., 1982), (Nunn et al., 1985), (Jand and Foscolo, 2005), (Radmanesh et al., 2006). The empirical relations are function of operating conditions, type of feedstock, particle size, temperature, and heating rate. Concerning the fact that each correlation is valid for particular operating parameters and biomass feedstock, it is not applicable as a comprehensive approach.

Structural model have been developed for biomass in terms of the cellulose, hemicelluloses, and lignin fractions. The overall devolatilization model is a combination of the three reference components. The model is capable to predict the yield of gas species (Ranzi et al., 2008).

2.7. Syngas cleaning

As the syngas obtained from the gasifier contains particulate, tars, alkali compounds, and other contaminants, a gas cleaning unit is generally utilized before syngas application. Particulate and tars should be removed to avoid clogging of downstream processes. Sulfur compounds have to be removed particularly when catalysts are used in fuel synthesis applications otherwise there is the potential of catalyst poisoning or deactivation.

Physical methods such as cyclones are frequently employed to remove particulates. The particulate removal should be done before the syngas is cooled down in order to avoid tar condensation. Hot temperature metal and ceramic filters can also be applied to remove particulates.

Various techniques of tar removal have been developed (Milne and Evans, 1998). Physical removal by the use of wet scrubber is a common method to remove tar and alkali after gasification. The other techniques are catalytic or thermal conversion of tar to non-condensable gas. Sulfur in the biomass mostly forms into hydrogen sulfide (H_2S) and if necessary must be removed separately.

CO_2 capturing in biomass gasification process is in favor for biofuel fuel production such as hydrogen production. While, acid gas removal including CO_2 capturing for integrated black liquor and coal gasification combined cycle is essentially required; for the cases which the produced syngas burned in gas turbines or in lime kilns, generally, the CO_2 capturing units are not utilized.

CO_2 capturing technologies can be divided in four methods:

- Chemical absorption
- Physical absorption
- Solid adsorption
- Membrane

Membrane technology is an attractive method to capture $CO_{2,}$, but it has been not employed in industrial applications yet. Solid adsorption is applicable for limited gas volumes. Chemical and physical absorption have been shown to be the appropriate approaches for industrial gasification plants. A typical absorption process is shown in Figure 2.8. First, the syngas is cooled, and then injected at the bottom of the absorber while the solvent is fed at the top of the absorber to capture CO_2. The bottom stream of absorption column is heated and then sent to regeneration column to recover the solvent. Different amines formulas have been used as the chemical solvent. Among of physical solvents, methanol and Dimethyl of polyethylene glycol are more favorable due to their chemical stability and high absorption capacity. Rectisol and Selexol physical absorption technologies which respectively utilize methanol and dimethyl polyethylene glycol as the solvents are known in gasification plants for acid gas removal. As the Rectisol technology operate at low operating temperature compared to the Selexol technology, in the most integrated gasification combined cycle processes, Selexol technology is employed for acid gas removal (Chiesa and Lozza, 1999), (Persons, 2002), (Okeefe et al., 2002), (Foster Wheel, 2003).

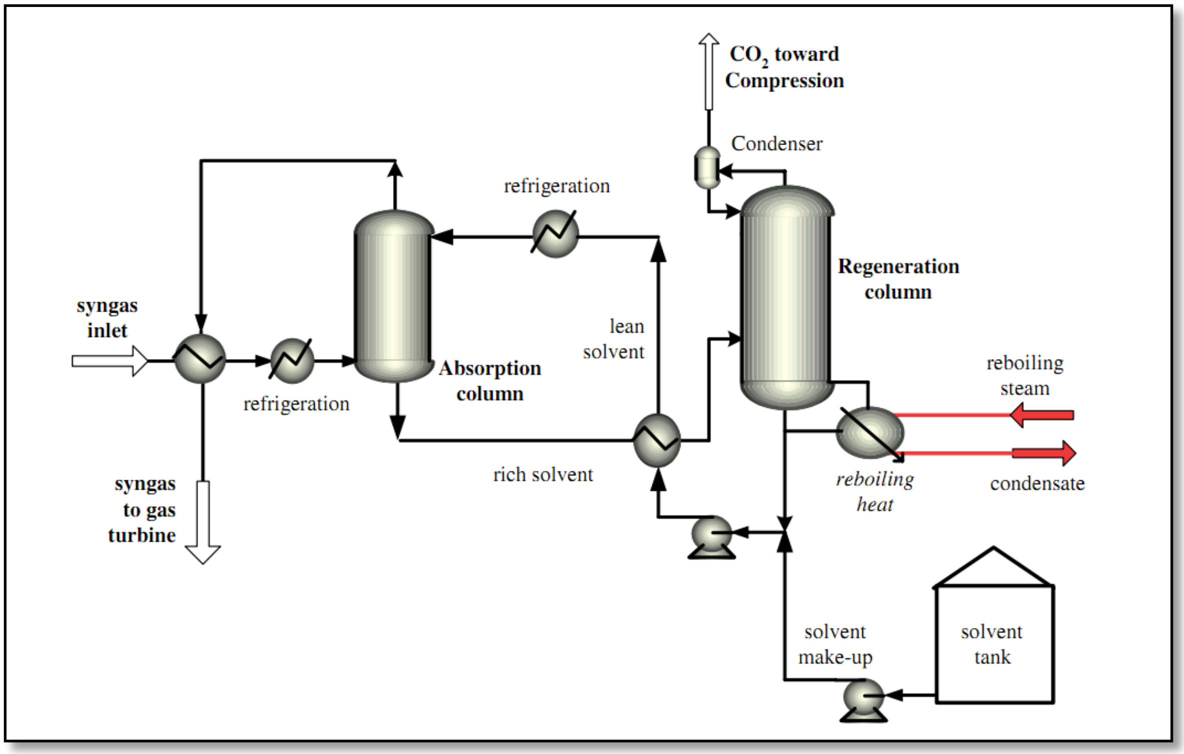

Figure 2.6. Typical absorption process, (Kanniche and Bouallou, 2007)

CHAPTER 3: Methodology

3.1. Main objective

The main objective of this study is to evaluate the integration of a wood biomass gasification process into a Canadian reference Kraft mill.

3.2. Specific objectives

The specific objectives of the present study include:

- To develop a complete model of the gasification process that includes biomass dryer, syngas cooling and cleaning, and heat and power unit.
- To assess the use of the syngas produced in biomass gasification process as an alternative fuel for firing the reference Kraft mill`s lime kiln.
- To evaluate the replacement of the bark boiler in the reference Kraft mill with an integrated biomass gasification combined cycle.

3.3. Overall methodology

3.3.1. Developing a model of biomass gasification process

In order to evaluate the integration of biomass gasification into a Kraft mill, a robust model of gasification process is required. Figure 3.1 illustrates the basic process steps of an integrated biomass gasification process.

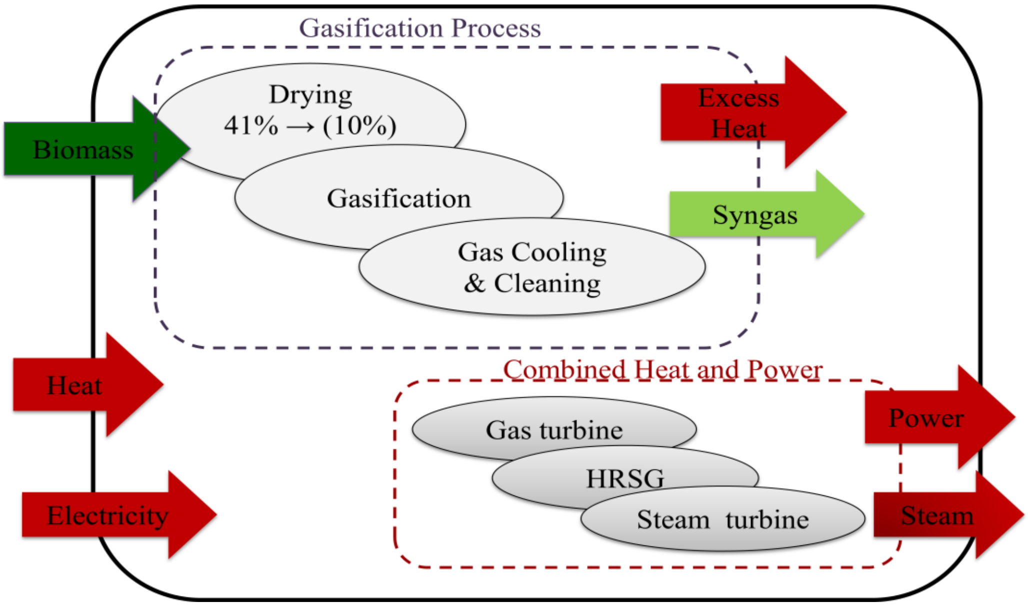

Figure 3.1. Basic process steps of an integrated biomass gasification process

In order to obtain mass and energy balances for the integration process, Aspen Plus software was used. All process steps except the gasifier model were simulated based on the commercial technologies in Aspen Plus. In the present project, the biomass dryer was simulated in Aspen Plus based on steam dryer from GEA Barr-Rosin technology. As well, the model of heat and power unit was implemented in Aspen Plus based on GE technology. Also, a modified equilibrium model for the biomass gasifier was developed in MATLAB. First of all, an equilibrium thermodynamic model based on the minimization of Gibbs free energy was generated. Then, to identify the non-equilibrium parameters, the syngas compositions from the generated equilibrium model were compared with a large number of experimental data of woody biomass gasification. Subsequently, the methane yield and carbon conversion were specified and estimated as the two non-equilibrium factors. The corresponding atoms of carbon and hydrogen are deducted from the ultimate analysis of biomass input stream and the estimated methane yield is considered as the final methane yield. The predicted syngas compositions and heating value from modified equilibrium model were evaluated by comparison with several existing commercial woody biomass gasification plants.

3.3.2. Integration of biomass gasification process into a reference Kraft mill

A Canadian reference Kraft mill has been created and simulated in CADSIM Plus in our research group based on the typical western Canadian mills were used in this study. Two integration gasification concepts were considered. Figure 3.2 and Figure 3.3 show the two scenarios schematically. The first scenario is a biomass gasification lime kiln process in which the syngas produced from wood residues was applied as an alternative lime kiln fuel. The use of gasified wood residues proposes the revenues of non-fossil fuels replacements in lime kilns. Besides, the use of gasified wood has the potential to significantly reduce greenhouse gas emissions. Depending on natural gas and fuel oil prices, the economics of the first scenario can vary. In this concept, the gasification process was sized so that the total required lime kiln fuel could be supplied from the gasified residues.

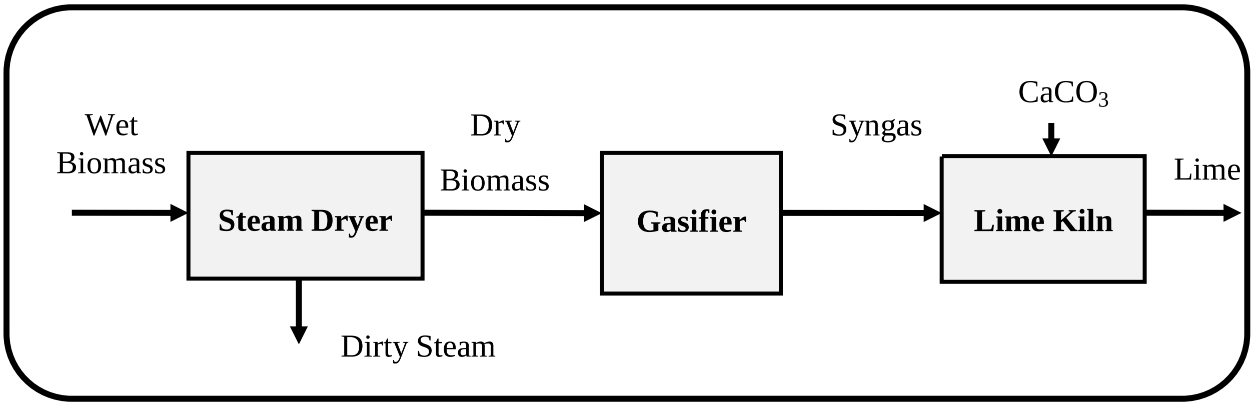

Figure 3.2. Flow diagram for biomass gasification lime kiln process

The second scenario is replacing the bark boiler with an integrated biomass gasification combined cycle. In this scenario, the produced syngas was fired in a gas turbine, and then the gas turbine exhaust was cooled in a heat recovery steam generator (HRSG) to generate steam for the steam turbine. The size of the gasification plant in the second concept was selected to process the same amount of wood residues as the reference Kraft mill bark boiler. The generated steam and electricity were adjusted to the heat and power system of the reference mill.

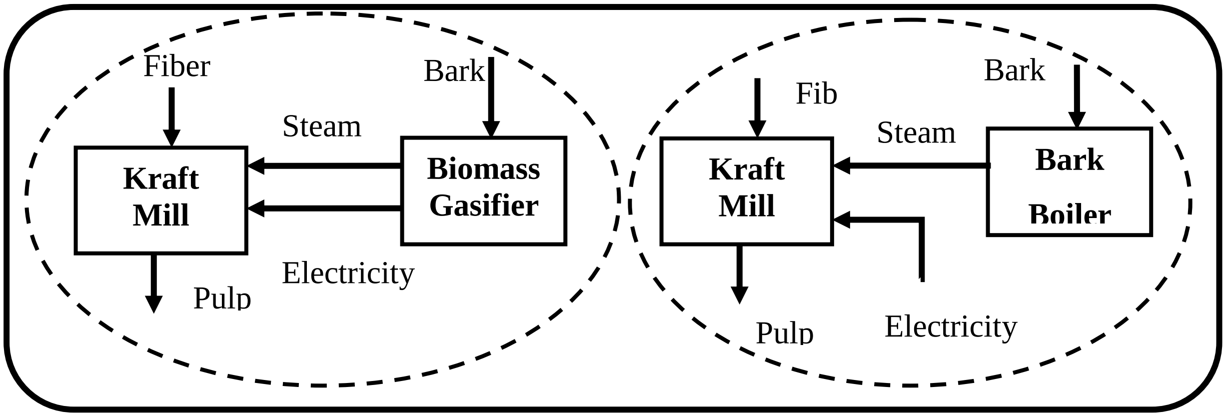

Figure 3.3 Flow diagram for replacing bark boiler with a BIGCC

3.3.3.Technical and economic analysis of integrated biomass gasification process

For both scenarios economic and technical analyses were performed. The capital and operating costs of each of the process steps were calculated based on literature data and experimental data extracted from commercial biomass gasifiers. Moreover, greenhouse gas emissions were estimated by quantifying emissions of CO_2. In the second scenario, the capital cost for a new bark boiler was used to evaluate the replacement of bark boiler with an integrated biomass gasification process.

CHAPTER 4: Model Development

A steady state model of the gasification process was developed in Aspen Plus and MATLAB and linked to a simulated reference Kraft mill in CADSIM Plus for pre-benchmarking and energy system analysis. The biomass dryer was simulated in Aspen Plus based on the biomass steam dryer technology from GEA Barr-Rosin Company. The dry basis ultimate and proximate analysis of biomass was utilized as the gasifier input stream. To develop a modified equilibrium model for biomass gasifier, a semi-empirical pyrolysis model was employed to estimate the methane yield as a pyrolysis gas product. The details of developing the modified equilibrium model and the pyrolysis model are given in the present chapter. Also, syngas cooling and cleaning units were simulated in Aspen Plus. Literature data and operating parameters of commercial technologies were utilized to specify the unit operation parameters and specifications. The proximate and ultimate analyses of mill wood residues were extracted from literature based on the feedstock type which is a combination of Maple and Aspen woods. Modeling of each of the unit operations is discussed below.

4.1. Biomass dryer

The biomass feed stream is considered to be a solid non-conventional stream in Aspen Plus. The ultimate and proximate analyses of the feedstock are used to calculate the General Enthalpy and General Density. Biomass drying is simulated in Aspen Plus based on the GEA Barr-Rosin data (Figure 4.1). REAC-DRY is a RYIELD reactor in Aspen Plus which is used to separate moisture from the wet biomass into the vapor phase. A FORTRAN calculator block is employed to set the moisture content of dry biomass to 10%. After raising temperature of the biomass in steam dryer, water vapor is separated from the dry biomass in the FLSH-DRY. The design parameters of exergy dryer licensed from GEA Barr-Rosin were used to simulate the biomass dryer (Gribik et al., 2007). The dry biomass and steam exit dryer temperature estimated by simulation are respectively 100 °C and 150 °C.

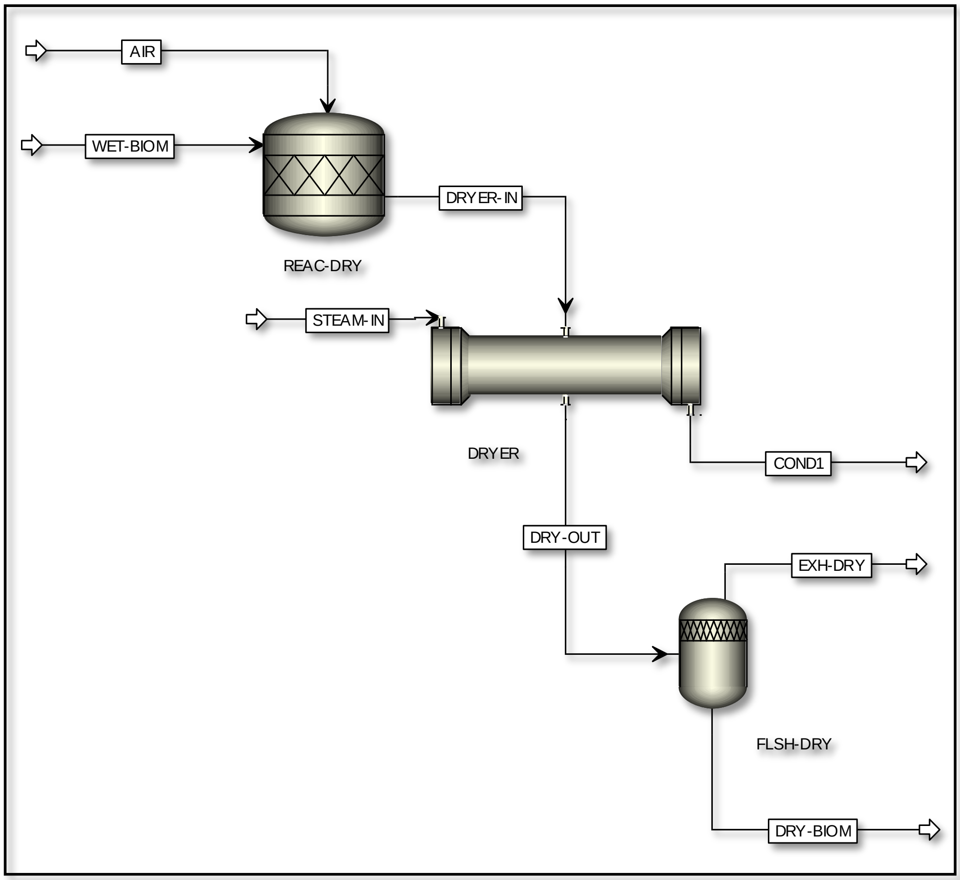

Figure 4.1. Aspen Plus process for biomass dryer

4.2. Biomass gasifier

As the gasifier is the heart of the process, accuracy and reliability of the gasifier model is critical. Modified equilibrium model for the gasification was developed. The equilibrium model gives a reasonable estimation of syngas composition when temperature is high enough and the reactor residence time is greater than the time required for completing gasification reactions. Since this condition does not generally apply for gasifiers, the equilibrium models are not able to predict the syngas composition accurately. Carbon conversion and methane yield are two important parameters that influence the gasification performance. As these two parameters cannot be estimated through equilibrium modeling, they are considered as two non equilibrium factors.

A thermodynamic equilibrium model based on the Gibbs free energy minimization is implemented in MATLAB software. The developed model is validated with available experimental data. A modified thermodynamic equilibrium model of biomass gasification is developed in MATLAB. In order to develop the model, four steps are considered (Figure 4.2):

1. Equilibrium modeling
2. Specifying non-equilibrium parameters
3. Calculation of non-equilibrium parameters
4. Model evaluation

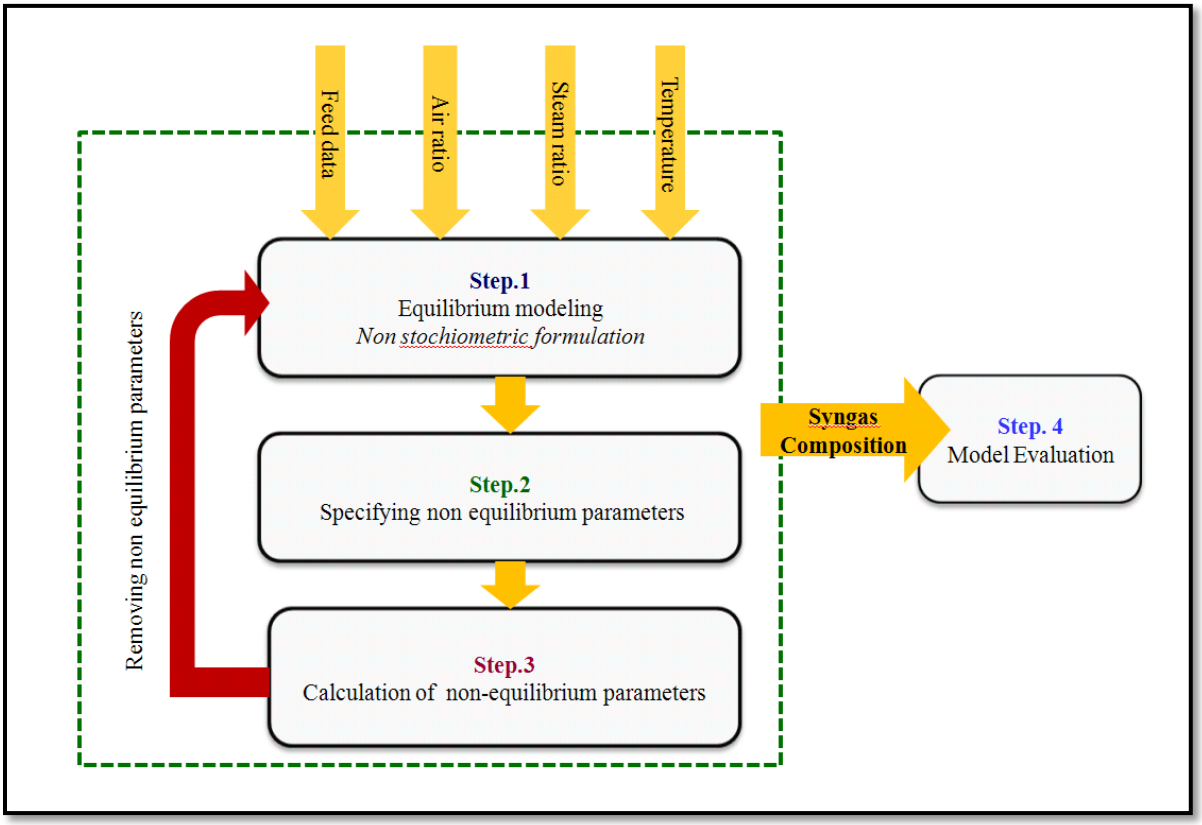

Figure 4.2. Developing steps of the modified equilibrium model

4.2.1. Equilibrium modeling based on the RAND algorithm

Numerous types of models from complex models considering fluid dynamics to simple black box model could be utilized to estimate performance of a biomass gasifier. In fact, selection of the model depends on the objective of modeling. In the present study, the overall estimation of biomass gasification performance is sufficient. Hence, black box modeling is chosen. Equilibrium modeling as a useful tool to evaluate the integration of biomass gasification into Kraft pulp mill from an energy saving and emissions reduction points of view. The non-stochiometric equilibrium approach was selected to develop a basic simple thermodynamic equilibrium model. In stochiometric modeling, a clearly well defined set of reactions is required. Although, non-stochiometric modelling requires only biomass feed composition it is an appropriate method for unknown reaction mechanisms and biomass feed streams where chemical compositions are not well defined (Li et al., 2004).

In the subsequent section, the equilibrium composition in the gasifier is predicted at constant temperature and pressure through thermodynamic calculation. The non-stochiometric approach based on the minimization of free Gibbs energy using RAND algorithm is selected for implementing a simple equilibrium model. The non-stochiometric approach is more flexible for the unknown reaction mechanism processes such as biomass gasification. The RAND algorithm formulated by (White et al., 1958) is a minimization method. At each iteration the element-abundance constraints is satisfied and the Gibbs free energy is minimized. The detail of RAND algorithm is illustrated as follows (Smith and Missen, 1982): The common approach for solving this simple constrained optimization problem is to use the method of Lagrange multipliers to remove the constraints (White et al., 1958):

$$\text{£}(\mathrm{n},\lambda) = \sum_{\mathrm{i}=1}^{\mathrm{N}} \mathrm{n_i}\mu_\mathrm{i} + \sum_{\mathrm{k}=1}^{\mathrm{M}} \lambda_\mathrm{k} \left(\mathrm{b_k} - \sum_{\mathrm{i}=1}^{\mathrm{N}} \mathrm{a_{ki}} \mathrm{n_i}\right) \tag{34}$$

$$\left(\frac{\partial \text{£}}{\partial n_i}\right)_{n_{j\neq i},\lambda} = \mu_i - \sum_{k=1}^{M} a_{ki}\lambda_k = 0 \tag{35}$$

$$\left(\frac{\partial \text{£}}{\partial \lambda_k}\right)_{\lambda_{j\neq k},n} = b_k - \sum_{i=1}^{N} a_{ki} n_i \tag{36}$$

Where λ is a vector of M unknown Lagrange multipliers. For an ideal solution, the chemical potential can be expressed as:

$$\mu_i = \mu_i^* + RT ln \frac{n_i}{n_t} \tag{37}$$

So, the Equation (34) can be written as:

$$\frac{\mu_i^*}{RT} + \ln n_i - lnn_t - \sum_{k=1}^{M} \varphi_k a_{ki} = 0 \tag{38}$$

$$\varphi_k = \frac{\lambda_k}{RT} \tag{39}$$

Where

$$n_t = \sum_{i=1}^{N'} n_i + n_z \tag{40}$$

The element abundance constraint is:

$$\sum_{i=1}^{N'} a_{ki} n_i - b_k = 0; \qquad k = 1,2,\ldots,M \tag{41}$$

By linearization of Equation (38) about an arbitrary estimation (n^m, φ^m), we have:

$$\frac{-1}{RT}\sum_{j=1}^{N'} \left(\frac{\partial \mu_i}{\partial n_j}\right)_{n^{(m)}} \delta n_j^{(m)} + \sum_{k=1}^{M} a_{ki} \delta\varphi_k^{(m)} = \frac{\mu_i^{(m)}}{RT} - \sum_{k=1}^{M} a_{ki} {\varphi_k}^{(m)} \tag{42}$$

Where

$$\delta\varphi_k^{(m)} = \varphi_k - {\varphi_k}^{(m)} \tag{43}$$

$$\delta n_j^{(m)} = n_j - {n_j}^{(m)} \tag{44}$$

Element abundance constraints are expressed as:

$$\sum_{j=1}^{N'} a_{ki}\, \delta n_j^{(m)} = b_k - b_k^{(m)} \tag{45}$$

$$b_k^{(m)} = \sum_{j=1}^{N'} a_{ki} n_j^{(m)} \tag{46}$$

Equations (42) and (45) constitute a set of (N'+M) linear equations in the unknowns $\delta n^{(m)}$ and $\delta \varphi^{(m)}$. These equations are solved and then new values of n and φ are estimated from:

$$\varphi^{(m+1)} = \varphi^{m} + \omega^{(m)} \delta\varphi^{(m)} \tag{47}$$

$$n^{(m+1)} = n^{m} + \omega^{(m)} \delta n^{(m)} \tag{48}$$

ω is a step-size parameter. The iterations are repeated until the convergence is achieved. For ideal solution, the number of linear equations number that should be solved will be reduced from (N'+M) to (M+1). The chemical potential for ideal solution can be written as

$$\mu_i = \mu_i^*(T,P) + RTln\frac{n_i}{n_t} \tag{49}$$

So we have

$$\frac{1}{RT}\left(\frac{\partial \mu_i}{\partial n_j}\right) = \frac{\delta_{ij}}{n_j} - \frac{1}{n_t} \tag{50}$$

Where δ_{ij} is the Kronecker delta. By substitution of Equation (40) in (35), $\delta n^{(m)}$ to be obtained in terms of φ:

$$\delta n_j^{(m)} = n_j^{(m)}\left(\sum_{k=1}^{M} a_{ki}\varphi_k + u - \frac{\mu_j}{RT}^{(m)}\right) \tag{51}$$

Where the additional variable u is defined by

$$u = \frac{\sum_{j=1}^{N'} \delta n_j^{(m)}}{n_t^{(m)}} \equiv \frac{\delta n_t^{(m)}}{n_t^{(m)}} \tag{52}$$

Substitution of Equation (51) in (35) yields the M linear equations:

Substitution of Equation (51) in (35) yields the M linear equations:

$$\sum_{i=1}^{M}\left(\sum_{k=1}^{N'} a_{ik}a_{jk}\, n_k^{(m)}\right)\varphi_i + b_j^{(m)}u = \sum_{k=1}^{N'} a_{jk}\, n_k^{(m)}\, \frac{\mu_k}{RT}^{(m)} + b_j - b_j^{(m)} \qquad (53)$$

A further equation is obtained by using Equations (52) and (51) to give:

$$\sum_{i=1}^{M} b_j^{(m)}\varphi_i - n_z u = \sum_{k=1}^{N'} n_k^{(m)}\, \frac{\mu_k^{(m)}}{RT} \qquad (54)$$

At each iteration of RAND algorithm, a set of *(M+1)* linear Equations (54) and (53) are solved using Equation (51) to calculate $\delta n^{(m)}$are solved. The RAND algorithm is easily extendable for multiphase systems. Equation (54) is written as:

$$\sum_{i=1}^{M} b_{j\alpha}^{(m)}\varphi_i - n_{z\alpha}u_\alpha = \sum_{k=1}^{N'} n_{k\alpha}^{(m)}\, \frac{\mu_{k\alpha}^{(m)}}{RT} \quad \alpha = 1,2,\ldots,\pi \qquad (55)$$

Where α refers to a phase. So, the algorithm consists of iteratively solving the set of *(M+* π*)* linear equations while:

$$\max\left|\frac{\delta n_i^{(m)}}{n_i^{(m)}}\right| < 0.5 \times 10^{-5} \qquad (56)$$

The Newthon-Raphson method is employed to linearize the ln(n) terms.

4.2.2. Specification of non equilibrium factors

The equilibrium calculations of gasification model were performed for a number of biomass gasification experimental tests. The predictions of syngas composition from the equilibrium model are compared to the three series of empirical results for a wide range of operating conditions ((Campoy et al., 2009), (Lv et al., 2003), (Narvaez et al., 1996)). The experimental data include high temperature air and steam biomass gasification processes in which atmospheric fluidized bed gasifiers are utilized. The biomass type and gasifier conditions for the experimental tests are reported in Table 4.1.

Table 4.1. The experimental set-up characteristics

Reference	Biomass type	Biomass type	Gasification agent	Temperature, °C
(Campoy et al., 009)	Wood pellets	BFBG	Air+Steam+Oxygen	755-840
(Lv et al., 2003)	Pine sawdust	FBG	Air+Steam	700-900
(Narvaez et al., 1996)	Pine sawdust	BFBG	Air	700-580

The predicted mole composition of major gas species including CO, CO_2, H_2, and CH_4 were compared with the above experimental data in Figures 4.3-4.7. As Shown in Figure 4. 3 to 4-5, the equilibrium model gives a reasonable prediction of CO, H_2, and CO_2 composition. On the other hand, Figure 4.6 shows that the equilibrium methane composition is considerably underestimated in comparison with the experimental data. The equilibrium methane concentration is less than 1%; although, the empirical methane content is between 2-12 mole percent. The deviation can be explained by the fact that methane which is initially produced in biomass devolatilization process does not reform in the gasification step.

Furthermore, equilibrium modeling is not capable of estimating the carbon conversion. As illustrated in Figure 4.7, the empirical carbon conversion values are below the equilibrium predictions. Carbon conversion is considered here to be the amount of carbon converted into gas. Consequently, the deviation between equilibrium and actual data is considered with two non-equilibrium factors: methnae yield and carbon conversion. In fact, it is expected by removing the amounts of unconverted carbon and methane from input stream of the equilibrium model and considering them directly as final gasification products, the equilibrium model would be significantly improved.

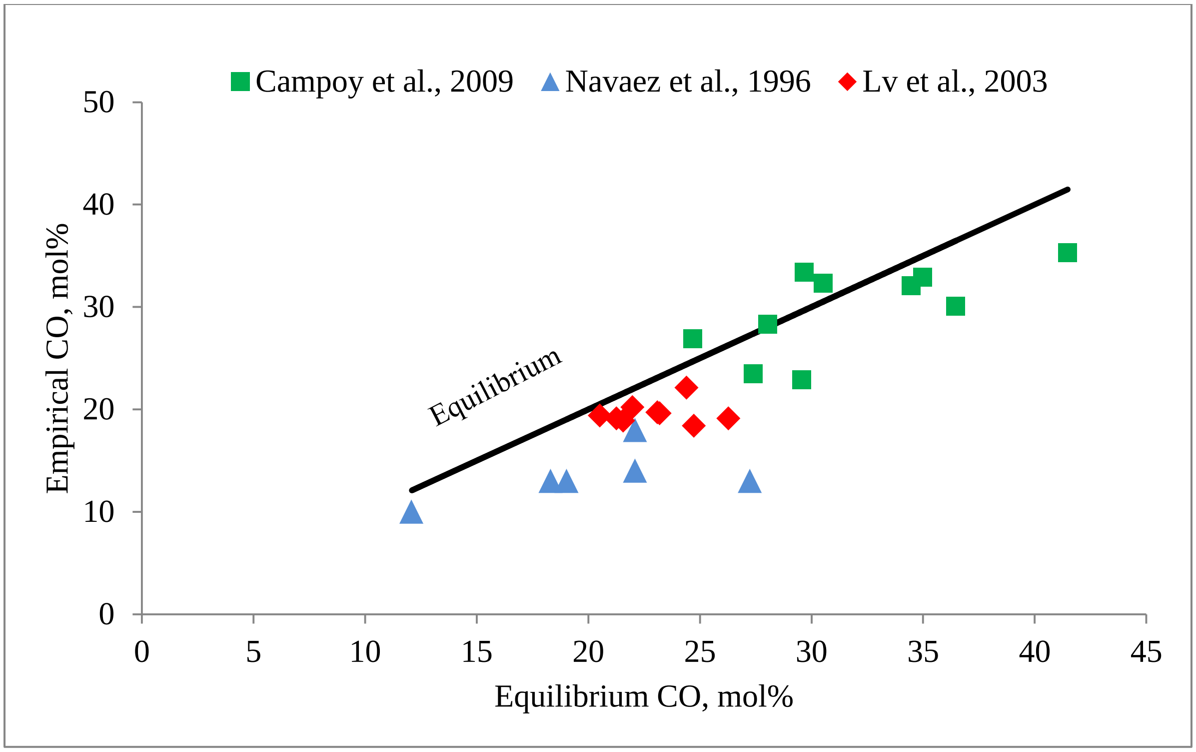

Figure 4.3. Comparison of equilibrium CO with the experimental data

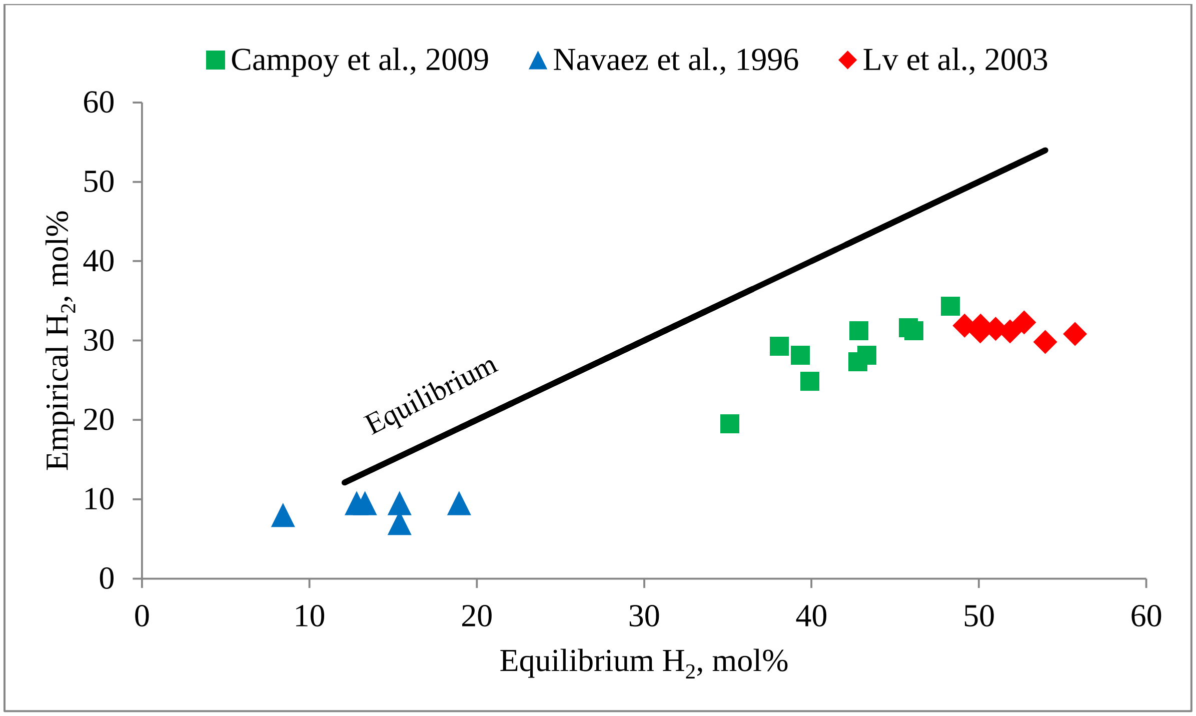

Figure 4.4. Comparison of equilibrium H_2 with the experimental data

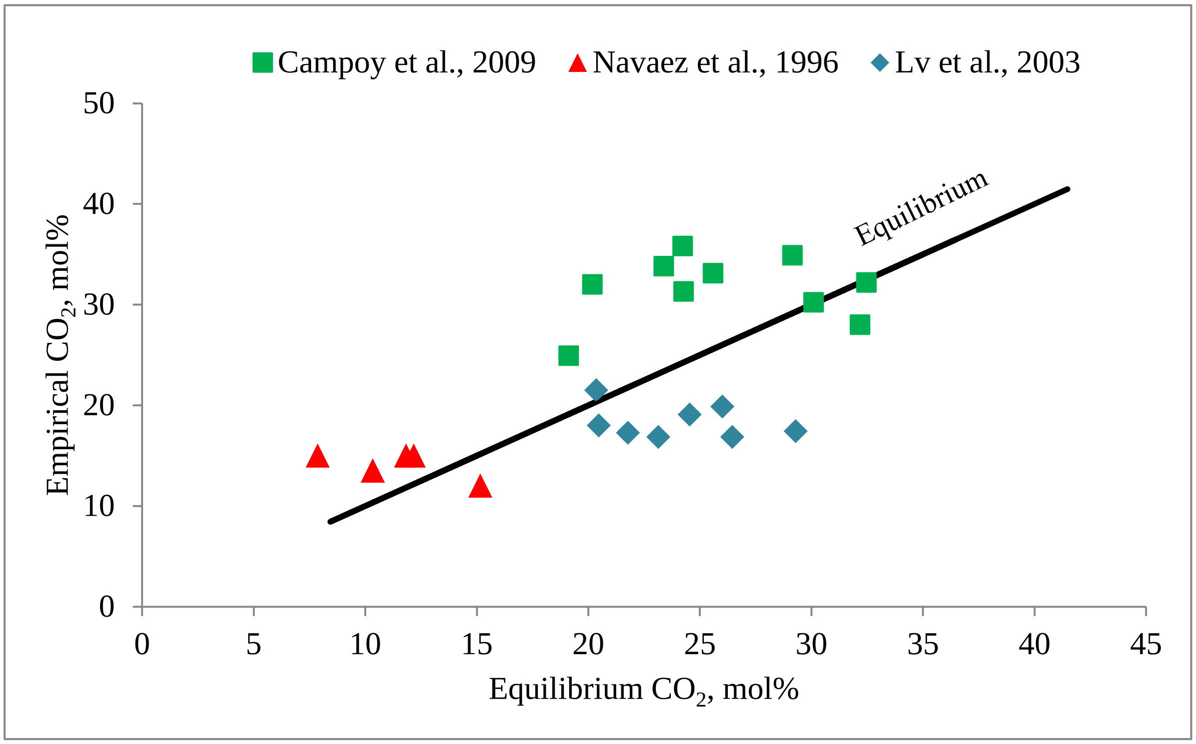

Figure 4.5. Comparison of equilibrium CO_2 with the experimental data

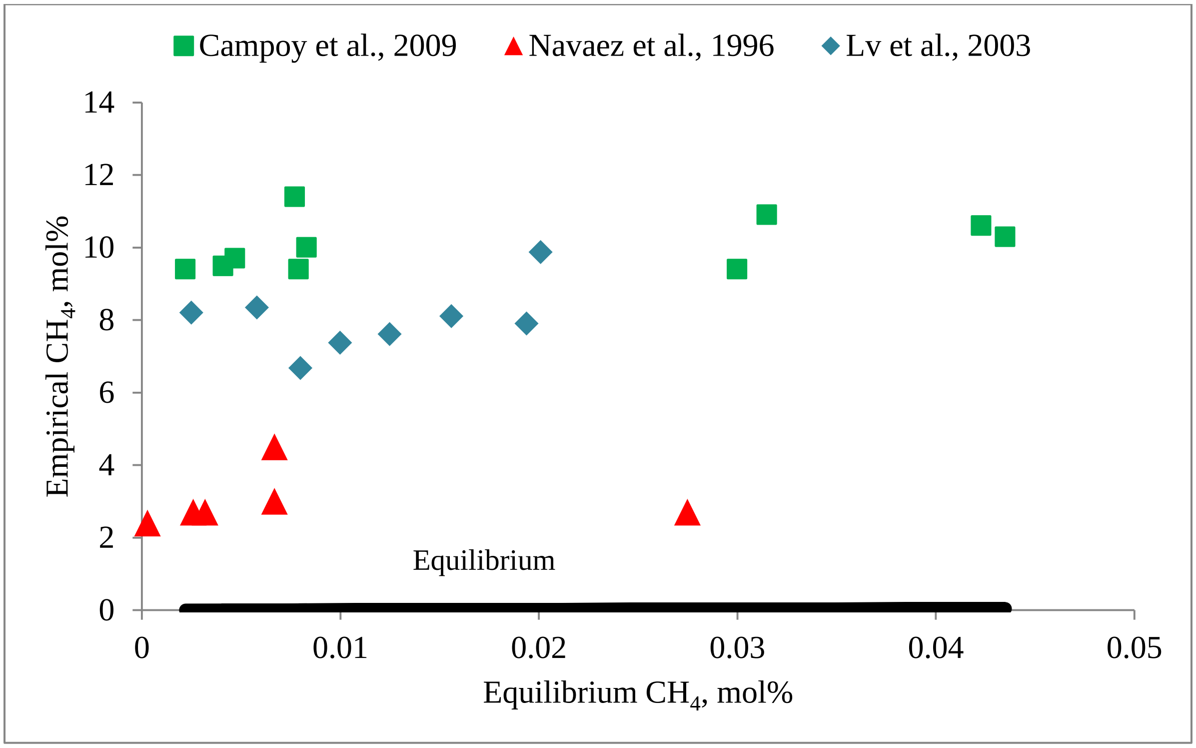

Figure 4.6. Comparison of equilibrium CH_4 with the experimental data

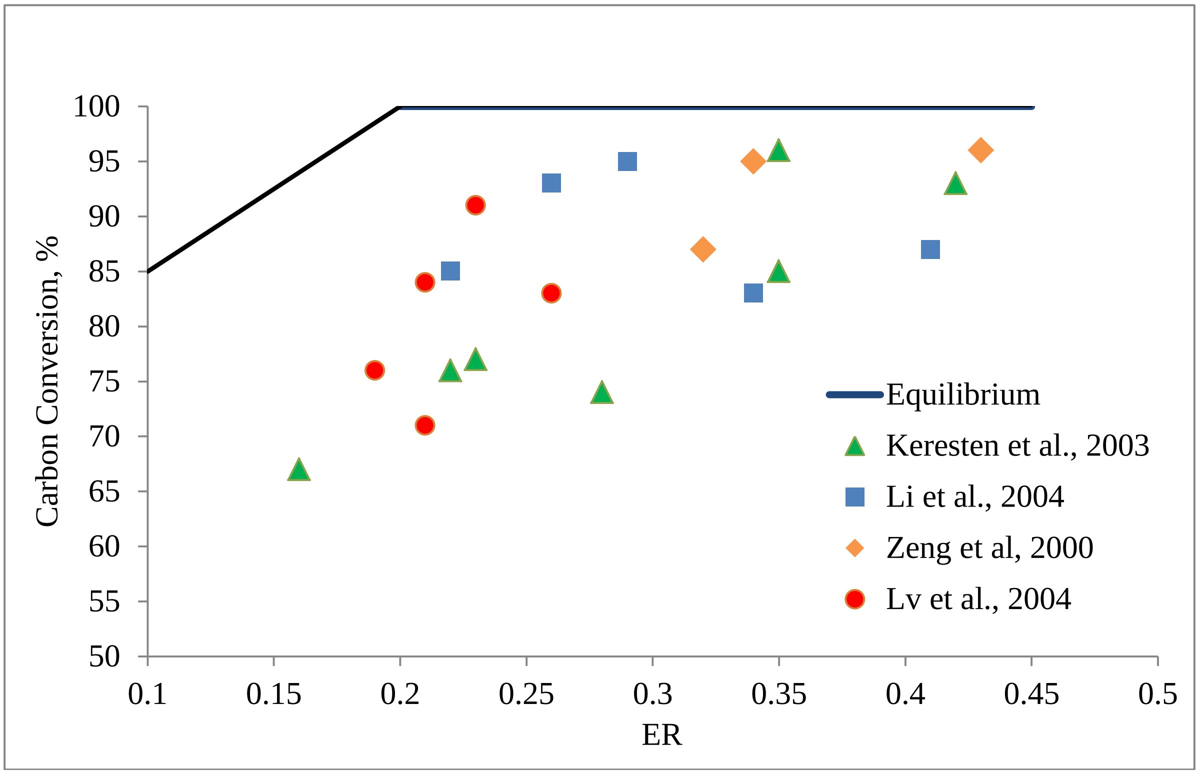

Figure 4.7. Carbon conversions over equivalence ratio for the experimental gasification data ((Kersten et al., 2003), (Li et al., 2004), (Zeng and van Heiningen, 2000), (Lv et al., 2004))

4.2.3. Methane yield calculation

The methane is considered to be originally formed in the biomass devolatilization process. The methane conversion is low because methane reforming requires the presence of a proper catalyst. Hence, the predicted methane yield from pyrolysis should estimate the final methane composition in the produced syngas. (Jand et al., 2006) confirmed that maximum yield obtained from steady state gasification tests is in acceptable agreement with the amount of methane released in wood devolatilization at high temperature. A semi-empirical pyrolysis model is applied to estimate the methane yield produced in the biomass pyrolysis step as demonstrated in the following section.

In order to calculate the amount of methane produced in pyrolysis step and to verify the carbon conversion to gaseous species, a flexible pyrolysis model that predicts volatile product composition is essential. Several models have been developed to estimate the volatile yields, but a general model of the composition of the volatile gases is still missing. In the present approach, a simplified model consisting of a mass balance complemented by two empirical ratios is used. To model the pyrolysis process, the volatile gases were assumed to consist of CO_2, CO, H_2O, H_2, and CH_4. The mass balances of the three elemental species, C, H, and O are expressed as:

$$Y_{gas}X_C(1-y_{ash}) = M_C(\frac{\gamma_{CO}}{M_{CO}} + \frac{\gamma_{CO2}}{M_{CO2}} + \frac{\gamma_{CH4}}{M_{CH4}}) \tag{57}$$

$$Y_{gas}X_{H_2}(1-y_{ash}) = M_{H_2}(\frac{\gamma_{H2}}{M_{H2}} + \frac{\gamma_{H2O}}{M_{H2O}} + 2\frac{\gamma_{CH4}}{M_{CH4}}) \tag{58}$$

$$Y_{gas}X_{O_2}(1-y_{ash}) = M_{O_2}(0.5\frac{\gamma_{H2O}}{M_{H2O}} + 0.5\frac{\gamma_{CO}}{M_{CO}} + \frac{\gamma_{CO2}}{M_{CO2}}) \tag{59}$$

$$\gamma_{CO} + \gamma_{CO_2} + \gamma_{CH4} + \gamma_{H_2O} + \gamma_{H_2} = 1 \tag{60}$$

Where γ is the mass fraction of gas species in the volatile gases and Y_{gas} is gas yield of pyrolysis product. There are six unknowns in the model. So, two more equations are required to estimate the gases species yield. Approximate relationships among the ratios of the gas products such as CO, CH_4, and CO_2, can be used for the modeling. Two empirical correlations expressed as the ratios of three gas components based on the data from literature are fitted. The approach for selecting the proper empirical ratios is explained as follows:

(Hajaligol et al., 1982) showed that the rate of production of each gaseous pyrolysis product, i, was described by the rate equation:

$$\frac{dV_i}{dt} = K_{o,i}e^{-\frac{E_i}{RT}}(V_{i^*} - V_i) \tag{61}$$

V_i : yield of product i at time t

V_{i^*}: ultimate yield of i at high temperature and long times

For two products 1 and 2, the integrated above equation is

$$\frac{\left[ln\frac{V_{1^*}}{V_{1^*} - V_1}\right]}{[ln\frac{V_{2^*}}{V_{2^*} - V_2}]} = \frac{K_{o,1}e^{-\frac{E_1}{RT}}t}{K_{o,2}e^{-\frac{E_2}{RT}}t} \tag{62}$$

If the yields of both species taken at the same temperature and reaction time and the activation energies are similar, Equation (62) represents only a weak function of temperature, and a logarithmic plot of the yield of one product versus the yield of the other product will give an approximately linear correlation for all times and temperatures. The activation energy of the gaseous component is shown in Table 4.2.

Table 4.2. Activation energy of volatilization gaseous products

	H_2	CH_4	CO	CO_2
Ei, KJ/mol, Beech wood, (Radmanesh et al., 2006)	93	45	50	34
Ei, KJ/mol, Saw dust, (Radmanesh et al., 2006)	110	51	41	55
Ei, KJ/mol, Sawdust, (Nunn et al., 1985)	-	69.45	61.09	59.83

In the case of CO and CH_4, the reported values of E reported are similar. Also, CO and CO_2 have comparable activation energies. So, the logarithms of ratios of yields of CO/CO_2 and CH_4/CO_2 show a reasonably linear relationship over temperature (Figure 4.8 and Figure 4.9).

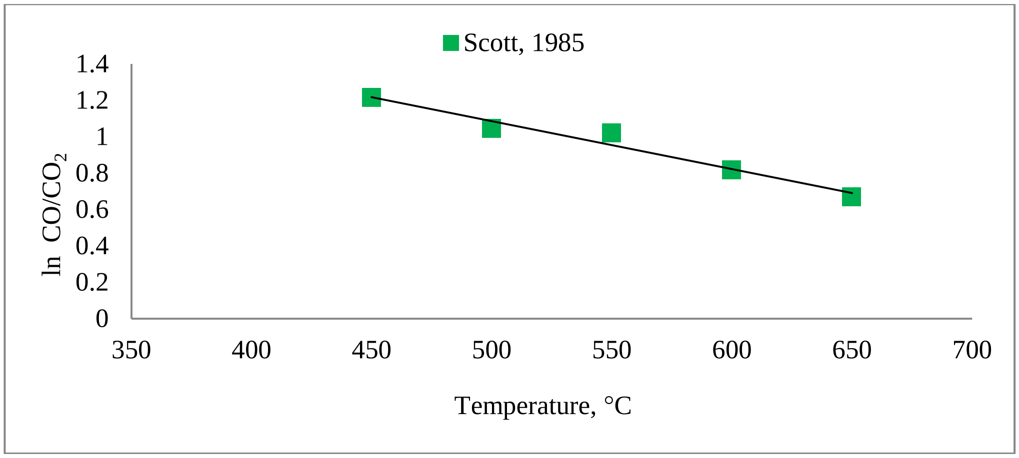

Figure 4.8. Logarithmic ratio of CO/CO_2 over temperature

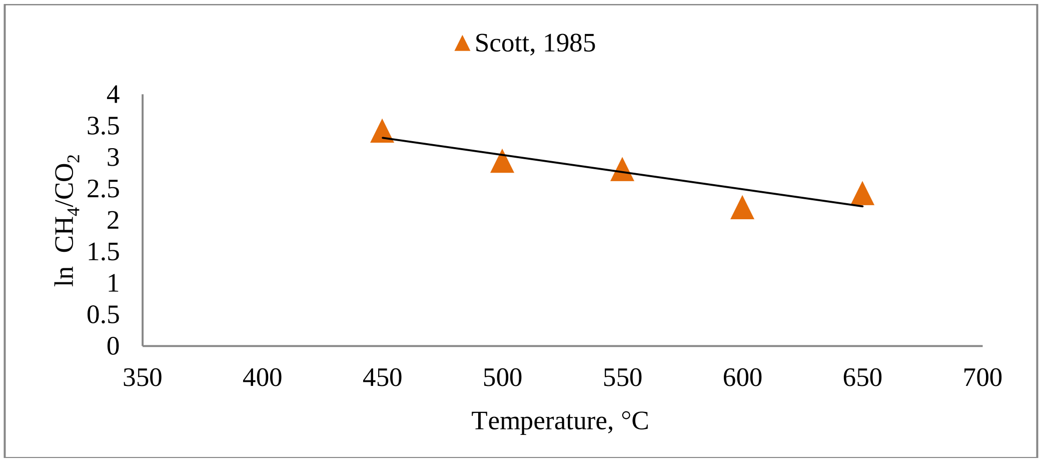

Figure 4.9. Logarithmic ratio of CH_4 /CO_2 over temperature

In order to estimate these pyrolysis product ratios, two models which express product ratios as a function of temperature based on the experimental pyrolysis data(Table 3) presented in the literature are fitted.

Table 3. Experimental data of pyrolysis gas yields

Reference	***Biomass type***	***Temperature (°C)***	***CO (mol%)***	***CO_2, (mol%)***	***H_2 (mol%)***	***CH_4 (mol%)***
(Radmanesh et al., 2006)	Beachwood	800	22.96	71.26	1.82	3.96
(Radmanesh et al., 2006)	Sawdust	800	18.74	74.97	1.50	4.80
(Grieco and Baldi, 2011)	Beachwood	877	35.5	38.2	9.3	15.4
(Grieco and Baldi, 2011)	Pine	877	37.6	36.1	8.8	15.5
(Grieco and Baldi, 2011)	Wood brich	900	48.04	34.32	1.09	16.55
(Gonzalez et al., 2005)	Almond shell	300	40.14	57.09	1.04	1.73
(Gonzalez et al., 2005)	Almond shell	400	36.87	52.70	2.12	8.30
(Gonzalez et al., 2005)	Almond shell	500	41.56	37.44	6.56	14.44
(Gonzalez et al., 2005)	Almond shell	600	37.21	32.77	12.43	17.60
(Gonzalez et al., 2005)	Almond shell	700	38.75	24.06	18.87	18.31
(Gonzalez et al., 2005)	Almond shell	800	34.54	18.87	27.82	18.77

Two models which express logarithms of $\frac{y_{CO}}{y_{CO_2}}$ and $\frac{y_{CH_4}}{y_{CO_2}}$ as functions of temperature logarithms are fitted using the experimental data (equations (63) and (64)). The evaluations of the fitted models are depicted in Figure 4.10 and Figure 4.11.

$$\ln\left(\frac{y_{CO}}{y_{CO_2}}\right) = lna + bln(T) \tag{63}$$

$$b = 3.72\ (2.79, 4.65)$$

$$lnc = -18.30\ (-24.37, -12.22)$$

$$SSE = 1.92$$

$$R - squared = 0.88$$

$$\ln\left(\frac{y_{CH_4}}{y_{CO_2}}\right) = lnc + dln(T) \tag{64}$$

$$d = 4.49\ (3.55, 5.42)$$

$$lnc = -25.44\ (-31.66, -19.21)$$

$$SSE = 0.15$$

$$R - squared = 0.95$$

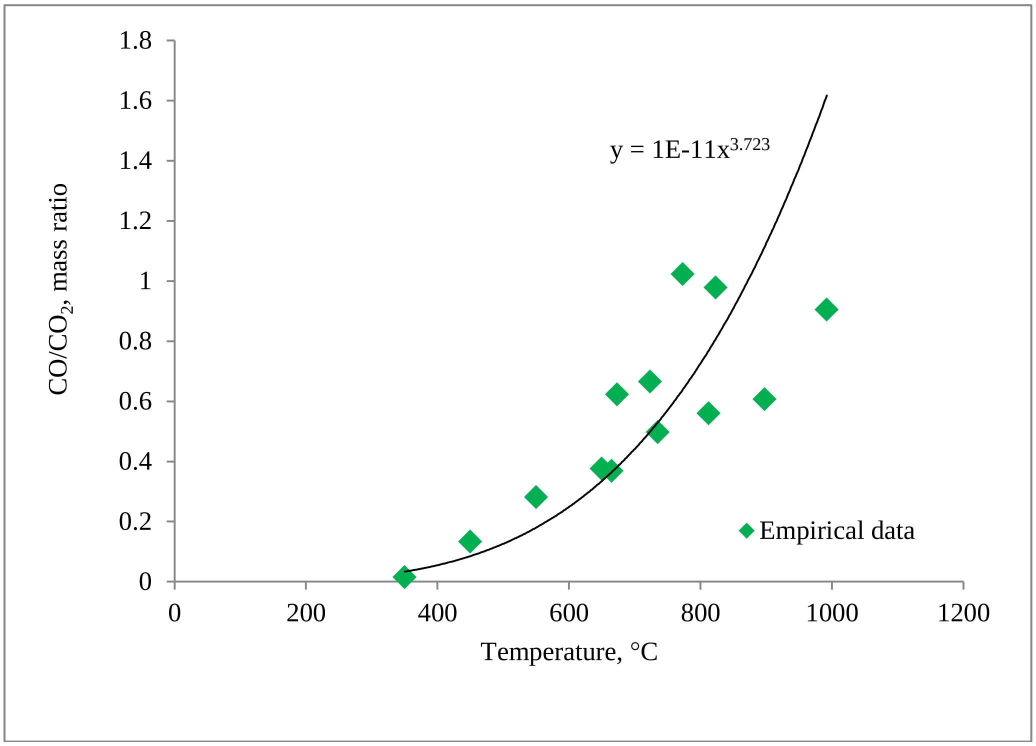

Figure 4.10. Evaluation of estimated y_{CO}/y_{CO2} *with empirical data*

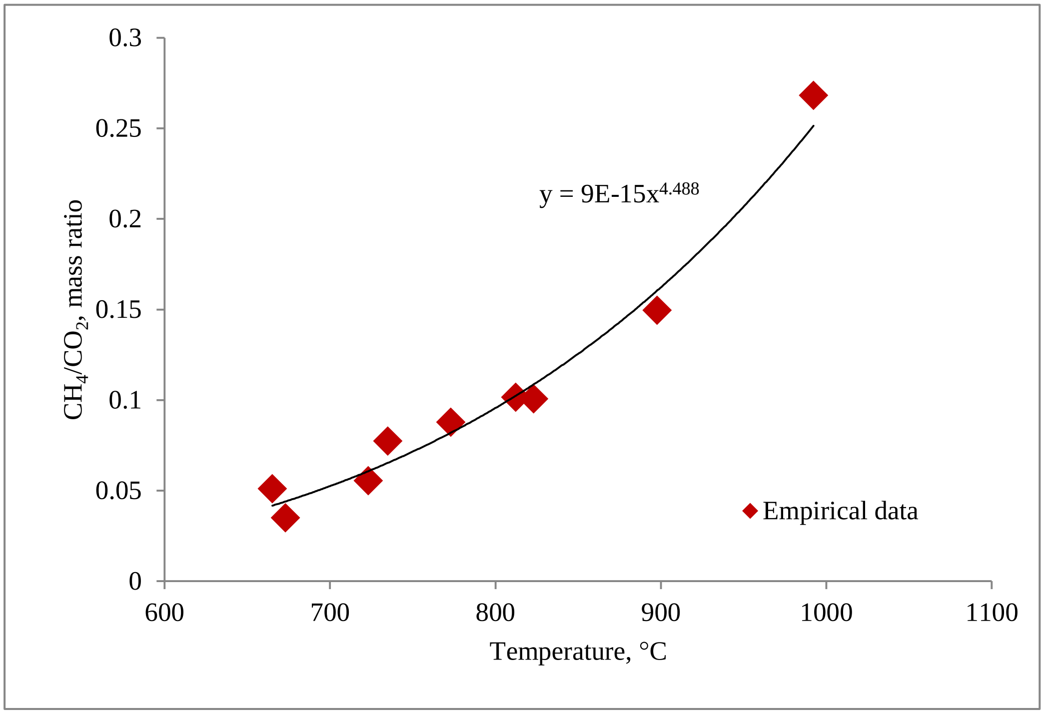

Figure 4.11. Evaluation of estimated y_{CH4}/y_{CO2} *with empirical data*

Subsequently, the two estimated pyrolysis product ratios together with equations (57) to (60) were solved in the MATLAB file to estimate pyrolysis gas products yields. The comparison of the estimated yields with a series of experimental data (Sun et al., 2010) is shown in Figure 4.12 to Figure 4.15. As illustrated in the Figures, the semi-empirical pyrolysis model has the good enough accuracy (less than 10% error) for estimation of pyrolysis gas products.

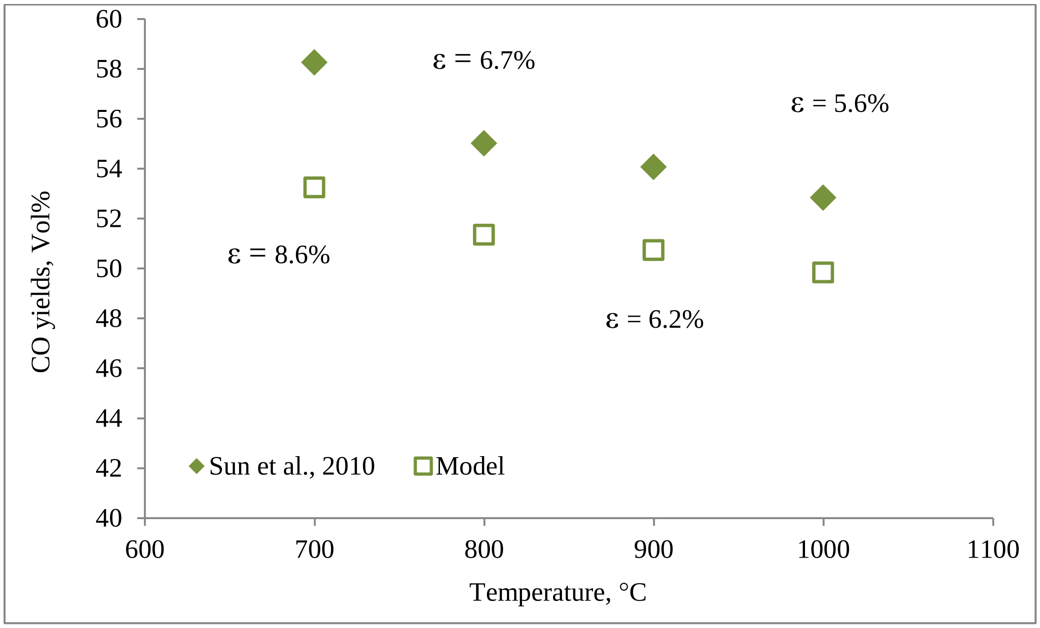

Figure 4.12. Comparison of the predicted CO yield with (Sun et al., 2010) data

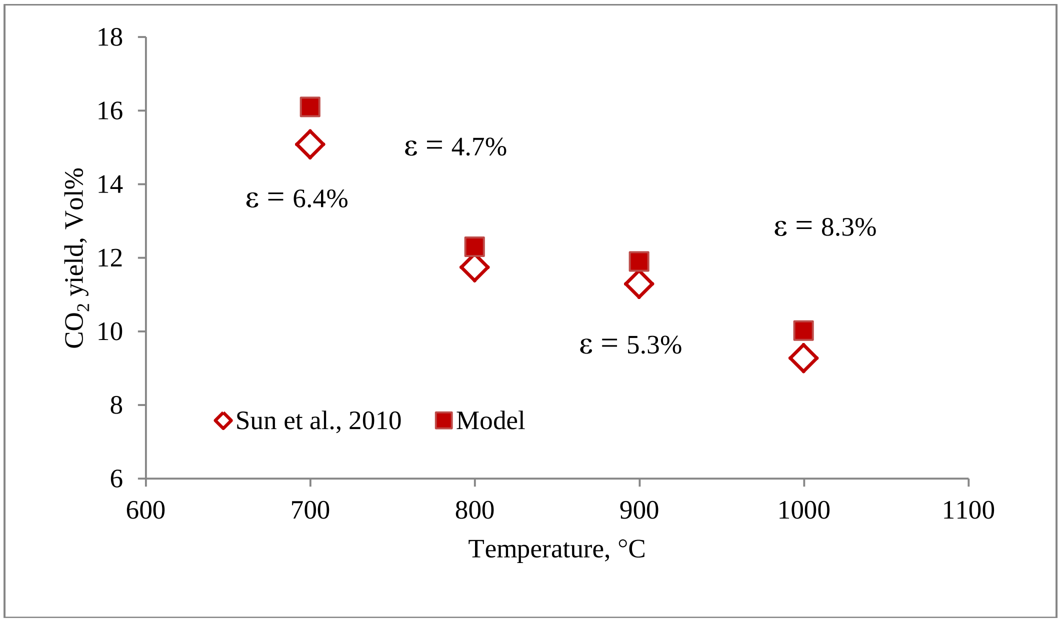

Figure 4.13. Comparison of the predicted CO_2 yield with (Sun et al., 2010) data

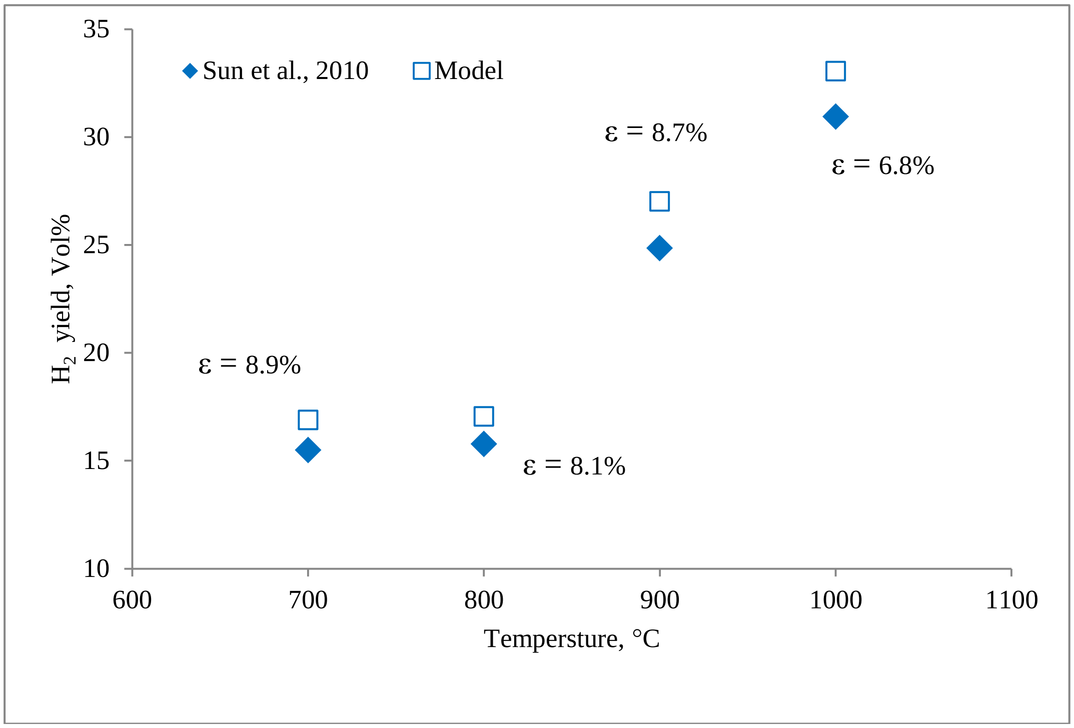

Figure 4.14. Comparison of the predicted H_2 yield with (Sun et al., 2010) data

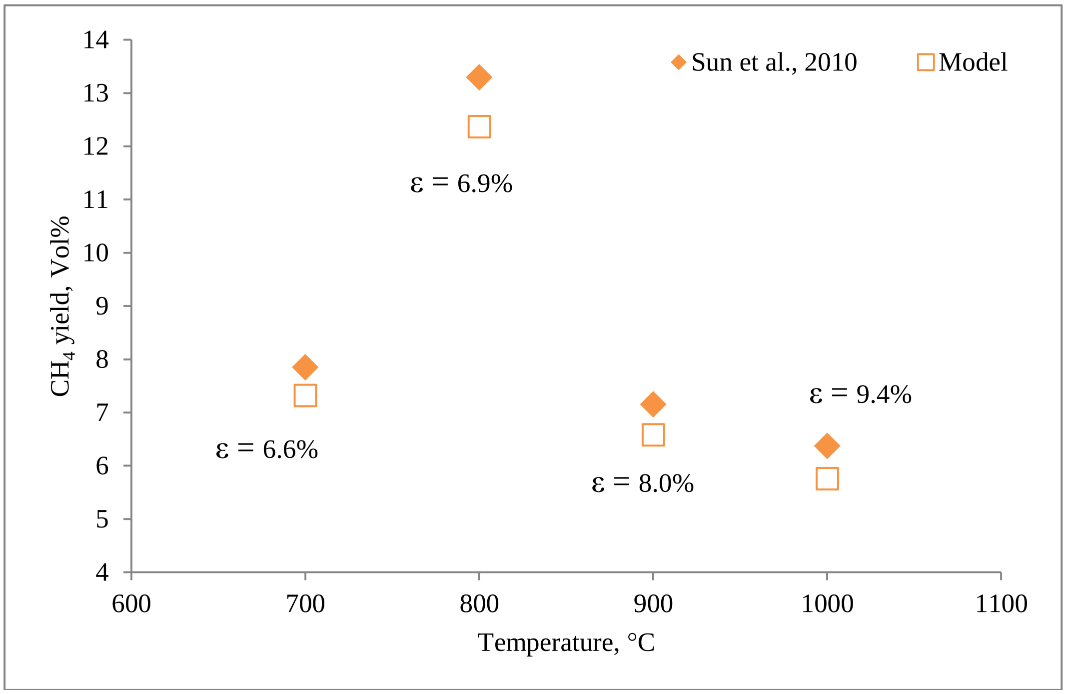

Figure 4.15. Comparison of the predicted CH_4 yield with (Sun et al., 2010) data

4.2.4. Gasifier model evaluation

After estimation of methane yield from the pyrolysis model, the corresponding atoms of hydrogen and carbon were deducted from the gasifier input stream. To estimate syngas composition, thermodynamic calculation was performed at constant temperature and pressure. Non-stochiometric formulation is selected because it does not require knowledge of an independent set of chemical reactions. The criterion of equilibrium is minimization of Gibbs free energy that is subject to elemental balance constraints. The evaluation of the modified equilibrium model with an experimental sawdust air gasification data for gasification temperature of 900 °C (Jand et al., 2006) is shown in Figure 4.17.

As pointed out in Chapter 2, several modified equilibrium models have been tried to improve the predictability of the gas yields in biomass gasification process. The problem, still, is that those equilibrium models are applicable for the specific gasification conditions. For instance, (Li et al., 2004) and (Jand et al., 2006) approaches which are close to the present study, the carbon conversion and methane yield as the two modification factors are estimated for particular gasification conditions. In (Li et al., 2004) paper, the fraction of carbon and hydrogen converted into methane is given as a function of ER:

$$\beta_{C\ to\ CH_4} = 0.11(1 - ER) \tag{65}$$

As can be observed simply from above function, this fraction is only depends on the equivalence ratio. Thus, it is obvious that for a specific value of ER, the amount of carbon converted to methane is a fixed value. But, experimental data provided evidence that the carbon conversion varies due to changes in other operating parameters such as temperature (Figure 4.16). The estimated unconverted carbon which is an inverse function of ER is in disagreement with empirical data (Jand et al., 2006).

Although the predictive capability of the modified equilibrium gasification model proposed by (Jand et al., 2006) is more accurate in comparison with (Li et al., 2004) model, the suggested empirical modification parameters are fixed factors which are not sensitive to operating conditions. For example, the amount of moles of methane generated from devolatilization step is fixed at 5.5 mol/kg for the specific operating conditions of the experimental test. As a result, the (Jand et al., 2006) approach in not applicable as an inclusive method to modify equilibrium modeling for other gasification conditions.

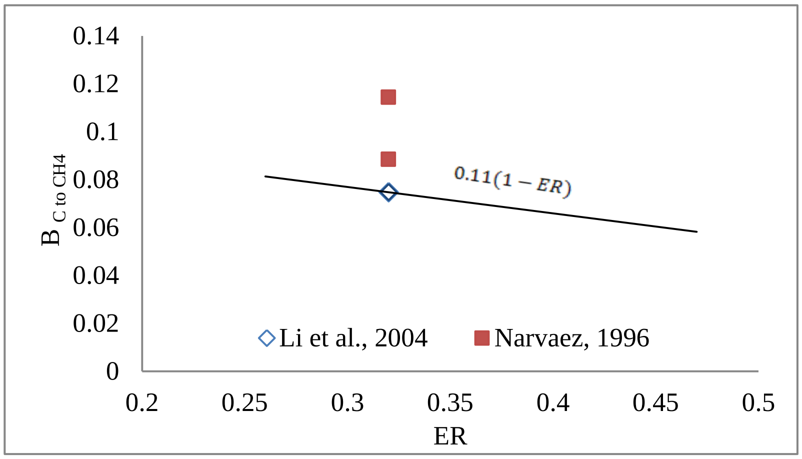

Figure 4.16. Evaluation the estimation of $\beta_{C\ to\ CH_4}$

Using the comprehensive pyrolysis model is a suitable technique to improve the prediction of methane yield in the gasification model for various gasifier types with different operating conditions. Figure 4.17 shows the performance of the modified model in comparison with the model proposed by (Li et al., 2004) and (Jand et al., 2006) for predicting the syngas composition generated from 500 kWth circulating fluidized-bed gasification facility (van der Drift et al., 2001). The gasifier is an atmospheric air-blown unit, called BIVKIN located at the Netherlands Energy Research Foundation. The authors give details of gasification data for 10 biomass types. The ultimate and approximate analysis of biomass used here is for the park wood. The gasification temperature and equivalence ratio respectively are 861 °C and 0.38. Figure 4.17 shows a considerable improvement of the estimated syngas composition from the modified model with those from the equilibrium model. In addition, noticeable improvement in the predictive capability of the model compared to the results achieved from the (Li et al., 2004) and (Jand et al., 2006) can be observed.

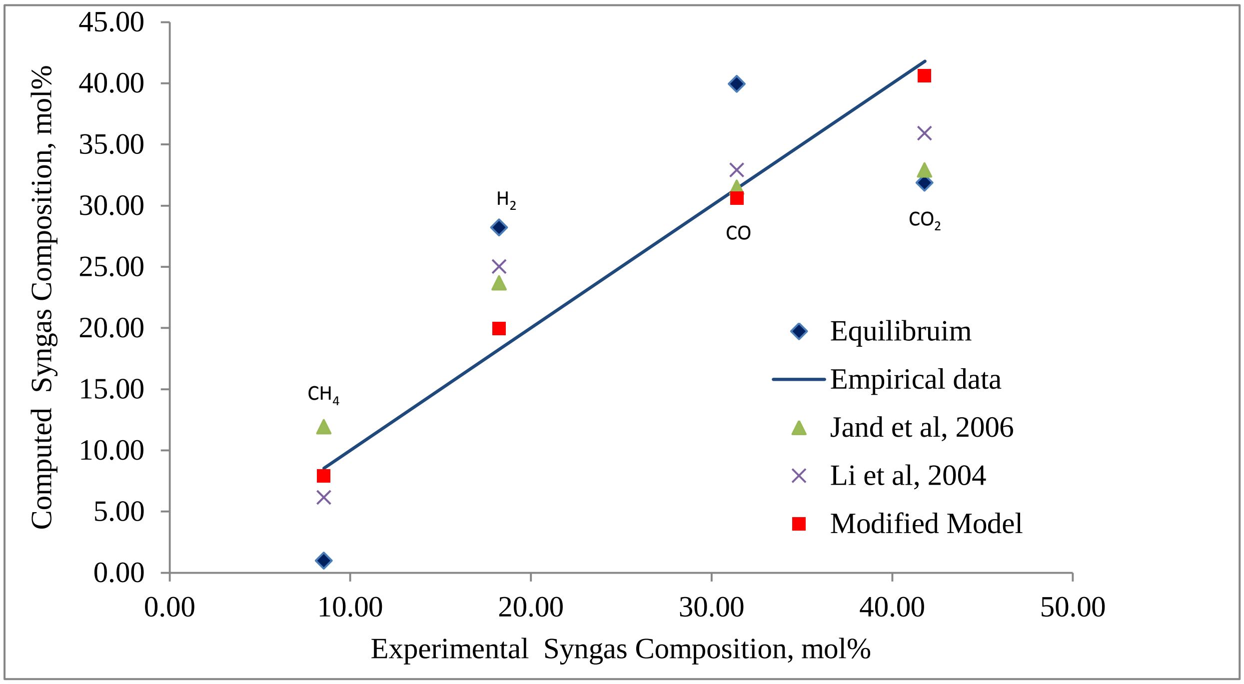

Figure 4.17. Model evaluation for a typical gasification test with the CFB gasifier at 861° C

4.3. Syngas cooling and cleaning

CO and H_2 are the major components of the produced syngas. H_2S and CO_2 are referred to acid gases. As H_2S and COS create acidic solution which is corrosive and since CO_2 is an important source of greenhouse gas emissions, the removal of these gasses is crucial. The necessary quality of syngas for different applications is shown in Table 4.4.

Table 4.4. Essential quality of syngas for different applications, (Gills, 2008)

Application	Power	Hydrogen	Chemical (F-T, DME, …)
Sulfur (wppm)	10–15	<1	0.01–1
CO_2 (vol %)	–	<0.1	0.05–2.0

In biomass gasification plant presented in literature when the syngas is used for heat and power generation purposes generally low temperature acid gas removal technology is not employed. In this part, SELEXOL system for CO_2 and H_2S capturing was simulated in Aspen plus. As mentioned in chapter 2, MDEA, Rectisol, and SELEXOL physical absorption technologies mostly have been employed in commercial gasification plants. The selection of acid gas removal technology depends on several factors such as syngas purity, operating temperature, and pressure, solvent loss, and cost. However, SELEXOL process shows good performance for acid gas removal. The SELEXOL process can operate at higher temperatures, can cost less, and can efficiently separate CO_2 (Doctor et al., 1993). The captured CO_2 can be used in biorefinery cases such as lignin extraction in which CO_2 is used for precipitating lignin. In fact, for the two proposed integration scenarios in which the gasifed wood residue is burnt in the lime kiln or sent to a gas turbine, just hot clean up by a filter is needed to remove alkali particles.

4.3.1. SELEXOL Unit

Several SELEXOL arrangements have been proposed based on the design objectives. The dual stage SELEXOL unit (Figure 4.18) is considered for acid gas removal of H_2S and CO_2 using dimethylether of polyethylene glycol (DEPG) solvent. Approximately 30% of the solvent from the bottom of CO_2 absorber after cooling is sent to the H_2S absorber. The rich solvent from the H_2S absorber goes to the SELEXOL stripper to remove H_2S from the syngas. The rest of the loaded solvent from the bottom of the CO_2 absorber is sent to a series of CO_2 recovery vessels for storage.

As the SELEXOL solvent is more selective toward H_2S than to CO_2, the amount of solvent for CO_2 absorption is much larger than the amount of solvent for H_2S absorbtion. The hot syngas exiting the gasifier passes through a syngas cooler and a water scrubber. The shifted syngas is further cooled before going to the acid gas removal (AGR) process which is a physical absorption process with SELEXOL solvent. The sour water drained from the syngas coolers is sent to the syngas treatment unit. The clean water from the sour gas treatment unit is sent to the scrubber and for slurry preparation. In the first stage of the dual-stage SELEXOL unit, H_2S is separated in the stripper and sent to the Claus unit. In the second SELEXOL stage, CO_2 is separated and sent to the compression unit for sequestration.

The schematic diagram of Aspen Plus simulation of the SELEXOL process is depicted in Figure 4.18. Peng-Robinson property package is used in the simulation. The syngas is cooled to 40 °C before being sent to the H_2S absorber. The syngas stream is sent through a H_2S absorber where the SELEXOL solvent passes countercurrent to the syngas stream. The solvent formula is CH_3O

$(C_2H_4)_xCH_3$ where x is between 3 and 9 (Robinson and Luyben, 2010). In the Aspen Plus simulation, the dimethyl ether of polyethylene glycol (x=5) is selected as the solvent. The rich solvent stream from the bottom of the H_2S absorber enters the stripping column to regenerate the solvent. The rich solvent is sent through a stripper where the solvent is regenerated by stream stripping and then cooled and recycled to the absorber. After that the H_2S captured stream is sent to the CO_2 absorber to capture CO_2. The required amount of solvent for CO_2 absorbtion is more than that applied in the H_2S absorber. The part of the bottom stream of the CO_2 absorber that is not recycled to the H_2S absorber enters the CO_2 sequestration unit.

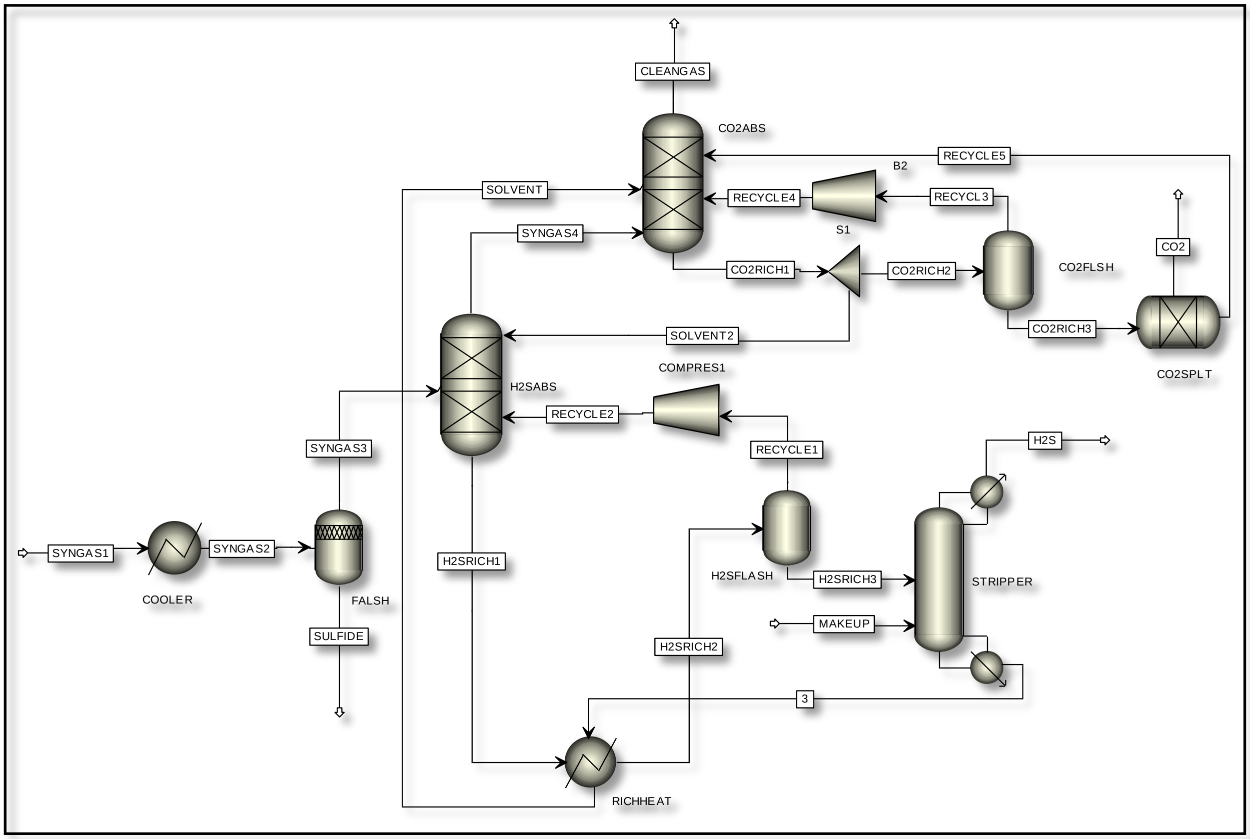

Figure 4.18. Schematic diagram of dual stage SELEXOL process in Aspen Plus

4.4. Combined heat and power generation

The simulation of a gas turbine in Aspen Plus (Figure 4.20), was carried out based on GEE F technology gas turbines (General Electric Website, 2003). The produced syngas together with compressed air (1.65 MPa) are sent to the gas combustor. The combustor and gas turbine firing temperatures are maintained respectively at 1377 °C and 1327 °C. The gas turbine isentropic efficiency is set to fix the exhaust temperature at 567 °C. Then, the flue gas carries the heat to the recovery steam generator (HRSG) where steam is generated at medium and low pressure levels. The generated high and low pressure steams are applied in steam turbine to generate power.

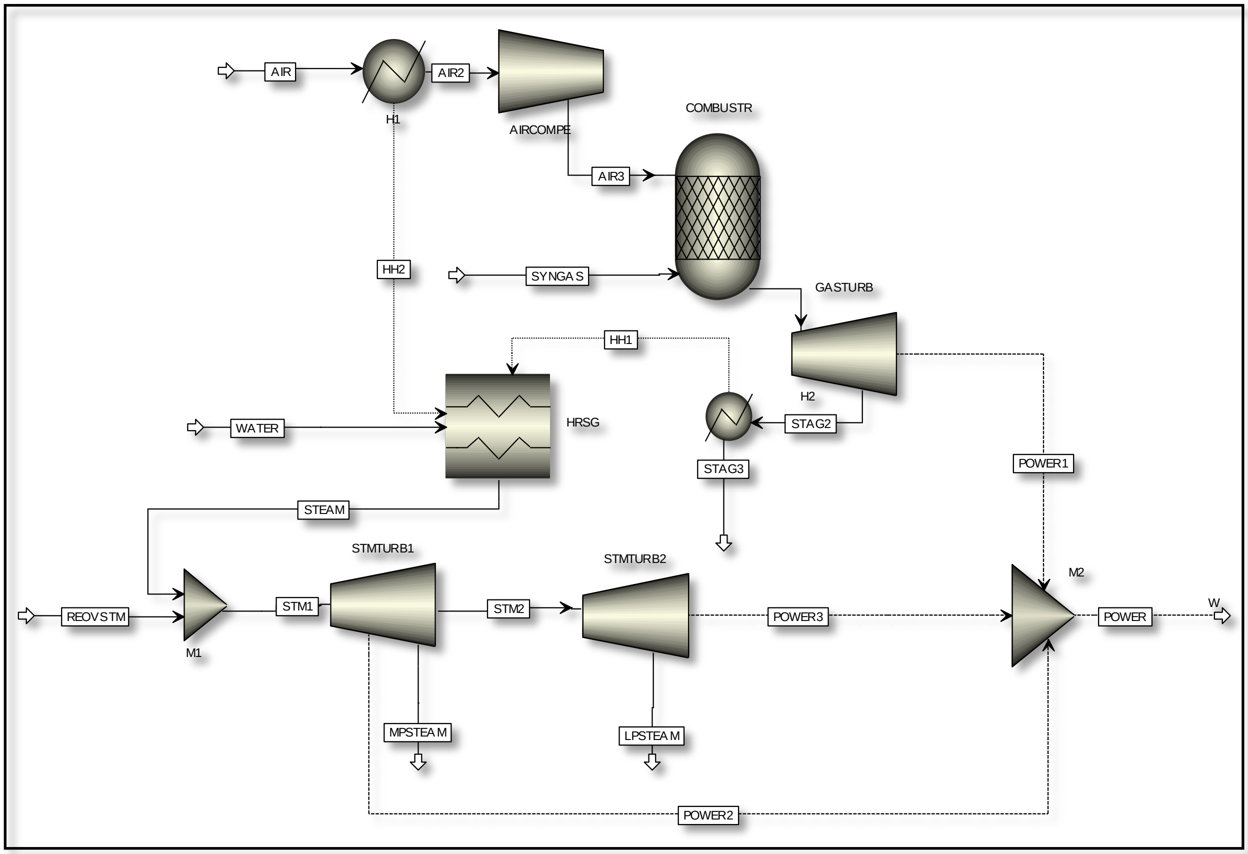

Figure 4.20. Schematic diagram of power plant in Aspen Plus

CHAPTER 5: Results and Discussion

5.1. Reference Kraft mill

The reference pulp and paper mill utilized as a case study is based on three Canadian Kraft mills. The annual production capacity is 820 adt/d (air dried tones per day) of dissolving pulp. Batch digesters are utilized in the mill. High pressure steam is generated by Tomlinson recovery boiler and bark boiler. The electricity demand of the Kraft mill is provided by a steam turbine with intermediate extraction of steam at medium and low pressure levels. The power generation in the steam turbine is 15 MW. The key input parameters for the mill are shown in Table 5.1. The data is based on the exciting reference Kraft mill simulation which has been created by our research group members in CADSIM Plus® software. It is a specialized program for the pulp and paper industry which models the process with mass and energy balances.

Table 5.1. Key parameters for the reference Kraft mill

Pulp Mill	Pulp Production, adt/d	820
	Wood consumption, t/d	1 860
	Bark, t/d	461
Steam	Mill consumption, t/h	154
	Total steam production, t/h	156
	Recover boiler steam production, t/h	104
	Recover boiler steam production, t/h	52
	MP Steam, t/h	36
	LP steam, t/h	94.5
Power	Produced, MW	15
Fuel	Lime kiln natural gas, MW	17

5.2. Feedstock's characteristics

The reference mill fiber supply is a combination of Maple and Aspen woods. The Proximate and ultimate analyses of the feedstock were extracted from the literature (Scott et al., 1985), (Neves et al., 2011). The characterizations of the mill feedstocks are given in Table 5.2.

Table 5.2. Reference Kraft mill Woody biomass data

	Maple	Aspen
Lignin	24	13.7
Hemicellulose	23.7	18
cellulose	44.7	34.3
Moisture	5.33	7.55
Ash	0.59	4.38
Ultimate Analysis, dry		
C	48.5	51
H	6.1	6.4
O	44.9	42.1
N	0.5	0.53
S	0	0
HHV, MJ/kg	20	17.9
Percent,%	65	35

5.3. Biomass dryer

The steam dryer simulation in Aspen Plus is used to calculate the required heat demand to reduce moisture content of biomass feed from 41% to 10%. The performance results for the dryer are shown in Table 5.3. About 461 t/d of 41% moisture biomass is fed to the drying system.

Table 5.3. Biomass dryer key results

Wet biomass flow, t/d	461
Moisture content, %	41
Heat demand, MW	6
Steam production, MW	4.5
Dry biomass moisture content, %	10
Electricity consumption, GJ	2.5

5.4. Biomass gasifier

In this part, first the sensitivity of the modified equilibrium model to the operating parameter variation was assessed. Moreover, the developed model was implemented for the reference mill feedstock, and the performance and efficiency of the biomass gasifier was evaluated

5.4.1. Model analysis

The modified equilibrium model is tested for the biomass feedstock of three Canadian mills. The RAND algorithm is implemented in MATLAB. Thermodynamic properties required for the equilibrium model are obtained from JANAF thermodynamic data (M.W.Chase et al., 1985). The composition of the producer gas and the calorific value of syngas are determined for a range of gasification temperature and equivalence ratio. The influence of these operating parameters is illustrated in the following section. The ultimate analysis for biomass feedstock of the three mills is shown in Table 5.4.

Table 5.4. The ultimate analysis of biomass feedstock

	Mill.1			Mill.2		Mill.3		
Biomass type	Spruce	Pine	Fir	Maple	Aspen	Jack Pine	Black Spruce	Pine
C	51.9	52.6	52.3	50.6	45.4	53.3	51.9	49.4
H	6.1	6.1	6.3	6	4.8	6.2	6.1	7.67
O	40.9	40.9	40.5	41.7	43.1	40.3	40.9	42.19
N	0.3	0.2	0.1	0.3	0.5	0.1	0.3	0.1
S	0	0	0	0	0	0.1	0	0.05
Ash	0.8	0.2	0.8	1.4	0.2	0	0.8	0.59
HHV, MJ/kg	20	21.3	21.1	20	17.9	22.3	20	22.3
Percent,%	20	70	10	65	35	10	80	10

In order to analyze the sensitivity of the developed model to the changes of temperature and equivalence ratio, ER, as the two most important gasifier operating parameters, the model is implemented for a wide range of temperature and ER.

Figure 5.1 shows the changes in the syngas composition against temperature. As the syngas composition is the result of several endothermic and exothermic reactions, the effect of gasifier temperature on the syngas composition is a complicated function of several variables such as the type of biomass and gasifying agent, and ER. As shown in Figure 5.1, for the utilized biomass feedstock and air gasification with (ER=0.25), the CO content increases and the H_2 content and the CO_2 content decrease with temperature. Figure 5.3 shows the variation of heating value of the produced syngas against gasification temperature for the three woody biomass feeds. As depicted in Figure 5.3, the heating value increases slightly with temperature due to the increase on the yield of CO. However, this is different for the cases in which high temperature is caused due to an increase in ER. (Zainal et al., 2001) showed that the calorific value of the produced syngas is reduced as a result of the higher temperature due to elevated ER.

The equivalence ratio (ER) is an important operational variable in biomass gasification with air. In the gasification model, it varies from 0.20 to 0.45. As shown in Figure 5.2, all combustible products (CO, H_2, and CH_4) decrease with an increase in ER and the formation of higher amounts of CO_2. The effect of ER on the heating value of the gas is represented in Figure 5.4. On increasing ER, the heating value of the gas is decreased.

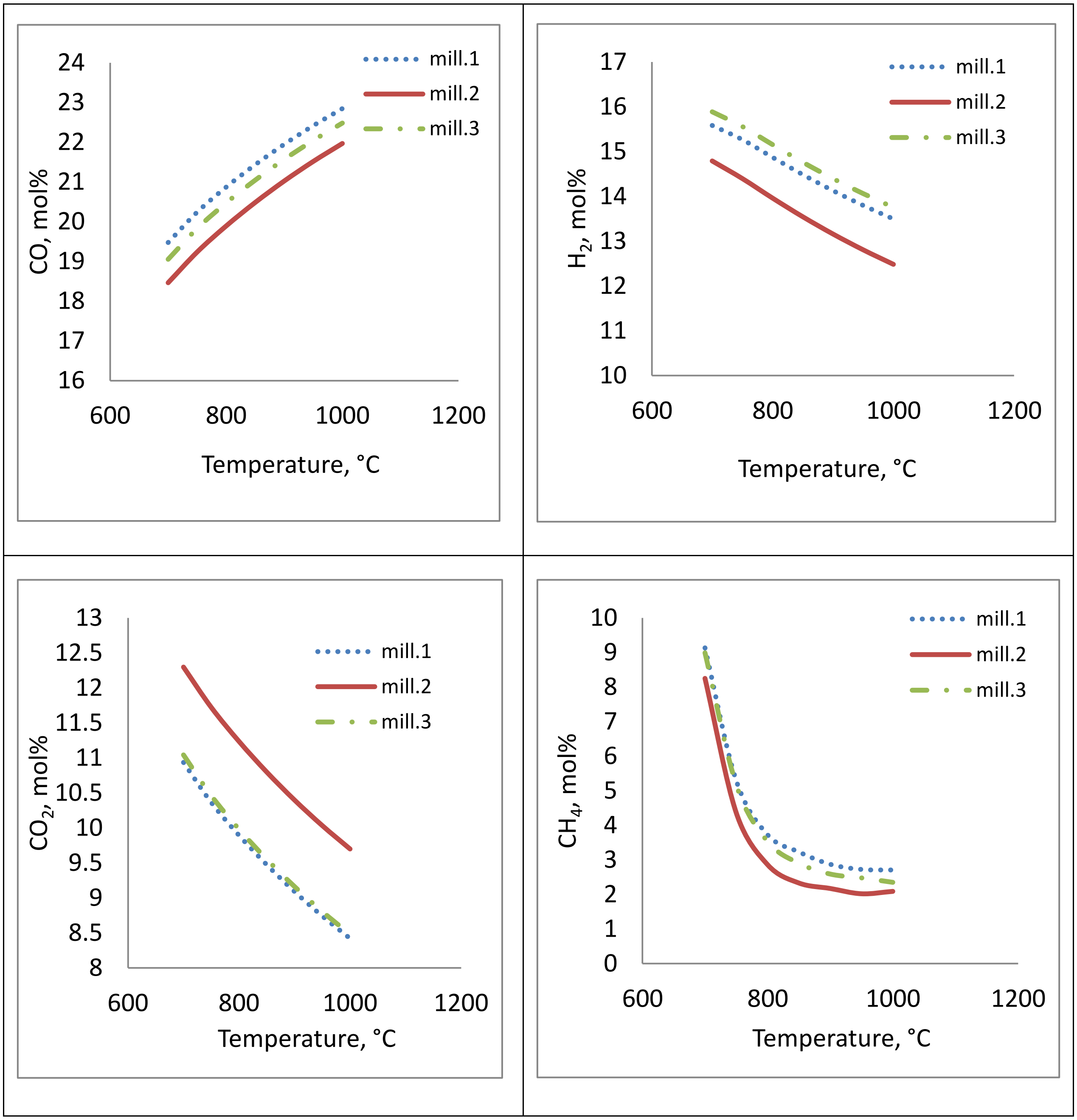

Figure 5.1. Effect of temperature on syngas composition

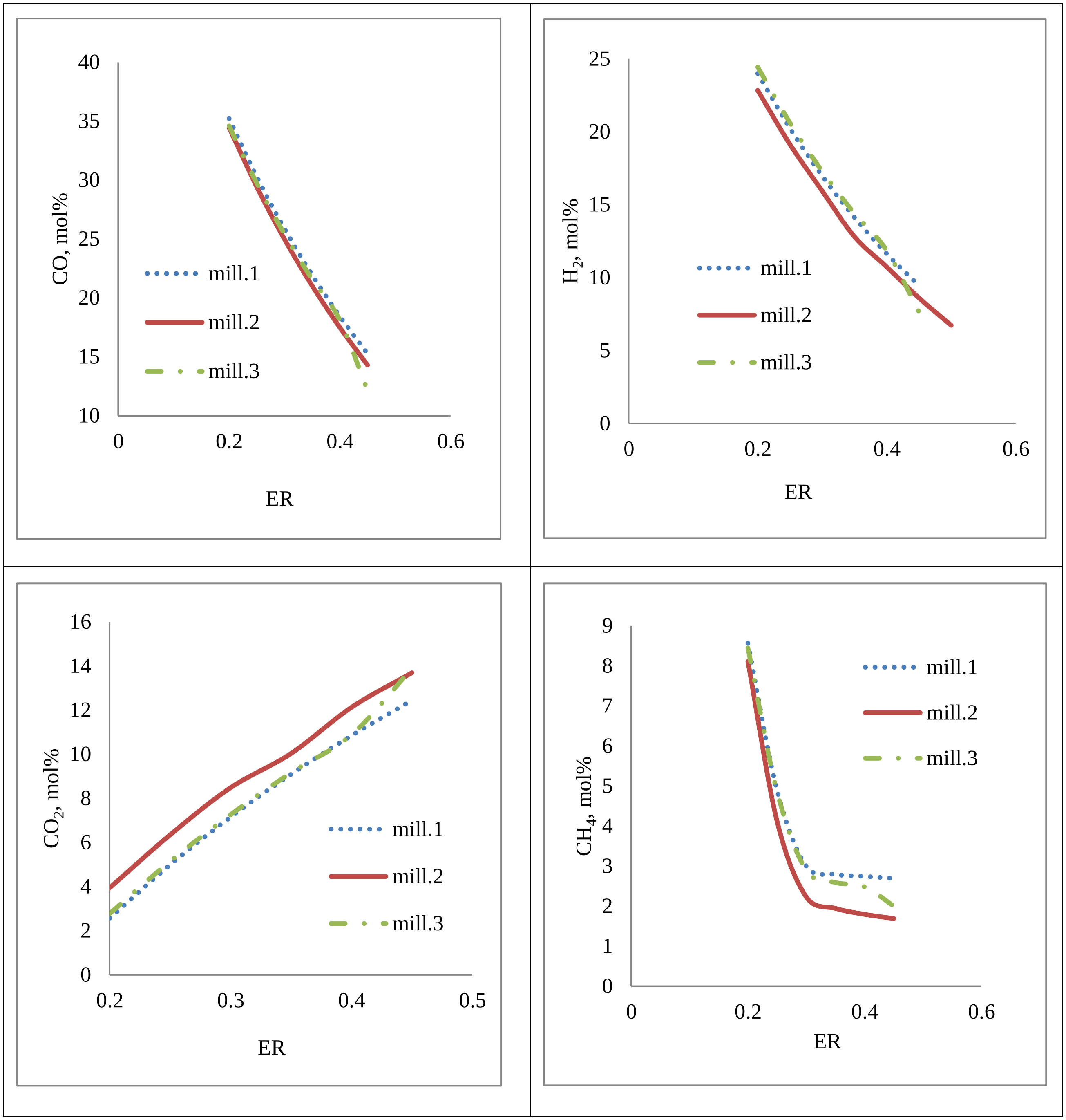

Figure 5.2. Effect of ER on syngas composition

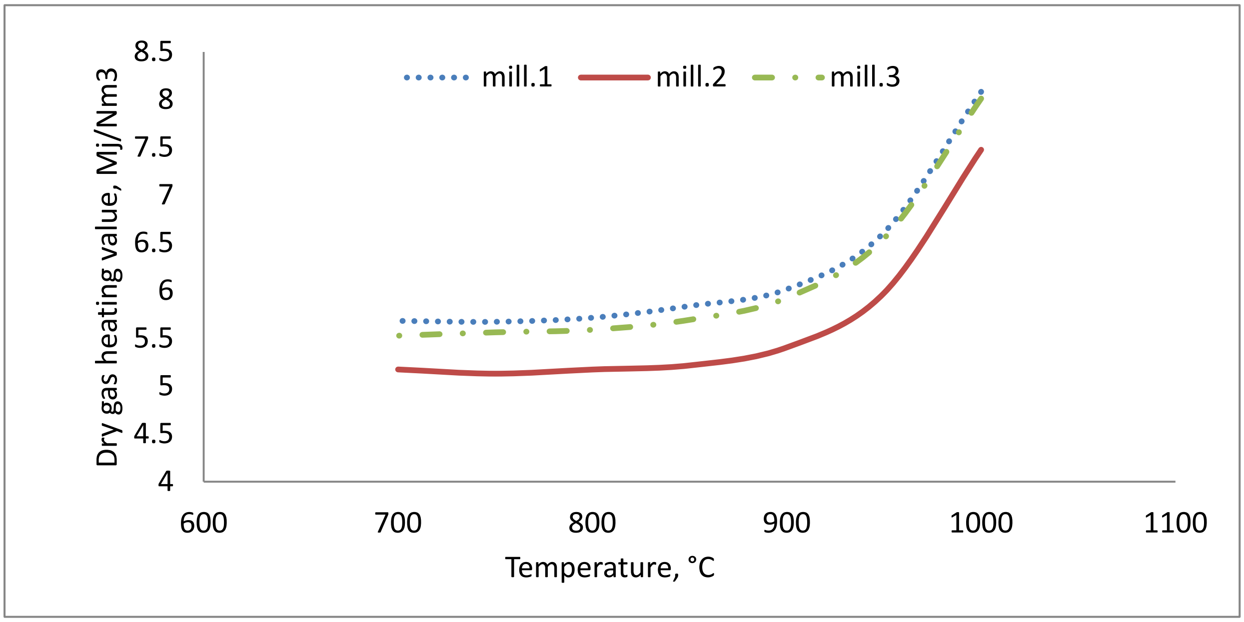

Figure 5.3. Effect of temperature on syngas heating value

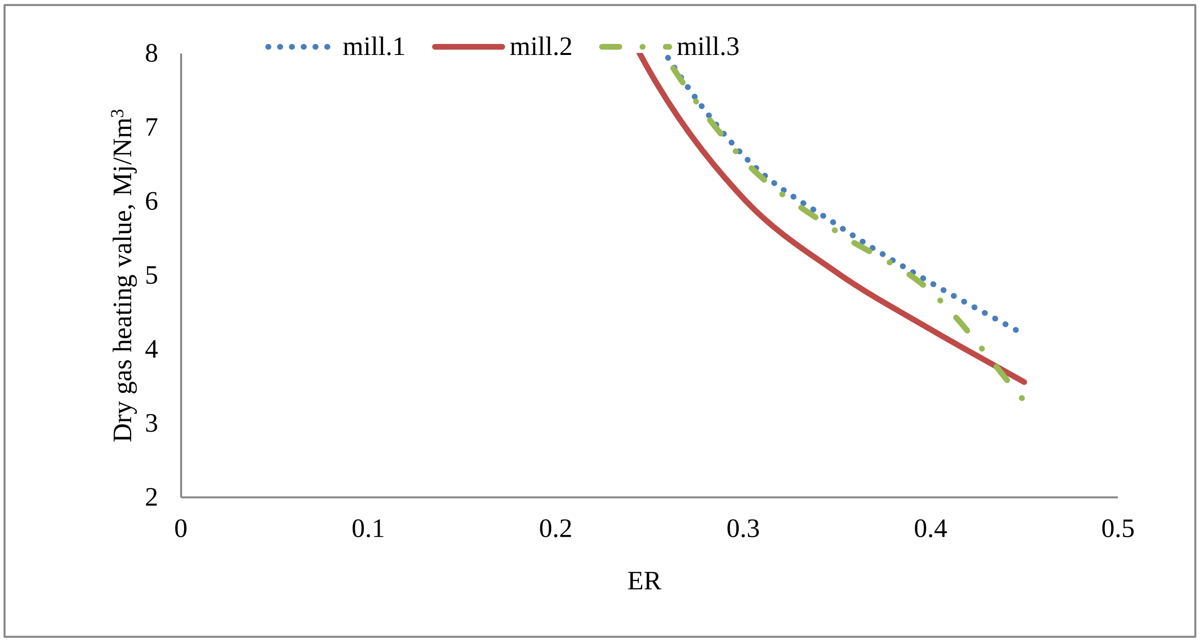

Figure 5.4. Effect of ER on syngas heating value

5.4.2. Gasifier type

The selection of the gasifier type depends on the several factors such as feedstock type, syngas, application, design capacity, and gasifier cost. A literature investigation was made to identify the appropriate commercial gasification technology for the proposed integration concepts and to collect reliable gasification data and evaluate the gasification economics. As mentioned in chapter 2, for large-scale processes fluidized beds generally are more advantageous. Considering that the large-scale operation of fixed bed biomass gasifiers poses several problems; industrial biomass gasifiers generally are bubbling fluidized bed or circulating fluidized bed reactors. Fluidized bed gasifier is an appropriate choice for biomass gasification because of temperature homogeneity, suitable gas-solid mixing, rapid heating of the biomass feedstock, and the possibility of including catalyst particles in the bed inventory to enhance the reforming reactions (Jand et al., 2006). In Table 5.5., operating conditions and syngas compositions for several commercial air wood fluidized bed gasification technologies are presented (Ciferno and Marano, 2002). As the Lurgi and Foster Wheeler technologies have been used for the lime kiln gasification applications, and since the heating of values of the produced syngas are larger than for the other technologies, the gasifier required data were extracted from data sheets for these technologies.

Table 5.5. Commercial biomass gasifier data

	EPI	Tampella	SEI	Foster wheeler	Lurgi	Sydkraft
Gasifier type	BFB	BFB	BFB	CFB	CFB	CFB
Feed flow,(t/d)	100	45	181	14.5	84-108	-
Temperature, °C	650	850-950	650-815	900	800	950-1000
Pressure, kPa	100	2 000-2 500	100	100	100	1 800
Air, kg/kg feed	2.0	0.4	1.45	1.7	1.25	-
Steam, kg/kg feed	-	0.5	-	-	-	-
Syngas flow, M^3/h	8793	-	48445	1181	9 700-12 500	-
Exit temperature, °C	621	300-350	800	700	600	-
Heating value, MJ/m^3	5.6	4-6	5.7	7.5	5.8	5
Syngas composition						
H_2	5.8	11.3	12.7	15-17	20.2	11
CO	17.5	13.5	15.5	21-22	19.6	16
CO_2	15.8	12.9	15.9	10-11	13.5	10.5
H_2O	dry	17.7	dry	dry	dry	12
CH_4	4.65	4.8	*5.72*	5-6	3.8	6.5
H_2S	-	-	-	-	-	-
N_2	51.9	40.2	47.9	46-47	42.9	44
H_2/CO ratio	0.3	0.8	0.8	0.7	1	0.7

5.4.3. Gasifier results

The modified equilibrium model of a biomass gasifier is validated with the industrial data from the Foster Wheeler and Lurgi gasification technologies. The comparison is presented in Table 5.6. It is obvious that the model results match well with the industrial data. The Foster Wheeler gasifier is an atmospheric circulating fluidized bed with operating temperature of 1000 °C. The gasifying agent is air and the biomass feed is wood. The produced syngas can be employed for electricity production or for firing in lime kilns. The Lurgi gasifier also is an atmospheric circulating fluidized bed which applied to produce the lime kiln fuel. The biomass feed is bark and the operating temperature is 800 °C.

Table 5.6. Comparison of the model results for Foster wheeler and Lurgi gasifiers

	Foster wheeler	Model	Error,%	Lurgi	Model	Error,%
Heating value, MJ/m^3	7.50	6.68	10.87	5.80	6.96	20.01
Syngas composition						
H_2	16.00	17.36	8.50	20.20	22.48	11.29
CO	21.50	22.76	5.86	19.60	22.36	14.08
CO_2	10.00	8.09	19.14	13.50	11.48	14.96
H_2O	dry	dry	-	dry	dry	-
CH_4	5.00	4.01	19.80	3.80	3.19	16.05
H_2S	-	-	-	-	-	-
N_2	46.50	47.63	2.43	42.90	39.82	7.18
H_2/CO ratio	0.70	0.76	8.99	1.00	0.82	17.63

The model developed in this work is applied to predict the syngas composition. The key results of the gasification of wood residues for the reference Kraft mill are shown in Table 5.7.

Table 5.7. Biomass gasifier results

Dry biomass feed, t/d	305
Air flow, t/hr	549
Air flow, kg/kg feed	1.8
Steam flow, t/hr	-
Gasification temperature, °C	900
Gasification pressure, kPa	100
Syngas composition, vol%	
H_2	15.93
CO	21.06
CO_2	8.84
H_2O	Dry
CH_4	4.43
H_2S	-
N_2	49.72
Carbon conversion, gas, %	85
Cold gas efficiency, %	63.7
Higher heating value, HHV,	6.46

5.5. Case study 1

The lime kiln process is currently the largest fossil fuel consumer in a Kraft mill, and therefore has a crucial importance to avoid increased dependency on fossil fuels. On average, a lime kiln process necessitates 8GJ/t CaO. Most of the lime kilns in the North America are fired with natural gas. Canadian natural gas prices in 2010 varied between 3–6$/GJ [*] (Natural Resources Canada Report, 2011). At a natural gas price of $6/GJ, the lime kiln energy cost estimated for a typical lime kiln of a Kraft mill with pulp production of 1 000 adt/d is about 3-5 M$/year. As the fossil fuels price rate continues to increase nowadays (Figure 5.5), gasified wood residue is an encouraging choice to heat lime kilns. In fact, high fossil fuels cost and the imposition of greenhouse gas emissions allowances have made biomass gasification a competitive alternative to heat lime kilns. So in this part of study, the technical, environmental, and economics of the lime kiln wood gasification process is evaluated.

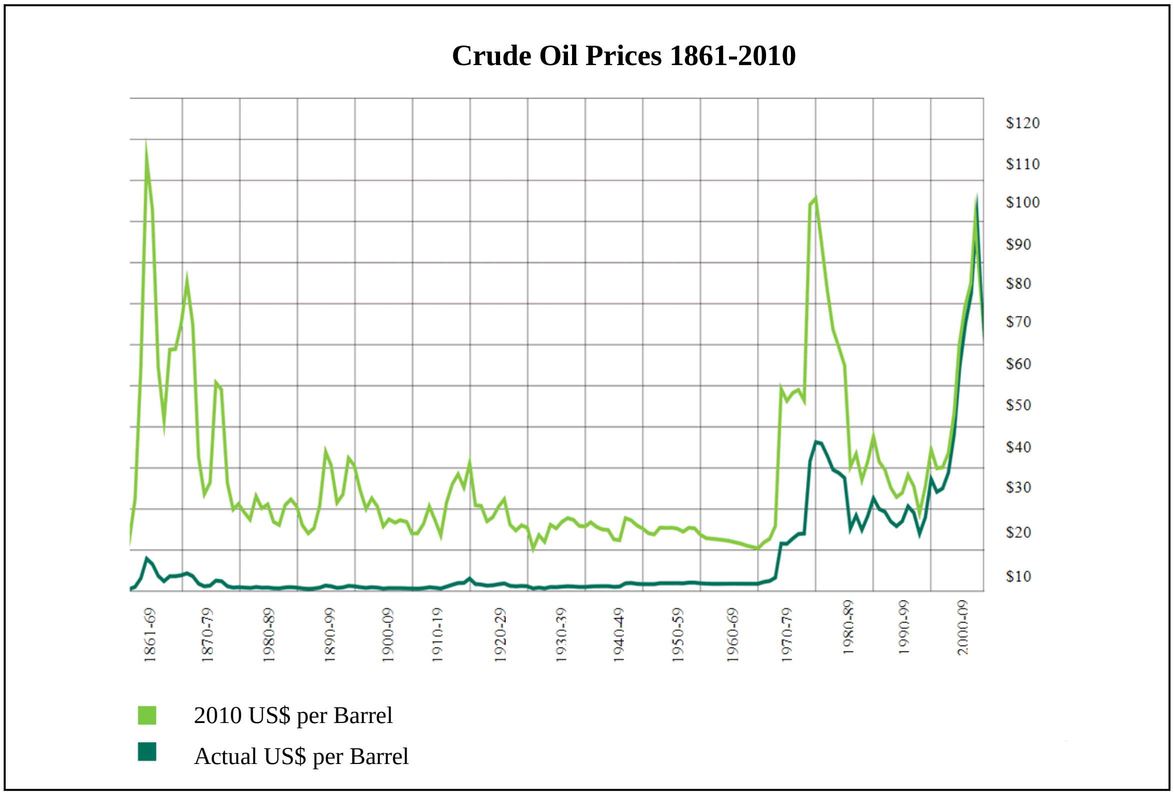

Figure 5.5. Historical chart of crude oil prices,(BP Statistical Review, 2010)

---

[*] All data are given in Canadian dollar for the present year

The schematic diagram of a CFB lime kiln gasification process is illustrated in Figure 5.6. The process includes biomass drying, feeding system, CFB gasifier, and cyclone separator. To have the same combustion properties as fossil fuels for the gasified wood residues, the moisture content of the woody biomass feed of the lime kiln gasifier should be less than 15%. High moisture content of biomass feed increases the produced syngas volume flow which causes decrease of lime kiln temperature. Therefore, for a feedstock with moisture content higher than 15%, a biomass drying system is essential. Generally, atmospheric CFB gasifier are utilized in lime kiln applications because of flexibility to the feed disturbances, high heat capacity, uniform temperature profile, intensive mixing, and suitability for large-scale processes compared with fixed bed gasifiers.

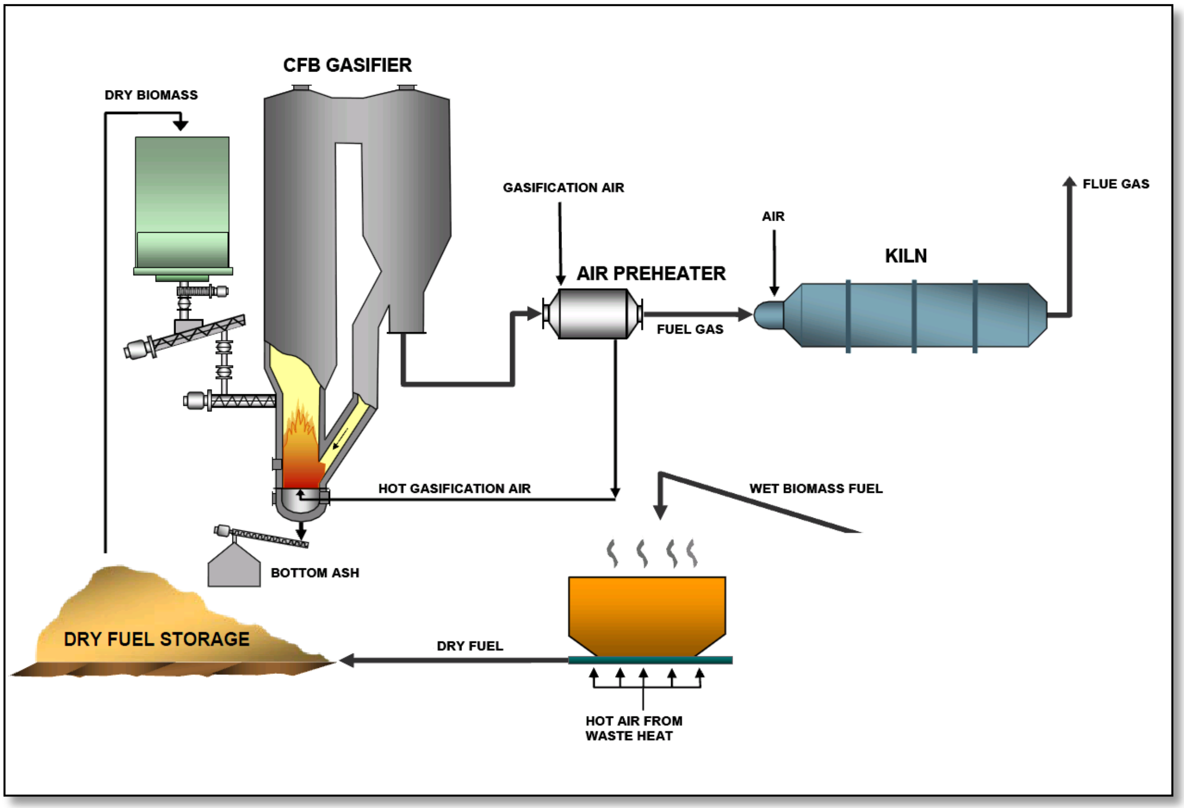

Figure 5.6. Schematic diagram of a CFB lime kiln gasification process, (Salo, 2009)

The reference Kraft Lime kiln mill with production capacity of 150 t/d of CaO has been simulated in CADSIM Plus. 17 MW of natural gas is utilized to heat the lime kiln. The lime kiln data are shown in Table 5.8.

Table 5.8. Reference Kraft mill lime kiln data

Parameter	Reference mill
Mud feed, t/d	350
Lime product, t/d	150
Natural gas, t/d	31
Combustion air, t/d	560
Required kiln heat, MW	17

A summary of the results for the first case study is presented in Table 5.9. The comparison of the characteristics of produced syngas with natural gas and fuel oil is shown in Table 5.10. The lower heating value of the syngas (6.5 MJ/kg) compared to heating values of the natural gas and fuel oil is the reason that the higher volume flow of syngas is needed to achieve the same heating rate. As a result, there is the possibility of affecting the lime kiln capacity. As shown by data provided in Table 5.10, the lower heating value of produced syngas causes lower flame temperature which may require additional modifications, however these are not addressed here. For now, in supplying required heat of calcination in the lime kiln, higher flow of syngas is assumed.

Table 5.9. Reference Kraft mill lime kiln data

	Base Case	Case Study 1
Wet biomass feed, t/d	NA	461
Air flow, t/d	NA	549
Steam flow, t/hr	NA	-
Gasification temperature, °C	NA	900
Gasification pressure, kPa	NA	100
Syngas composition, vol%		
H_2	Natural Gas	15.93
CO	Natural Gas	21.06
CO_2	Natural Gas	8.84
H_2O	Natural Gas	dry
CH_4	Natural Gas	4.43
H_2S	Natural Gas	-
N_2	Natural Gas	49.72
Gas to lime kiln, t/d	31	246
Gas temperature to lime kiln, °C	25	400
Air to lime kiln, t/d	560	427
Cold gas efficiency	NA	64
HHV dry, MJ/kg	48	6.5
Lime kiln heat, MW	17.22	18.5

Table 5.10. Comparison of syngas characteristics with natural gas and fuel oil

	Syngas	Natural gas (Ralston, 2002)	Fuel oil (Ralston, 2002)
LHV dry, MJ/kg	5.8	48.15	39.97
HHV dry, MJ/kg	6.5	53.28	42.33
Composition, ultimate analysis			
C	16.85	74.72	87.12
H	2.12	23.3	10.75
O	27.14	1.22	0
N	46.30	0.76	0
S	0	0	2.1
Ash	0	0	0.03
Moisture	7.60	0	0
Adiabatic flame Temperature(AFT),dry °C	1 813	2 055	2 118

In order to evaluate the performance of the lime kiln gasification process integrated with the reference Kraft mill, the key results of the simulation are compared with results from the Pietarsaari pulp mill (Siro, 1989). The whole lime kiln fuel requirement at the Pietarsaari pulp mill in Finland has since 1983 been supplied from woody waste gasification. The Atmospheric Circulating Fluidized Bed (CFB) gasifier by Foster Wheeler Energia Oy has been used. The same technology has been utilized at two Swedish pulp mills and one mill in Portugal. The biomass feed is combination of bark and sawdust. The summary of data is showed in Table 5.11.

Table 5.11. Comparison of the results with Pietarsaari mill

	Pietarsaari mill	Reference mill
Pulp production, adt/d	1 370	820
Average steam consumption, t/d	11 200	3 700
Lime kiln feed flow, t/d	804	350
Lime kiln effect, MW	35	18.5
Drying gas temperature, °C	150	150
Dry syngas moisture content, %	15	10
Gasification temperature, °C	900	900
Dry syngas composition, mol%		
CO	14.5-22	21.06
H_2	15.5-18	15.93
CH_4	4.3-7.2	4.43
CO_2	10.2-12.9	8.84
N_2	44-53.6	49.72
HHV, MJ/Nm^3	5.5-7	6.3

5.6. Case study 2

The objective of this scenario is to evaluate the integration of biomass gasification combined heat and power cycle to the reference Kraft mill. This case study assumes the full replacement of the existing bark boiler in the reference Kraft mill. The plant is dimensioned to process the same amount of biomass as the bark boiler. Figure 5.7. illustrates the schematic diagram of the biomass gasification combined cycle. Biomass is first dried, and then gasified to generate syngas, which is then cooled and cleaned, and after that fired in a gas turbine. The exhaust stream of the gas turbine enters the heat recovery steam generator (HRSG). Finally, the generated steam is sent to the steam turbine. The required LP and MP steams of the reference mill are extracted from steam turbine. An atmospheric air-blown gasifier is considered in this case study, because for an integrated gasification combined cycle which generates less than 80 MW_e, the cost of air separation unit makes the IBGCC unprofitable (Jin et al., 2009) .

The syngas leaving the gasifier is cooled to 400°C in a syngas cooler. The steam generated in the cooler is sent to heat recovery steam generator, HRSG, to increase amount of steam generation. By cooling the syngas, alkali components convert to suspended particulates in the syngas. Hot gas filtration is then considered in the process to remove alkali vapours. The cold gas efficiency is 63.7% on a higher heating value basis.

The produced syngas enters the gas turbine at temperature around 400 °C. As commercial combined cycles are designed to operate with natural gas with calorific value of about 50 MJ/Nm^3, new combined cycle technology should be developed for gasified biomass application with lower calorific value of 5-7.50 MJ/Nm^3. General Electric offers the 7F syngas turbine with a compressor capable for higher flow/pressure ratios. Also, the gas turbine involves a new combustion system for syngas applications. However, the operating data has not been published. In fact, the necessary syngas flow to rise the turbine inlet temperature is higher than that required with natural gas. As the result, a mismatch between compressor and gas turbine is occurring. To adjust this mismatch the (Larson et al., 2003) approach is used. The air compressor pressure ratio is increased and air flow is decreased to de-rate the gas turbine for syngas applications.

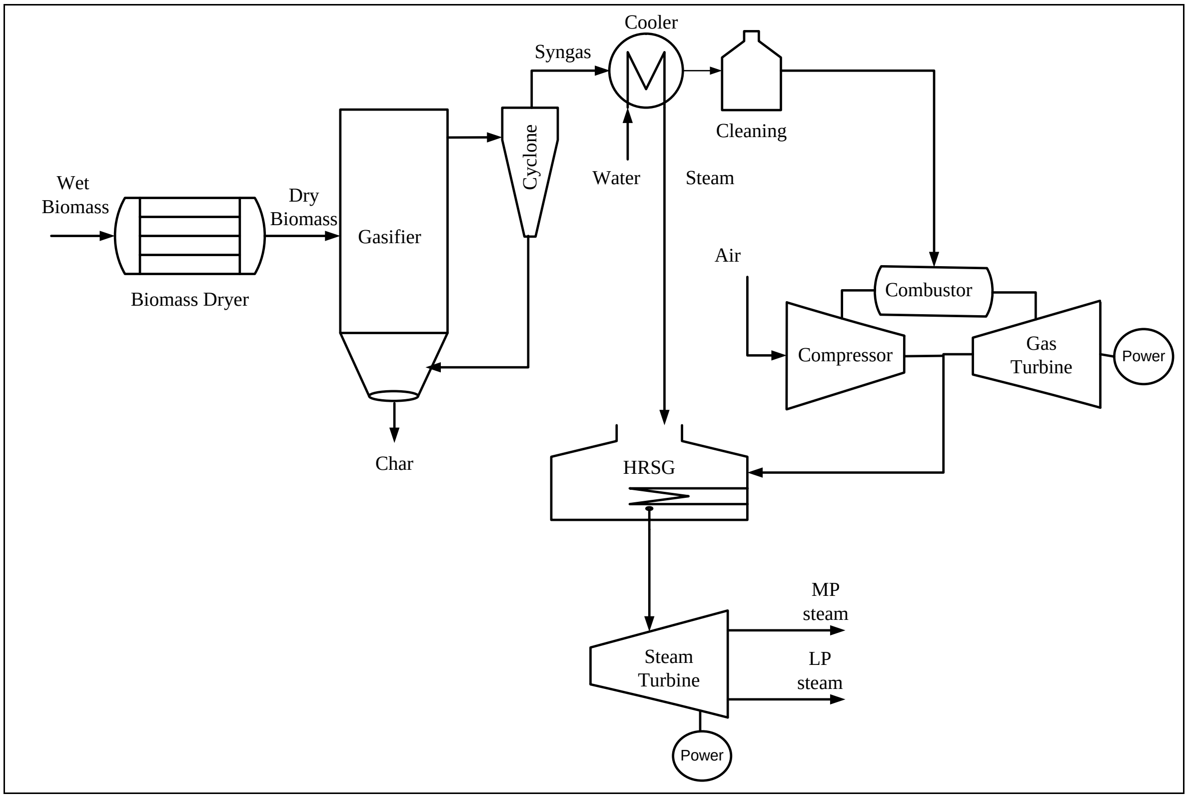

Figure 5.7. Schematic diagram of the biomass gasification combined cycle

The comparison of biomass gasifier performance with the bark boiler is illustrated in Table 5.12. The existing bark boiler together with the recovery boiler generate the steam for the Kraft process. The bark boiler burns 23 t/d of natural gas and 461 t/d of bark fuel to generate 1 243 t/d of steam at temperature of 400 °C and pressure of 6 000 kPa. The generated steam from the recovery boiler together with generated steam from the bark boiler is fed to a gas turbine to provide 850 t/d of MP steam and 2 500 t/d of LP steam. The amount of generated electricity is about 13.7 MW. The integrated gasification plant produces a gross electrical of 23 MW_e. The performance of the plant is based on the net electrical efficiency. As shown in Table 5.12, the electrical efficiency of the gasification system is about 23%, which is significantly higher than for the bark boiler which is about 12%.

Table 5.12. Performance data for IBGCC

	Bark boiler	Gasifier
Biomass, t/d	461	561
Natural gas, t/d	23	-
Generated steam in recovery boiler, t/d	1 250	1 250
Generated steam in recovery boiler, temperature, °C	400	400
Generated steam in recovery boiler, Pressure, kPa	6 000	6 000
Generated steam in bark boiler, t/d	2 500	-
MP(1000KPa) steam to process, t/d	850	900
LP(400 KPa) steam to process, t/d	2 300	2 200
Gas turbine power generation, MW_e	13.7	16.5
Steam turbine power generation, MW_e	-	6.5
Electricity generation, MW_e	13.7	23
Electricity efficiency, HHV,%	11.90	23.20

5.7. Gas emission reduction

Integrated biomass gasification has the potential to decrease CO_2 emission. Also, other emissions such as SO_2 and NO_x emissions would be decreased. Because the reduction of CO_2 emissions is considerably more than the other emissions, here just CO_2 emission reductions are considered. CO_2 emissions from lime kilns are estimated using the same method applied for the stationary fossil fuel combustion devices ((ICFPA report, 2005)). The main CO_2 emission sources in lime kilns are (Miner and Upton, 2002):

- **CO_2 released from burned fossil fuels in the kiln**

The required heat for the lime kiln reaction is generally provided by burning fossil fuels. In most of the industry's lime kilns, natural gas is utilized and just in few lime kilns in industry, fuel oil is used. The average rate of CO_2 emission from fossil fuel burning based on the lime kilns data collected from NCASI in 1996, is estimated about 100 kgCO_2/ton pulp (Miner and Upton, 2002).

- **CO_2 released from $CaCO_3$ in the calcining process**

The amount of calcium carbonate-derived CO_2 is significant. In average 250 (kg lime/t pulp) is used in a Kraft mill recovery cycle (Green et al., 1992). This amount of lime necessitates 446 (kg$CaCO_3$/t pulp) which release 196 (kgCO_2/t pulp). It should be mentioned that CO_2 emission which is originated from wood chips not to be considered in greenhouse gas emissions inventories. The combustion of biomass fuels such as wood, and wood waste produces carbon dioxide. However,based on the (EPA., 2000) report: "in the long run the carbon dioxide emitted from biomass consumption does not increase atmospheric carbon dioxide concentrations, assuming the biogenic carbon emitted is offset by the uptake of CO_2 resulting from the growth of new biomass. As a result, CO_2 emissions from biomass combustion have been estimated separately from fossil fuel-based emissions and are not included in the U.S".

For the first scenario in which gasified biomass is utilized to fire in the lime kiln, The reduction of CO_2 emissions are calculated on the basis of decreases in fossil fuel use. The corrected emission factor for natural gas of 55 900 tCO_2/TJ (Intergovernmental Panel on Climate Change (IPCC), 1997b) is considered to calculate CO_2 emission for the case in which natural gas is utilized to heat the reference mill lime kilns. As the amount of 31 t/d of natural gas supplied to the lime kiln, the calculated CO_2 emission reduction for the first scenario is about 30 400 tCO_2/y. The predicted CO_2 emission reduction for the second scenario is about 23 500 tCO_2/y. The predicted CO_2 emissions for both scenarios are shown in Table 5.13. The results show that biomass gasification process has the potential to obtain considerable environmental benefits.

Table 5.13. Predicted CO_2 emissions reduction

	Natural gas (t/d)	CO_2 emission factor (t CO_2/TJ)	Annual CO_2 emission reduction (t/y)
Case study 1	31	55 900	30 400
Case study 2	23	55 900	23 500

5.8. Economic analysis

In order to analyze the feasibility of biomass gasification process, the economic aspects should be considered. In this part, cost estimation including investment and production cost are determined for the biomass gasification process. Accuracy of economic results is considered about ±30% of the actual cost (Caputo et al., 2005). Total capital and operating costs are calculated for both case studies. The (Swanson, 2009) methodology which applied to predict the capital cost is shown in Table 5.14. The equipment costs are estimated for main equipments which are dryer, gasifier, gas cleaning and cooling unit, and power unit. The capital cost adjusted based on the six-tenths factor rule to adjust the equipment cost for the considered equipment capacities. (Peters and Timmerhaus, 1991):

$$C_2 = C_1\left(\frac{q_2}{q_1}\right)^{\theta} \qquad (66)$$

C_2: The cost of the equipment at capacity q_2

C_1: The cost of the equipment at capacity q_1

θ: Exponential factor = 0.6

The direct costs which include piping, electricity, instruments are estimated via an installation factor.

Table 5.14 Total Capital Investment estimation methodology

Parameter	Method
Total equipment cost (TEC)	Commercial and literature data
Direct cost (DC)	Installation factor*(TEC)
Indirect cost (IC)	0.89* TEC
Contingency	0.2*(DC+IC)
Working capital (WC)	0.15*(DC+IC+ Contingency)
Total capital investment (TCI)	(DC+IC+WC+ Contingency)

The operating costs include raw material costs, labor costs, transport cost, maintenance, and insurance costs. Material costs are shown in Table 5.15. In spite of a large demand for forest residues, there is no common market price for forest residues biomass. Numerous parameters influence the cost of biomass: type of residue, location, moisture content, availability, size, energy content, harvesting method, transportation distance, etc. So defining a specific price for biomass is not easily produced, as the prices can vary significantly. (Bradley, 2008) estimated average prices ($/odt) for mill residues, bark piles and harvest residues in Eastern Ontario (2012 estimates) of 20, 5 and 29.

Table 5.15. Material costs adjusted to 2010 $

Variable cost	Cost
Biomass, CND$/t	20 [a]
Electricity, CND$/MW.h	130 [b]
Process Steam, CND $/t	9.2 [c]
Natural gas, CND$/GJ	6 [d]

a (Bradley, 2008)
b (National Energy Board report, 2011)
c (Peters and Timmerhaus, 1991)
d (Natural Resources Canada Report, 2011)

The labor costs are computed as the function of the 2011 labor fee (Statistics Canada Report, 2011) which fixed to 61 363 $/y, and the number of personnel. The 60% of labor salaries is considered as the overhead (Aden and National Renewable Energy Laboratory (U.S.), 2002). Also, 2% of the total capital cost is considered for the maintenance and insurance costs (Aden and National Renewable Energy Laboratory (U.S.), 2002).

The cost estimation for the steam dryer is determined based on the GEA-Barr-Rosin design data and then adjusted for the capacity of 461 t/d and 561 t/d of bark feed with 41% moisture. For the estimation of equipment costs for gasifier, gas cooling and cleaning unit, and power unit, several experimental and literature data is utilized (Bridgwater et al., 2002),(EnergyE2. and Foster Wheeler Energia Oy Reportm, 2002) ,(Caputo et al., 2005), (Isaksson et al., 2008), (Jin et al., 2009), (Swanson et al., 2010).

The capital and operating costs for different units of the gasification process for the both case studies are shown in Table 5.16 and Table 5.17.

Table 5.16. Capital costs for different units, (MM $)

Case Study 2	Case Study 1	Unit
4.70	3.90	Biomass dryer
6.90	6.20	Gasifier with cyclone
3.80	-	Syngas cooling and cleaning
10.20	-	Power unit
52.70	21.70	Direct cost (DC)
46.90	19.30	Indirect cost (IC)
19.90	8.20	Contingency
17.60	7.40	Working capital (WC)
137.10	56.60	Total capital investment (TCI)

To compare the economics of the gasified wood residues as the alternative fuel for replacing natural gas, internal rate of return (IRR), and the payback period are determined. The difference between the annual operating costs of the lime kiln gasification process and the base case is assumed as the cash flow. An inflation rate of 3% is considered for each year.

The net present value (NPV) is evaluated by considering all cash inflows and outflows (Caputo et al., 2005):

$$NPV = \sum_{k=1}^{L} \frac{F_k}{(1+IR)^k} \tag{67}$$

Where IR is interest rate for each year, F_k is the cash flow at the end of the k period, L is the plant life.

Table 5.17. Annual operating costs for different units, ($1000/y)

Case Study 2	Case Study 1	Unit
3 590	2 310	Biomass feedstock
276	227	Steam
859	430	Operating labor
2 743	1 131	Maintenance
515	258	Overhead
2 743	1 131	Tax and insurance
10 726	5 487	Annual operating cost

NPV are calculated for 20 years plant life for the estimated TPI and at ±30% TPI. The interest rate is considered 9% for each year (Caputo et al., 2005). The CO_2 emission reduction also is considered as the revenue for both scenarios for calculating NPV. The carbon tax of 30 $/t$CO_2$

is assumed to be equal to the carbon tax for the current year (http://www.carbontax.org, 2011). The NPV results are shown in Table 5.18.

Table 5.18. NPV results, ($1000)

	TPI	(+30% TPI)	(-30% TPI)
NPV(20 years) for case study1	-6 905	-13 501	1 207
NPV(20 years) for case study2	79 00	26 147	70 720

As shown in Table 5.18 for the first case study negative NPV values are reached, while positive NPV are obtained for the second case study. The payback period, τ, is estimated as the first year in which the sum of cash flows is greater than the capital investment:

$$\sum_{k=1}^{\tau} \frac{F_k}{\left(1 + IR'\right)^k} \geq 0 \qquad (68)$$

The payback time is estimated 1.2 years for the second case study. The gasification power plant based on the estimated NPV and payback period is cost efficient. The profitability of lime kiln gasifier depends on fuel prices and also CO_2 emission allowances. For the present cost values of natural gas fuel and biomass, the economic profitability for the first case study is dependent on capital investment costs. Table 5.19 shows the predicted annual cost comparing natural gas and syngas from biomass gasification for the reference Kraft mill. As the results are illustrated in Table 5.19, gasification is an attractive alternative for replacement fuel oil in lime kiln units.

Table 5.19. Replacement of natural gas with syngas, annual cost comparison

Product	Quantity	Cost ($1000)	Income ($1000)
Biomass	461 t/d	2 310	-
Natural gas	-31 t/d		5 570
CO_2 emissions	-30 360 tco_2	-	6 330
Other cost	-	3 140	
Total		5 450	11 900
Balance			6 450

CHAPTER 6: Conclusions and Recommendations

6.1. Conclusion

This thesis had studied the integration of biomass gasification into a Canadian Kraft mill. A models of biomass gasification process including dryer, gasifier, syngas cleaning, and heat and power units have been implemented. Regarding that the available thermodynamic equilibrium model for biomass gasifiers miss estimate the yield of the gaseous products, a modified equilibrium model has been developed to improve the predictability of the gasifier model. After modeling the process, two case studies have been considered to investigate the performance of the integrated gasification process to the Kraft mill: The use of gasified wood to fire the lime kiln, and the replacement of the exciting bark boiler with an Integrated Biomass Gasification Combined Cycle. The technical analysis, economic performances, and CO2 emission balances associated with implementation of biomass gasification in the mill have been studied. The following main conclusions can be drawn:

- At the high temperature biomass gasification, the predicted yields of carbon monoxide, carbon dioxide, and hydrogen in gaseous phase by the equilibrium model are comparable with the empirical data. While, the estimated methane yield is significantly lower than real methane.

- Based on the fact that methane formed as a result of biomass devolatilization does not reform through the gasification reactions, using a semi empirical pyrolysis model by applying the experimental data available in the literature to estimate the methane yield can considerably improve the performance of the equilibrium model.

- The modified model estimates product gas yields, product heating values in good agreement with empirical data from an atmospheric high temperature circulating fluidized bed gasifier. The proposed model shows higher performance by comparing the modified model results with the equilibrium data, and with the other suggested modified models data.

- For the reference mill, biomass gasification could contribute to decreased global CO_2 emissions in both scenarios. The estimated CO_2 emission reeducation for the first scenario which produced syngas from gasifier applied to fire the lime kiln is 30 4000 t/y of CO_2 and for the second scenario which replacement of existing bark boiler with an Integrated Biomass Gasification Combined cycle is 23 5000 t/y CO_2.

- The replacement of the existing bark boiler with integrated gasification combined cycle if the necessity of new bark boiler installation considered is technically and economically viable. On the other hand, the profitability of use of the syngas for firing in lime kiln depends on fossil fuel price and capital investment.

6.2. Recommendations

Further work should be done in order to evaluate the feasibility of larger scale integrated biomass gasification process to the Kraft mill to supply simultaneously lime kiln fuel and to generate the Kraft steam and power demand. Furthermore, as several heat integration possibilities between the gasification plant and the Kraft processes are presented, the possible integration scenarios should be investigated. Finally the integration of biomass gasification combined heat and power to the Kraft jointly with two other biorefinery possibilities which are lignin extraction, and furfural and ethanol production from hemicellulose could be analyzed.

References

ABDUL SALAM, P., KUMAR, S. & SIRIWARDHANA, M. 2010. The status of biomass gasification in Thailand and Combodia. *Energy Environment Partnership (EEP) Report,* available at http://www.eepmekong.org.

ADEN, A. & NATIONAL RENEWABLE ENERGY LABORATORY (U.S.) 2002. Lignocellulosic biomass to ethanol process design and economics utilizing co-current dilute acid prehydrolysis and enzymatic hydrolysis for corn stover. *Technical report NREL/TP-510-32438,*. National Renewable Energy Laboratory.

ALTAFINI, C. R., WANDER, P. R. & BARRETO, R. M. 2003. Prediction of the working parameters of a wood waste gasifier through an equilibrium model. *Energy Conversion and Management,* 44**,** 2763-2777.

ANDERSSON, E. & HARVEY, S. 2006. System analysis of hydrogen production from gasified black liquor. *Energy,* 31**,** 3426-3434.

AZAR, C., LINDGREN, K. & ANDERSSON, B. A. 2003. Global energy scenarios meeting stringent CO2 constraints - cost-effective fuel choices in the transportation sector. *Energy Policy,* 31**,** 961-976.

BERGLIN, N. & BERNTSSON, T. 1998. CHP in the pulp industry using black liquor gasification: thermodynamic analysis. *Applied Thermal Engineering,* 18**,** 947-961.

BP STATISTICAL REVIEW 2010. BP Statistical Review of World Energy. *Avaiable at http://www.bp.com*.

BRADLEY, D. 2008. canada biomass availability and cost. *www.tradecommissioner.gc.ca*.

BRIDGWATER, A. V., TOFT, A. J. & BRAMMER, J. G. 2002. A techno-economic comparison of power production by biomass fast pyrolysis with gasification and combustion. *Renewable & Sustainable Energy Reviews,* 6**,** 181-248.

CAMPOY, M., GOMEZ-BAREA, A., VIDAL, F. B. & OLLERO, P. 2009. Air-steam gasification of biomass in a fluidised bed: Process optimisation by enriched air. *Fuel Processing Technology,* 90**,** 677-685.

CAPUTO, A. C., PALUMBO, M., PELAGAGGE, P. M. & SCACCHIA, F. 2005. Economics of biomass energy utilization in combustion and gasification plants: effects of logistic variables. *Biomass & Bioenergy,* 28**,** 35-51.

CHIESA, P. & LOZZA, G. 1999. CO2 emission abatement in IGCC power plants by semiclosed cycles: Part A - With oxygen-blown combustion. *Journal of Engineering for Gas Turbines and Power-Transactions of the Asme,* 121**,** 635-641.

CIFERNO, J. P. & MARANO, J. J. 2002. Benchmarking Biomass Gasification Technologies for Fuels, Chemicals and Hydrogen Production. *U.S. Department of Energy& National Energy Technology Technology Laboratory Report*.

CONSONNI, S., KATOFSKY, R. E. & LARSON, E. D. 2009. A gasification-based biorefinery for the pulp and paper industry. *Chemical Engineering Research & Design,* 87**,** 1293-1317.

CORELLA, J. & SANZ, A. 2005. Modeling circulating fluidized bed biomass gasifiers. A pseudo-rigorous model for stationary state. *Fuel Processing Technology,* 86**,** 1021-1053.

DE DIEGO, L. F., GARCIA-LABIANO, F., ABAD, A., GAYAN, P. & ADANEZ, J. 2002. Modeling of the devolatilization of nonspherical wet pine wood particles in fluidized beds. *Industrial & Engineering Chemistry Research,* 41**,** 3642-3650.

DE KAM, M. J., MOREY, R. V. & TIFFANY, D. G. 2009. Biomass Integrated Gasification Combined Cycle for heat and power at ethanol plants. *Energy Conversion and Management,* 50**,** 1682-1690.

DEMIRBAS, A. 2009. Biofuels securing the planet's future energy needs. *Energy Conversion and Management,* 50**,** 2239-2249.

DI BLASI, C. 2008. Modeling chemical and physical processes of wood and biomass pyrolysis. *Progress in Energy and Combustion Science,* 34**,** 47-90.

DOCTOR, R. D., MOLBURG, J. C., THIMMAPURAM, P., BERRY, G. F., LIVENGOOD, C. D. & JOHNSON, R. A. 1993. Gasification Combined-Cycle - Carbon-Dioxide Recovery, Transport, and Disposal. *Energy Conversion and Management,* 34**,** 1113-1120.

DORNBURG, V. & FAAIJ, A. P. C. 2001. Efficiency and economy of wood-fired biomass energy systems in relation to scale regarding heat and power generation using combustion and gasification technologies. *Biomass & Bioenergy,* 21**,** 91-108.

ENERGYE2. & FOSTER WHEELER ENERGIA OY REPORTM 2002. FINAL TECHNICAL REPORT of STRAW GASIFICATION FOR CO-COMBUSTION IN LARGE CHP-PLANTS. *PROJECT NO: 1999/C77/13 AND 1999/C77/15*.

EPA-CHP 2007. Biomass Combined Heat and Power Catalog of Technologies *U.S. Environmental Protection Agency, Combined Heat and Power Partnership,* Available at http://www.epa.gov/chp/.

EPA., U. S. E. P. A. 2000. Inventory of U.S. greenhouse gas emissions and sinks: 1990–1998. *Report No. EPA 236-R-00-001EPA.*

FOSTER WHEEL 2003. Potential for improvment in gasification combined cycle power generation with CO2 capture. *Report.PH4/19.*

FRANCEY, S., TRAN, H. & JONES, A. 2009. Current status of alternative fuel use in lime kilns. *Tappi Journal,* 8**,** 33-39.

GAUTAM, G., ADHIKARI, S. & BHAVNANI, S. 2010. Estimation of Biomass Synthesis Gas Composition using Equilibrium Modeling. *Energy & Fuels,* 24**,** 2692-2698.

GENERAL ELECTRIC WEBSITE 2003. Available at http://www.ge-energy.com/.

GILLS, B. K. 2008. Climate Change: A Global Call to Action. *Globalizations,* 5**,** 83-87.

GOMEZ-BAREA, A. & LECKNER, B. 2010. Modeling of biomass gasification in fluidized bed. *Progress in Energy and Combustion Science,* 36**,** 444-509.

GONZALEZ, J. F., RAMIRO, A., GONZALEZ-GARCIA, C. M., GANAN, J., ENCINAR, J. M., SABIO, E. & RUBIALES, J. 2005. Pyrolysis of almond shells. Energy applications of fractions. *Industrial & Engineering Chemistry Research,* 44**,** 3003-3012.

GREEN, R. P., HOUGH, G. & TECHNICAL ASSOCIATION OF THE PULP AND PAPER INDUSTRY. ALKALINE PULPING COMMITTEE. 1992. *Chemical recovery in the alkaline pulping processes,* Atlanta, GA, U.S.A., TAPPI Press.

GRIBIK, A. M., MIZIA, R. E., GATLEY, H. & PHILLIPS, B. 2007. Economic and Technical Assessment of Wood Biomass Fuel Gasification for Industrial Gas Production. *Idaho National Laboratory*.

GRIECO, E. & BALDI, G. 2011. Analysis and modelling of wood pyrolysis. *Chemical Engineering Science,* 66**,** 650-660.

HAJALIGOL, M. R., HOWARD, J. B., LONGWELL, J. P. & PETERS, W. A. 1982. Product compositions and kinetics for rapid pyrolysis of cellulose. *Ind Eng Chem Process Des Dev,* 21**,** 457–465.

HANNULA, I. & KURKELA, E. 2010. A semi-empirical model for pressurised air-blown fluidised-bed gasification of biomass. *Bioresource Technology,* 101**,** 4608-4615.

HEYENE, S. 2010. Process Integration Opportunities for Synthetic Natural Gas (SNG) Production by Thermal Gasification of Biomass. *Ph.D. thesis* Department of Energy and Environment**,** Göteborg, Sweden

HOLMBERG, H. & AHTILA, P. 2005. Evaluation of energy efficiency in biofuel drying by means of energy and exergy analyses. *Applied Thermal Engineering,* 25**,** 3115-3128.

HTTP://WWW.CARBONTAX.ORG 2011.

HUANG, H. J. & RAMASWAMY, S. 2009. Modeling Biomass Gasification Using Thermodynamic Equilibrium Approach. *Applied Biochemistry and Biotechnology,* 154**,** 193-204.

ICFPA REPORT 2005. Calculation Tools for Estimating Greenhouse Gas Emissions from Pulp and Paper Mill. *National Council for Air and Stream Improvement, Inc. (NCASI),* Available at http://www.wbcsd.org.

INTERGOVERNMENTAL PANEL ON CLIMATE CHANGE (IPCC) 1997b. Revised 1996 IPCC guidelines
for national greenhouse gas inventories. *IPCC National Greenhouse Gas Inventory Program,* Workbook (Vol. 2).

ISAKSSON, J., HELANTI, V. & SHENASSA, R. 2008. Biomass Gasification for Lime Kilns. *TAPPI Engineering, pulping & Enviromental Conference*.

JAND, N., BRANDANI, V. & FOSCOLO, P. U. 2006. Thermodynamic limits and actual product yields and compositions in Biomass gasification processes. *Industrial & Engineering Chemistry Research,* 45**,** 834-843.

JAND, N. & FOSCOLO, P. U. 2005. Decomposition of wood particles in fluidized beds. *Industrial & Engineering Chemistry Research,* 44**,** 5079-5089.

JARUNGTHAMMACHOTE, S. & DUTTA, A. 2007. Thermodynamic equilibrium model and second law analysis of a downdraft waste gasifier. *Energy,* 32**,** 1660-1669.

JARUNGTHAMMACHOTE, S. & DUTTA, A. 2008. Equilibrium modeling of gasification: Gibbs free energy minimization approach and its application to spouted bed and spout-fluid bed gasifiers. *Energy Conversion and Management,* 49**,** 1345-1356.

JAYAH, T. H., AYE, L., FULLER, R. J. & STEWART, D. F. 2003. Computer simulation of a downdraft wood gasifier for tea drying. *Biomass & Bioenergy,* 25**,** 459-469.

JIN, H. M., LARSON, E. D. & CELIK, F. E. 2009. Performance and cost analysis of future, commercially mature gasification-based electric power generation from switchgrass. *Biofuels Bioproducts & Biorefining-Biofpr,* 3**,** 142-173.

KANNICHE, M. & BOUALLOU, C. 2007. CO2 capture study in advanced integrated gasification combined cycle. *Applied Thermal Engineering,* 27**,** 2693-2702.

KAUSHAL, P., ABEDI, J. & MAHINPEY, N. 2010. A comprehensive mathematical model for biomass gasification in a bubbling fluidized bed reactor. *Fuel,* 89**,** 3650-3661.

KERSTEN, S. R. A., PRINS, W., VAN DER DRIFT, A. & VAN SWAAIJ, W. P. M. 2003. Experimental fact-finding in CFB biomass gasification for ECN's 500 kW(th) pilot plant. *Industrial & Engineering Chemistry Research,* 42**,** 6755-6764.

KINOSHITA, C. M., YUE, W. & TAKAHASHI, P. K. 1991. Chemical-Equilibrium Computations for Gasification of Biomass to Produce Methanol. *Energy Sources,* 13**,** 361-368.

LARSON, E. D., CONSONNI, S. & KATOFSK, R. E. 2003. A Cost-Benefit Assessment of Biomass Gasification Power Generation in the Pulp and Paper Industry. *Final Report,* Princeton University.

LI, X., GRACE, J. R., WATKINSON, A. P., LIM, C. J. & ERGUDENLER, A. 2001. Equilibrium modeling of gasification: a free energy minimization approach and its application to a circulating fluidized bed coal gasifier. *Fuel,* 80**,** 195-207.

LI, X. T., GRACE, J. R., LIM, C. J., WATKINSON, A. P., CHEN, H. P. & KIM, J. R. 2004. Biomass gasification in a circulating fluidized bed. *Biomass & Bioenergy,* 26**,** 171-193.

LIDE, D. R. & KEHIAIAN, H. V. 1994. *CRC handbook of thermophysical and thermochemical data,* Boca Raton, CRC Press.

LINDBLOM, M., LANDÄLV, I. 2007. Chemrec’s Atmospheric & Pressurized BLG(Black Liquor Gasification) Technology-Status and Fiture Plans. *Chemrec AB* Floragatan 10B.

LV, P. M., CHANG, J., XIONG, Z. H., HUANG, H. T., WU, C. Z., CHEN, Y. & ZHU, J. X. 2003. Biomass air-steam gasification in a fluidized bed to produce hydrogen-rich gas. *Energy & Fuels,* 17**,** 677-682.

LV, P. M., XIONG, Z. H., CHANG, J., WU, C. Z., CHEN, Y. & ZHU, J. X. 2004. An experimental study on biomass air-steam gasification in a fluidized bed. *Bioresource Technology,* 95**,** 95-101.

M.W.CHASE, J., C.A.DAVIES, J. D., JR., D.J. FRURIP, R. A. M. & SYVERUD, A. 1985. JANAF thermodynamic tables. *J Phys Chem Ref Data*, 14.

MANSARAY, K. G., GHALY, A. E., AL-TAWELL, A. M., UGURSAL, V. I. & HAMDULLAHPUR, F. 2000. Mathematical modeling of a fluidized bed rice husk gasifier: Part III - Model verification. *Energy Sources*, 22**,** 281-296.

MATHIEU, P. & DUBUISSON, R. 2002. Performance analysis of a biomass gasifier. *Energy Conversion and Management*, 43**,** 1291-1299.

MELGAR, A., PEREZ, J. F., LAGET, H. & HORILLO, A. 2007. Thermochemical equilibrium modelling of a gasifying process. *Energy Conversion and Management*, 48**,** 59-67.

MILNE, T. A. & EVANS, R. J. 1998. Biomass Gasifier Tars: Their Nature, Formation, and Conversion. *National Renewable Energy Laboratory Report*, NREL/TP-570-25357.

MINER, R. & UPTON, B. 2002. Methods for estimating greenhouse gas emissions from lime kilns at kraft pulp mills. *Energy*, 27**,** 729-738.

NAQVI, M., YAN, J. & FROLING, M. 2010. Bio-refinery system of DME or CH(4) production from black liquor gasification in pulp mills. *Bioresource Technology*, 101**,** 937-944.

NARVAEZ, I., ORIO, A., AZNAR, M. P. & CORELLA, J. 1996. Biomass gasification with air in an atmospheric bubbling fluidized bed. Effect of six operational variables on the quality of the produced raw gas. *Industrial & Engineering Chemistry Research*, 35**,** 2110-2120.

NATIONAL ENERGY BOARD REPORT 2011. Electricity - Current Market Conditions October-December 2011. *Available at http://www.neb.gc.ca*.

NATURAL RESOURCES CANADA REPORT 2011. Canadian Crude Oil, Natural Gas and Petroleum Products. *Review of 2009 & Outlook to 2030*, Avaiable at http://www.nrcan.gc.ca.

NEVES, D., THUNMAN, H., MATOS, A., TARELHO, L. & GOMEZ-BAREA, A. 2011. Characterization and prediction of biomass pyrolysis products. *Progress in Energy and Combustion Science*, 37**,** 611-630.

NIKOO, M. B. & MAHINPEY, N. 2008. Simulation of biomass gasification in fluidized bed reactor using ASPEN PLUS. *Biomass & Bioenergy*, 32**,** 1245-1254.

NUNN, T., HOWARD, J., LONGWELL, J. P. & PETERS, W. A. 1985. Product compositions and kinetics in the rapid pyrolysis of sweet gum hardwood. *Ind. Eng. Chem Process Des Dev*, 24.

OKEEFE, L. F., GRIFFITHS, J., WEISSMAN, R. C., DE PUY, R. A. & WAINWRIGHT, J. M. 2002. A Single IGCC Design for Variable CO2 Capture. *Fifth European Gasification Conference*.

PERSONS, E. 2002. Advanced Fossil Power System Comparisons Study. *NETL report*.

PETERS, M. S. & TIMMERHAUS, K. D. 1991. *Plant design and economics for chemical engineers,* New York, McGraw-Hill.

QUAAK, P., KNOEF, H. & STASSEN, H. 1999. Energy from biomass: a review of combustion and gasification technologies. *Energy Series Technical Papers,* No.422.

RADMANESH, R., COURBARIAUX, Y., CHAOUKI, J. & GUY, C. 2006. A unified lumped approach in kinetic modeling of biomass pyrolysis. *Fuel,* 85**,** 1211-1220.

RALSTON, P. E. 2002. Fuel and Combustion Equipment Standard Handbook of Plant Engineering *McGraw-Hill,* 3rd Edition.

RANZI, E., CUOCI, A., FARAVELLI, T., FRASSOLDATI, A., MIGLIAVACCA, G., PIERUCCI, S. & SOMMARIVA, S. 2008. Chemical Kinetics of Biomass Pyrolysis. *Energy & Fuels,* 22**,** 4292-4300.

RAO, M. S., SINGH, S. P., SODHA, M. S., DUBEY, A. K. & SHYAM, M. 2004. Stoichiometric, mass, energy and exergy balance analysis of countercurrent fixed-bed gasification of post-consumer residues. *Biomass & Bioenergy,* 27**,** 155-171.

RATH, J., STEINER, G., WOLFINGER, M. G. & STAUDINGER, G. 2002. Tar cracking from fast pyrolysis of large beech wood particles. *Journal of Analytical and Applied Pyrolysis,* 62**,** 83-92.

ROBINSON, P. J. & LUYBEN, W. L. 2010. Integrated Gasification Combined Cycle Dynamic Model: H2S Absorption/Stripping, Water-Gas Shift Reactors, and CO2 Absorption/Stripping. *Industrial & Engineering Chemistry Research,* 49**,** 4766-4781.

RODRIGUES, M., WALTER, A. & FAAIJ, A. 2007. Performance evaluation of atmospheric biomass integrated gasifier combined cycle systems under different strategies for the use of low calorific gases. *Energy Conversion and Management,* 48**,** 1289-1301.

RUGGIERO, M. & MANFRIDA, G. 1999. An equilibrium model for biomass gasification processes. *Renewable Energy,* 16**,** 1106-1109.

SCHUSTER, G., LOFFLER, G., WEIGL, K. & HOFBAUER, H. 2001. Biomass steam gasification - an extensive parametric modeling study. *Bioresource Technology,* 77**,** 71-79.

SCOTT, D. S., PISKORZ, J. & RADLEIN, D. 1985. Liquid products from the continuous flash pyrolysis of biomass. *Ind. Eng. Chem. Process Des. Dev.,* 24 (3)**,** pp 581–588.

SIRO, M. 1989. Operation Eperiences from Bark Gasification for a Lime Kilns. *Low Grade Fuels,* VTT Symposium 108**,** PP. 373-382.

SMITH, W. R. & MISSEN, R. W. 1982. *Chemical reaction equilibrium analysis : theory and algorithms,* New York, Wiley.

SMOOK, G. A. 1990. *Handbook of pulp & paper terminology : a guide to industrial and technological usage,* Vancouver ; Bellingham, Wangus Wilde Publications.

SOUZA-SANTOS, M. 2004. Solid fuels combustion and gasification. Modeling, simulation and equipment operation. *New York: Marcel Dekker Inc.*

STASSEN, H., PRINS, W. & VAN SWAAIJ, W. 2002. Thermal conversion of biomass into secondary products the case of gasification and pyrolysis. *Proceedings of the 12th European conference on biomass for energy,* Industry and climate protection**,** 38–44.

STATISTICS CANADA REPORT 2011. Average hourly wages of employees by selected characteristics and profession, unadjusted data, by province. *Availale at http://www40.statcan.ca*.

SUN, S. Z., TIAN, H. M., ZHAO, Y. J., SUN, R. & ZHOU, H. 2010. Experimental and numerical study of biomass flash pyrolysis in an entrained flow reactor. *Bioresource Technology,* 101**,** 3678-3684.

SWANSON, R. 2009. Techno-economic analysis of biomass-to-liquids production based on gasification. *Master thesis* Mechanical Engineering; Biorenewable Resources and Technology, Iowa State University.

SWANSON, R. M., PLATON, A., SATRIO, J. A. & BROWN, R. C. 2010. Techno-economic analysis of biomass-to-liquids production based on gasification. *Fuel,* 89**,** S2-S10.

TANG, H. Q. & KITAGAWA, K. 2005. Supercritical water gasification of biomass: thermodynamic analysis with direct Gibbs free energy minimization. *Chemical Engineering Journal,* 106**,** 261-267.

VAN DER DRIFT, A., VAN DOORN, J. & VERMEULEN, J. W. 2001. Ten residual biomass fuels for circulating fluidized-bed gasification. *Biomass & Bioenergy,* 20**,** 45-56.

WAHLUND, B., YAN, J. Y. & WESTERMARK, M. 2004. Increasing biomass utilisation in energy systems: A comparative study of CO2 reduction and cost for different bioenergy processing options. *Biomass & Bioenergy,* 26**,** 531-544.

WANG, M. M., ZHANG, J. S., ZHANG, S. Y., WU, J. H. & YUE, G. X. 2008. Experimental studies on gasification of the Shenmu coal char with CO_2 at elevated pressures. *Korean Journal of Chemical Engineering,* 25**,** 1322-1325.

WARNECKE, R. 2000. Gasification of biomass: comparison of fixed bed and fluidized bed gasifier. *Biomass & Bioenergy,* 18**,** 489-497.

WETTERLUND, E., PETTERSSON, K. & HARVEY, S. 2011. Systems analysis of integrating biomass gasification with pulp and paper production - Effects on economic performance, CO_2 emissions and energy use. *Energy,* 36**,** 932-941.

WHITE, W. B., JOHNSON, S. M. & DANTZIG, G. B. 1958. Chemical Equilibrium in Complex Mixtures. *The Journal of Chemical Physics,* 28**,** 751-755.

WIMMERSTEDT, R. & LINDE, B. 1998. Assessment of Technique and Economy of Biofuel Drying. *(No. 637):,* Värmeforsk.

ZAINAL, Z. A., ALI, R., LEAN, C. H. & SEETHARAMU, K. N. 2001. Prediction of performance of a downdraft gasifier using equilibrium modeling for different biomass materials. *Energy Conversion and Management,* 42**,** 1499-1515.

ZAINAL, Z. A., RIFAU, A., QUADIR, G. A. & SEETHARAMU, K. N. 2002. Experimental investigation of a downdraft biomass gasifier. *Biomass & Bioenergy,* 23**,** 283-289.

ZENG, L. & VAN HEININGEN, A. R. P. 2000. Carbon gasification of kraft black liquor solids in the presence of TiO_2 in a fluidized bed. *Energy & Fuels,* 14**,** 83-88.